Electro-reflectance in thin films of gold

ELECTRO - REFLECTANCE IN THIN FILMS OF GOLD

Author: J. N. Averitsiotis

Supervisor: Dr. R. P. Howson

Submitted for M.Sc. degree of

Loughborough University of Technology

Date of submission 1974

C O N T E N T S

SUMMARY

Optical measurements on evaporated thin films of gold in the visible region of the electromagnetic spectrum are shown to exhibit a distinct free carrier plasma edge in the region of 2.3eV.

It will be shown that it is possible to predict the optical properties of evaporated films of gold in the visible region as a function of their thickness and changes in free electron concentration. The optical constants due to free carrier effects have been separated from those due to bound electrons and used in computer programs for film behavior. A one carrier model was found adequate to account for free carrier dispersion with a relaxation time of 1.5×10^{-14} sec found for a $N/m^* = 8 \times 10^{28}\ m^{-3}$.

Measurements of the induced change in reflectance , i.e. the Electro - reflectance effect , in thin films of gold using the Electrolytic technique are shown to exhibit two main features. Firstly the peak of the Electro - reflectance spectrum occurs in the spectral region of the plasma edge of the thin gold films and secondly the Electroreflectance peak shifts to lower photon - energies as the thickness of the film becomes less than 200 Å . The dependence of the Electroreflectance Effect on the magnitude of the modulating voltage and the double layer capacity has also been studied.

A Schottky - type barrier which exists in a Schottky diode used succes - fully for the modulation of the optical properties of a very thin film of gold. The measurement of the Electroreflectance spectrum of a 70 Å thick film of gold was possible using the Schottky - diode technique.

Measurements of the Electrotransmittance effect in thin films of gold show a derivative - like spectrum exhibiting two peaks of opposite sign.

A new model is proposed to explain the observed features of the Electroreflectance spectrum of thin films of gold and previous plasma edge reflection modulation data of a gold - mirror electrode. Emphasis is given to the fact that intraband transitions only account for the Electroreflectance effect in metals.

Acknowledgements

I am greatly indebted to Dr. R. P. Howson for encouragmement and guidance throughout the duration of this project and for many helpful discussions.

Thanks are also due to my wife Rea for her constant encouragement and help with the manuscript.

List of Principal Symbols

C	Double layer capacity
c	Velocity of light
d	Width
ε_o	Permitivity of free space
ε_L	Lattice dielectric constant
$\bar{\varepsilon}_f$	Free - electrons dielectric constant
e	Electronic charge
I	Intensity
m^*	Carrier effective mass
m_e	Electron mass
Δn	Refractive index change
n	Real part of refractive index
$\bar{n}$	Complex refractive index
n_L	Refractive index of the electrolyte
N	Free carrier concentration
ν	Frequency
R	Reflectance
ΔR	Reflectance change
$\frac{\Delta R}{R}$	Modulation depth
$\bar{r}$	Complex Fresnel coefficient
τ	Electron free collision time
V_m	Modulating voltage
T	Transmittance
$\bar{t}$	Complex Fresnel transmission coefficient
ω_p	Plasma frequency
ω	Frequency
δ	Phase change

$\ominus$	Angle
k	Extinction coefficient
σ	Electrical conductivity
Φ	Angle

CHAPTER 1 - HISTORICAL REVIEW

1.1 Electrolytic Technique

The effect of Electroreflectance (ER) of gold (Au) was first observed by Feinleib /1/. He had used an Au mirror as a working-electrode and a platinum counter-electrode both immersed in aqueous 1M KCl. A modulating voltage of 2V peak-to-peak at 35 Hz, was applied on these electrodes. The detected ER signal, ΔR, divided by the D.C. reflectivity, R, was plotted against wavelength. This ER spectrum $\Delta R/R=f(\lambda)$, exhibited a major peak at about 2.35 eV.

Feinleib tried to explain the shape of the ER spectrum obtained by proposing that the observed effect was due to the modulation of the optical constants of the electrolyte in the double layer region, because of the applied low frequency modulating electric field.

Feinleib's quantitative results are today in doubt because no precaution was taken to avoid the formation of surface films or metal-chloride complexes or evolution and absorption of H and O on the surface of the Au electrodes.

Since Feinleib's observation, a large number of investigators have employed the same (Electrolytic) technique with remarkable success in elucidating the optical properties of gold.

The employment of the electrolytic technique for the study of the ER effect has the great advantage of the ease with which a high electric field can be created in the metal-electrolyte interface. It is

generally accepted today that the perturbation of the optical properties of a metal -electrolyte interface is due to the existence of an electrical double layer which provides the necessary high electric field at the interface between a metal and a solution. The term double layer is used in electrochemistry to describe the distribution of electrons, solvent molecules , and other species at the interface between a metal and an electrolyte solution. Although the exact nature of the double layer is still unknown , the consideration of the double layer in two sections : an outer or diffuse layer and an inner layer , seems very useful.

The force holding the ions in the outer layer is the coulombic interaction between the charge on the metal and the charged ions. The inner layer is one or two molecular diameters in thickness and the ions here are held partly by coulombic and partly by specific forces. The theory of the outer layer in its simplest form is due to Gouy and Chapman /2/. Stern developed more quantitatively their approach co nsidering the model,of the parallel plate condenser and taking into account the diffusion of the charge on the solution side. Stern proposed that the ions in the outer layer are restricted by their finite size and other factors to a plane (Stern plane) located a few Angstroms from the metal-electrolyte interface Fig.(1.1).

Fig.(1.2) represents the variation of potential across the electrical double layer according to Gouy's and Stern's models.

From recent,Grahame /3/, experimental data it seems that the above interpretation is not satisfactory , and that the inner region of the double layer should be very complex.

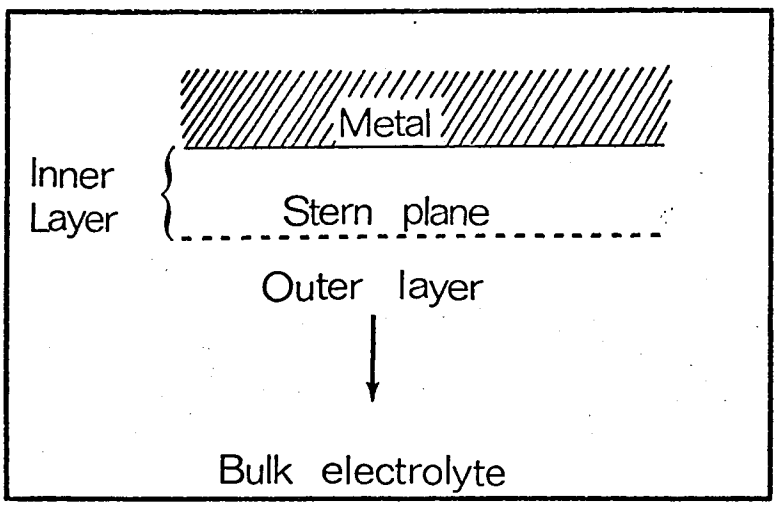

F i g . (1.1)

Schematic diagram of the electrical double layer.

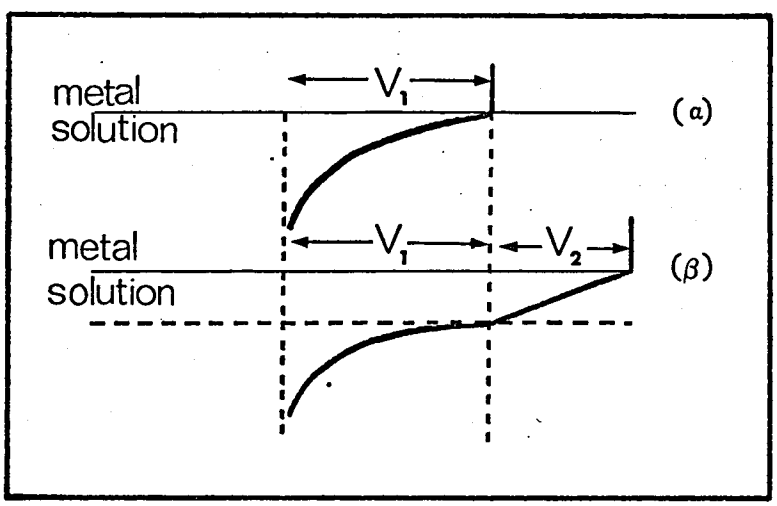

F i g . (1.2)

(α) represents the distribution of potentials in Gour-Chapman model, and (β) in Stern model respectively.

Grahame improved Stern's model by distinguishing between the plane of closest approach of diffuse layer ions (Stern plane) which he called the outer Helmholtz plane and the position of the centres of specifically adsorbed ions , the inner Helmholtz plane. Grahame's modification of the Stern's model is the basis of current theories of the double layer. So the diagramatic representation of the generally accepted model of the double layer is as in Fig.(1.3).

Not one of the present theories determines satisfactory the experimental data , and more research must be done to help the derivation of a more realistic model.

Working with Stern's model the total potential difference (V) in the double layer is given by :

$$V = V_1 + V_2 \qquad (1.1)$$

where V_2 is the potential difference between the metal - electrode and the Stern plane and V_1 is the Gouy-Chapman diffuse layer potential difference. The capacitances existingin the double layer are always the subject of interest because they are measurable quantities , and they determine the electrical characterista of the double layer,a fact which helps in the interpretation of the obtained ER spectra of the metal - electrolyte interface. Differentiation of Eq.1.1 with respect to the charge on the metal - electrode and with the assumption of no specific adsorption (i.e. all the charges assumed in the diffuse layer) gives :

$$\frac{1}{C} = \frac{1}{C_1} + \frac{1}{C_2} \qquad (1.2)$$

The double layer capacity therefore is given as a series combination

of the diffuse layer capacity C_1 and the inner layer capacity C_2 . It is obvious that C is controlled by the smaller of C_1 and C_2 .

The electric fields existing within the double layer are extremely large. A simple calculation considering the double layer capacity as an ordinary parallel plate condenser gives an idea of the order of magnitude of the electric field applied by the double layer on the surface of the metal. Considering that the distance between the outer Helmholtz plane and the surface of the metal is four Angstroms and that the applied modulating voltage is 1V then the change in the electric field on the double layer will be $E=IV/4\mathring{A} = 2 \times 10^7$ V/cm .

This large electric field definitely p erturbs the optical properties of the gold e lectrode - solution interface. The dependence of the electric fields , generated in the double layer region, on the externally applied voltages, can be seen considering the double layer as a combination of capacitances according to the present theories and experimental data. Takamura T. and co - workers /4/ have studied the reflectivity changes of gold as a function of the applied potential. It is obvious from their results that the optical properties of the gold - solution interface are affected by the applied potentials and consequently the electric fields present in the double layer.

The following precautions must be taken using the electrolytic technique :

I. Something which must be seriously considered with the electrolytic technique is the p urification of the electrolyte /5/.We can consider two types of impuruties :

a) organic substances or generally non - ionic impurities and

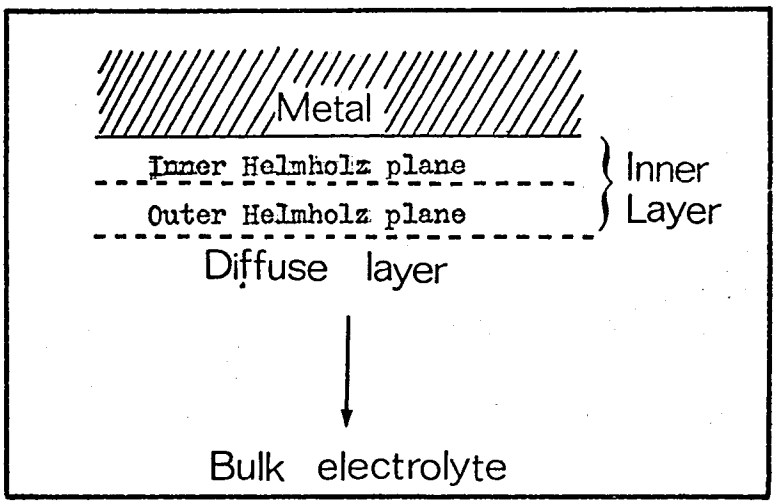

F i g . (1.3)

Schematic diagram of the electrical double layer as it is now accepted. Nonspecifically adsorbed ions remain on the outer Helmholz plane. Specifically adsorbed ions are assumed to form a monolayer with their centers in the inner Helmholz plane.

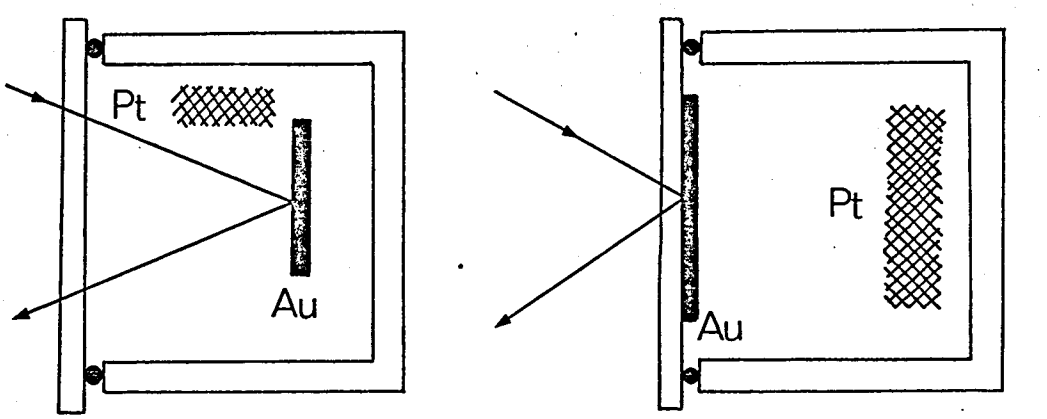

a) External reflection spectroscopy

b) Internal reflection spectroscopy

F i g . (1.4)

b) ionic impurities.

Pre - electrolysis of the solution by-passing a high current between a pair of platinum electrodes immersed in the electrolyte for several hours or days purifies the solution because it removes the ionic impurities. Purified activated charcoal has been used for the removal of the organic molecules from the solution. The technique consists in the circulation of the electrolyte through a column of activated charcoal for a period of at least 48 hours.

Both the above techniques have their disadvantages , but they are quite adequate. Pre - electrolysis introduces probably traces of platinum into the solution. Activated charcoal must be free from ionic impurities which probably have been introduced during its pre - treatment. The use of high purity chemicals and triple distilled water is of great advantage.

II. The value of the externally applied modulating voltage on the electrodes of the electrolytic cell must be less than the critical one. We difine as critical the value of the modulating voltage which brings the potentials of the gold electrode at the value where the formation of an oxide layer starts.

Takamura , T. and co-workers /4/ have studied in detail the formation of oxides on gold electrodes as a function of the applied potential in 0.2 M $HClO_4$, 0.5 M NaOH and H_2SO_4 . According to their report formation of stable gold oxide begins at about + 1.1V (relative to saturated calonel reference electrode , SCE). More accurate measurements indicate that the formation of oxide on the gold - electrode surface starts at 0.96 V. Formation of surface oxides reduces the reflectivity and shifts the peak of the ER spectrum of the gold electrode to longer wavelenths as they have proved experimentally .

The reflectivity-potential curve of gold exhibits a linear region from 0.0V to 0.8V relative to SCE characterised by a slight hysteresis. Consequently the value of the total applied potential on the Au electrode ,for ER studies, must be less than 0.8V SCE.

The electrolytes which are used with the electrolytic technique contain species which are not adsorbed on the surface of the gold electrode. The electrolytes frequently used are aqueous solutions of Na_2SO_4 , H_2SO_4 e to .

In the main two modes of the electrolytic technique have been used to study the ER effect :

a) Internal Reflection Spectroscopy (IRS) ,Fig.(1.4b) and

b) External (specular) Reflection Spectroscopy (ERS),Fig.(1.4a)

The main difference between IRS and ERS consists in the way in which the light falls onto the surface under examination. In IRS the light falls onto the surface passing through the gold . In ERS the light falls on the surface passing through the electrolyte. It is obvious that the IRS,in contrast to the ERS is used only with Au films (50 Å - 400Å) fabricated by vacuum deposition of the metal on the surface of a transparent glass or quartz.

The normalised internal re flectivity ($\Delta R/R$) is very sensitive and indicates small changes in the optical properties of the gold - electrolyte interface.This mode yields transmission - like absorption spectra of thin surface films when high angle s of incidence are employed.

Internal reflection spectroscopy has been used widely as a technique

for the investigation of the metal- electrolyte interface and the detection of electrode reaction products. Semitransparent gold electrodes have been fabricated /6/, by vacuum deposition for the above purposes , because of their importance to electrochemistry . But no one , to our knowledge , has studied the optical behaviour and specially the ER effect of gold films 75 - 100 Angstroms thick and its dependence on the film thickness.

On the other hand with ERS the optical properties of bulk metal - electrolyte interfaces can be studied.

Single and multiple reflection configurations have been used in relation with the IRS and ERS , where a single or large number of reflections of the incident light beam , take place respectively, on the gold surface under investigation , before coming out of the electrolytic cell and falling on the detector which is usually a photomultiplier.

The use of the multiple reflection configuration gives a large signal for ΔR but at the same time eliminates the effect of the film thickness on the ER spectrum. Howe ver, the single reflection configuration does not eliminate this effect.

Different angles of incident light - beam have also been employed but this matters only when polarised monochromatic light is used.

1.2 Ferroelectric Technique

A different technique for the elucidation of the ER spectrum of gold has been developed by Standler. Standler , H,L. /7/ has studied the modulation of the reflectivity of Au films deposited on $BaTiO_3$. The

ferroelectric polarization of the substrate was changing (reversing) repeatedly. A 60V , 350Hz square - wave voltage had been applied between the measured gold film and another metal film on the opposite face of the 0.02 cm thick ferroelectric substrate. Care had been taken to avoid stretching of the film caused by the piezoelectric strain of the crystal due to the modulating voltage. The great advantage of this method is the ease with which the ER effect at very low temperatures can be studied - this is impossible using the electrolytic method.

The above described method in contrast to the electrolytic method can be employed for ER studies in the infrared region of the spectrum.

The experimental ER spectrum , according to Stadler's measurements exhibits a peak at 2.3 eV and a dip at 3.7 eV. This technique proves experimentally the fact that the ER effect is not due to changes in the electrolyte but it is due to changes on the metal surface.

1.3 Hansen and Prostak Model

Hansen , W. and Prostak , A. /8/ have shown with computer calculations, based on Hansen's formula /9/ for the optical reflectance from a three layer structure that the reported /1/ peak in the ER spectrum of Au can not be explained with the assumption of the modulation of the optical constants of the electrolyte. On the other hand they have pointed out that the modulation of the optical constants of Au produces a peak at approximately 2.35 eV as Feinleib reported. Their results are vali d even if the disturbance in the optical properties of Au e xtends only 0.5 Angstroms into the gold. They assumed for each photon-energy, that a 0.5 Angstroms thick surface layer of the gold - electrode had its optical constants step between those of the bulk gold and those

appropriate to gold for a photon energy 0.1 eV different from that used for the bulk gold. They pointed out , also , that possible creation of Au chloride compounds on the surface of the gold electrode does not affect strongly the ER spectrum in the visible region. Their calculations for a Au - (chloride compound)-(KCl aqueous solution) did not give a major peak in the visible region of the spectrum.

Developing their multilayer model , Hansen and Prostak proposed that a shift of the plasma edge of gold , because of the applied electric field , accounts for the predominant peak at 2.35 eV.

The plasma frequency of a metal is given by /10/.

$$\omega_p^2 = \frac{4\pi N e^2}{m^*} \qquad (1.3)$$

where m^* is the effective electronic mass and N the concentration of the free electrons. An increase of the free electron concentration by an amount ΔN produces a plasma frequency shift

$$\Delta \omega_p = \frac{1}{2} \omega_p \frac{\Delta N}{N} \qquad (1.4)$$

which displaces the plot of reflectance of gold (R) to higher energies. So the field - induced modulation of the number of the free electrons produces a shift of the plasma edge of the metal. Hansen and Prostak proposed that the Fermi level is modulated by the modulation of the concentration and that other bands are unaffected by the modulating field. Also they postulated that the optical constants of the metal are shifted along the energy axis by the same fraction that ω_p is shifted.

Their model was verified experimentally by spectroscopic studies employing the internal and specular (external)reflection spectroscopy modes of the electrolytic technique, /11/,/12/.

This semiempirical model is physically unrealistic because it assumes a low frequency modulation of the Fermi level of the gold and generally of the metals.

1.4 McIntyre and Aspnes Model

McIntyre and Aspnes /13/ proposed a new model based on the assumption of a field induced very thin layer transition region of thickness $d \ll \lambda$, whose dielectric constant varies continuously the value of the dielectric constant of the metal and the dielectric constant of the electrolyte , as in Fig. (1.5).

They defined a mean value $\langle \Delta \bar{\varepsilon} \rangle$ for the dielectric constant of the transition region by averaging the changes of $\langle \Delta \bar{\varepsilon}(z) \rangle$over the transition region. Using the assumption $d \ll \lambda$ and defining , the normalized reflectivity change , for normal incidence , as

$$\frac{\Delta R}{R} = \frac{R(d) - R(0)}{R(0)} = \frac{R(d)}{R(0)} - 1 \qquad (1.5)$$

they derived the following expression , to first order in d/λ

$$\frac{\Delta R}{R} = \frac{8\pi n_1 d}{\lambda} \operatorname{Im}\left(\frac{\bar{\varepsilon}_2 - \bar{\varepsilon}_3}{\varepsilon_1 - \bar{\varepsilon}_3}\right) = \frac{8\pi n_1 d}{\lambda} \operatorname{Im}\left(\frac{\bar{\varepsilon}_2 - \varepsilon_1}{\varepsilon_1 - \bar{\varepsilon}_3}\right) \qquad (1.6)$$

All the quantities are defined in Fig. (1.5)

Two limiting cases have been considered: $\Delta\bar{\varepsilon} = \bar{\varepsilon}_2 - \varepsilon_1$ and $\Delta\bar{\varepsilon} = \bar{\varepsilon}_2 - \bar{\varepsilon}_3$,

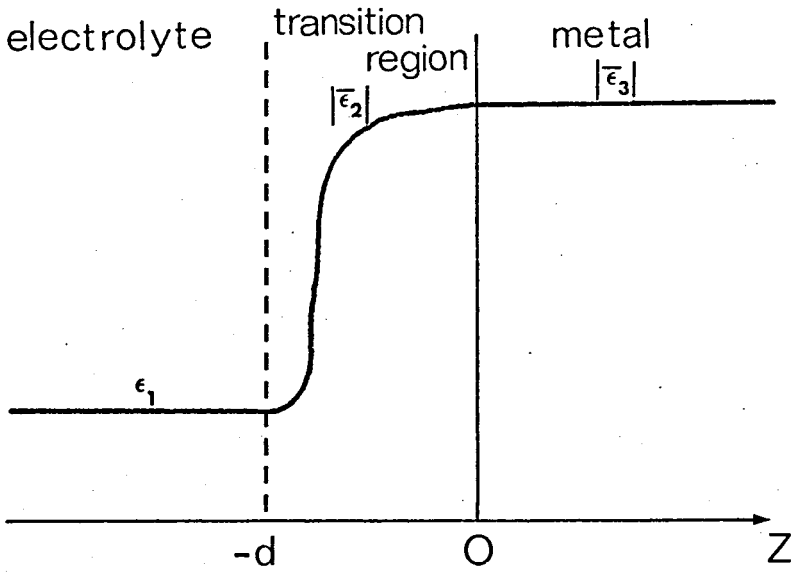

F i g. (1.5)

Schematic illustration of McIntyre's assumption.

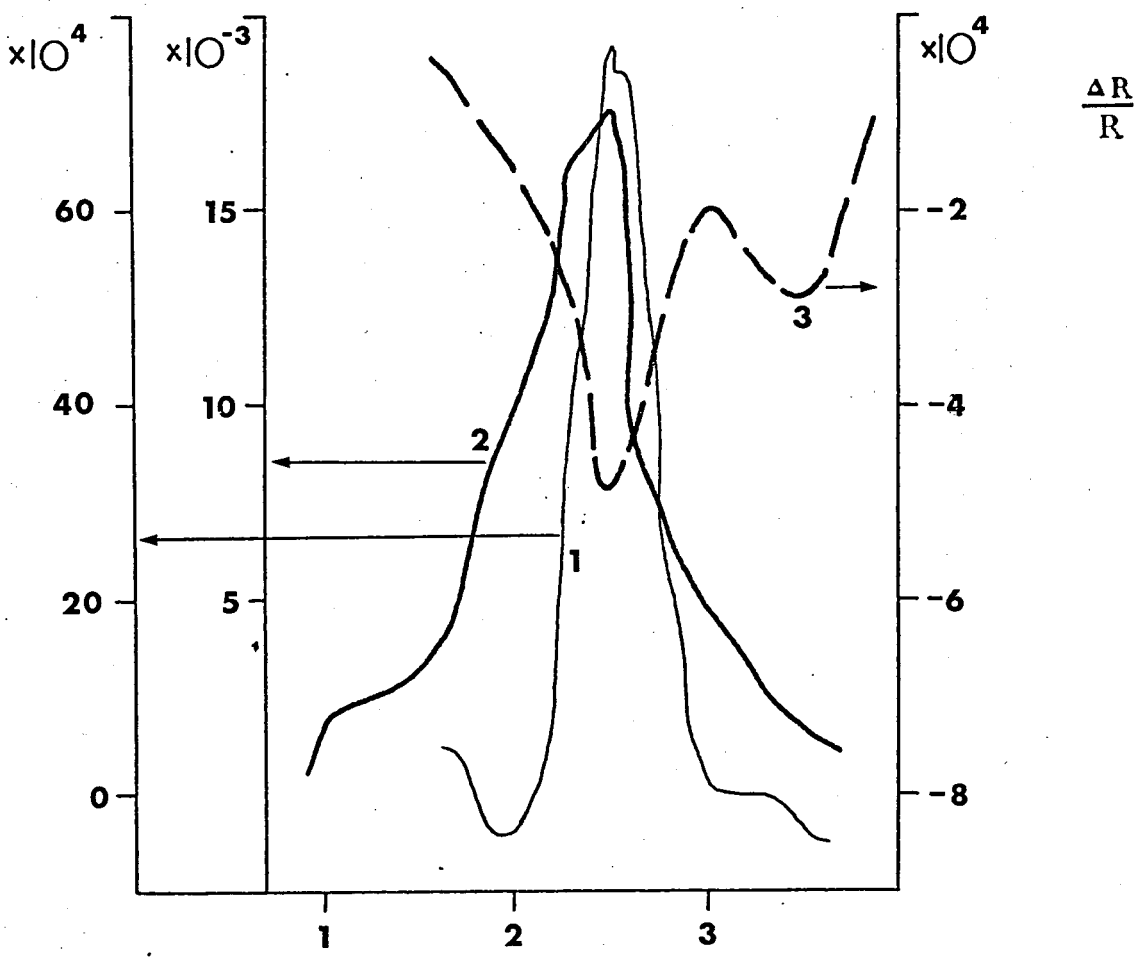

F i g. (1.6)

Experimental ER spectra of gold by: 1)J. Feinleib /1/, 2)Hansen /11/ and 3)McIntyre /14/.

corresponding to the electric field induced changes of the optical constants of the electrolyte and the metal respectively.

They have shown that the modulation of the ionic double layer refractive index is not the primary mechanism responsible for the ER effect of Ag and Au.

Assuming that the term of the dielectric function which is due to the interband transition contribution, remains constant with the applied on the surface of the electrode field', they derived expression showing the linear dependance of $\Delta R/R$ on the applied field and the differential double layer capacity.

According to their model , the change of the surface carriers density with the applied field accounts for the main characteristics of the ER spectra of Ag and Au. , and the influence of interband transitions appears through their contribution to the bulk - metal part of the dielectric constant , which is not modulated by the applied field as they have proved by their calculations.

Also from their model comes out the fact that the quantity $(1/R)(\partial R/\partial E)$, (where E , the applied field) , is always negative over the entire visible and ultra - violet wavelength region.

Their experimental results verify roughly their linear approximation theory /14/, /15/.

McIntyre and Aspnes model does not give physical insight to the mechanism of the ER effect in metals. The defined mean value $\langle\Delta\bar{\varepsilon}\rangle$ of the dielectric constant for the transition region is arbitrary and unrealistic. It is obvious /4/ that the charge distribution on the surface of the metal - electrode changes strongly with the applied voltage but it is unrealistic to assume the existence of a "step" in the density of charges between

the metal - electrode and the electrolyte, because this charge distribution does not represent the reality. It is more realistic to assume an exponential - like charge distribution in both sides of the metal-electrolyte interface.

1.5 Cheyssac et al Model

Cheyssac , Garrigos and others /16/ have suggested recently a new interpre tation in which the ER effect is associated with the surface of the Au electrode. According to their model when a light - wave falls on the surface of the metal , the excess electrons , moved by the e lectric field of the light wave , give rise to a surface current density. Involving the above assumption in the boundary conditions for the magnetic and electric fields of the light - wave , they found that the Fresnel reflection coefficient (r) , at normal incidence,is

$$r = \frac{n_E - n_M - p}{n_E + n_M + p} \qquad (1.7)$$

where n_E is the refractive index of the electrolyte , $n_M = n + ik$ the complex index of refraction of the metal and p is defined as

$$p = (\mu_o / \varepsilon_o)^{\frac{1}{2}} . g \qquad (1.8)$$

where g is the surface conductivity and is proportional to the density of excess electrons. When the electric field is modulated , the fractional change in the reflectivity R is

$$\Delta R / R = F \Delta p / p = F \Delta N / N \qquad (1.9)$$

with

$$F = -4 n_E p \frac{n_E^2 + k^2 - (p+n)^2}{\left[n_E^2 + k^2 - (p+n)^2\right]^2 + 4k^2 (p+n)^2} \qquad (1.10)$$

They have verified their theoretical model with experimental studies of the ER effect of gold , copper and silver. There are , of course discrepancies between their theoretical and experimental results.

CHAPTER 2 - EXPERIMENTAL TECHNIQUES

2.1 Preparation of Gold Films

The preparation of gold films is described step by step below. The apparatus used for the preparation is also described and emphasis is given to the preparation conditions.

2.1.1 The Evaporation System

An evaporation technique was employed for the production of samples of gold because of its flexibility and range of possible deposition conditions and also because basic evaporation methods are well established.

The apparatus used for the evaporation of gold is illustrated in Fig. (2.1). The vacuum system is enclosed by an 18" glass bell-jar, sealed by neoprene and pumped by a standard 4" diffusion pump. There was no cold trap but the system was capable of an ultimate pressure of better than 10^{-6} Torr. The chamber pressure was measured using a 1G2 ionization gange head mounted in the base plate.

An electron gun from Varian Associates was used to evaporate the source material. The substrates were mounted in a stainless steel frame and heated with a pair of 750 watt cylindrical quartz lamps mounted in a reflector and heating the substrates indirectly through an intermediate stainless steel plate. The substrate holder was able to take up to two slides at a time. The intermediate plate was necessary to convert the short wavelength radiation from the lamps into longer wavelengths which would be absorbed by the glass substrates. (See Figs. (2.2) and (2.3)).

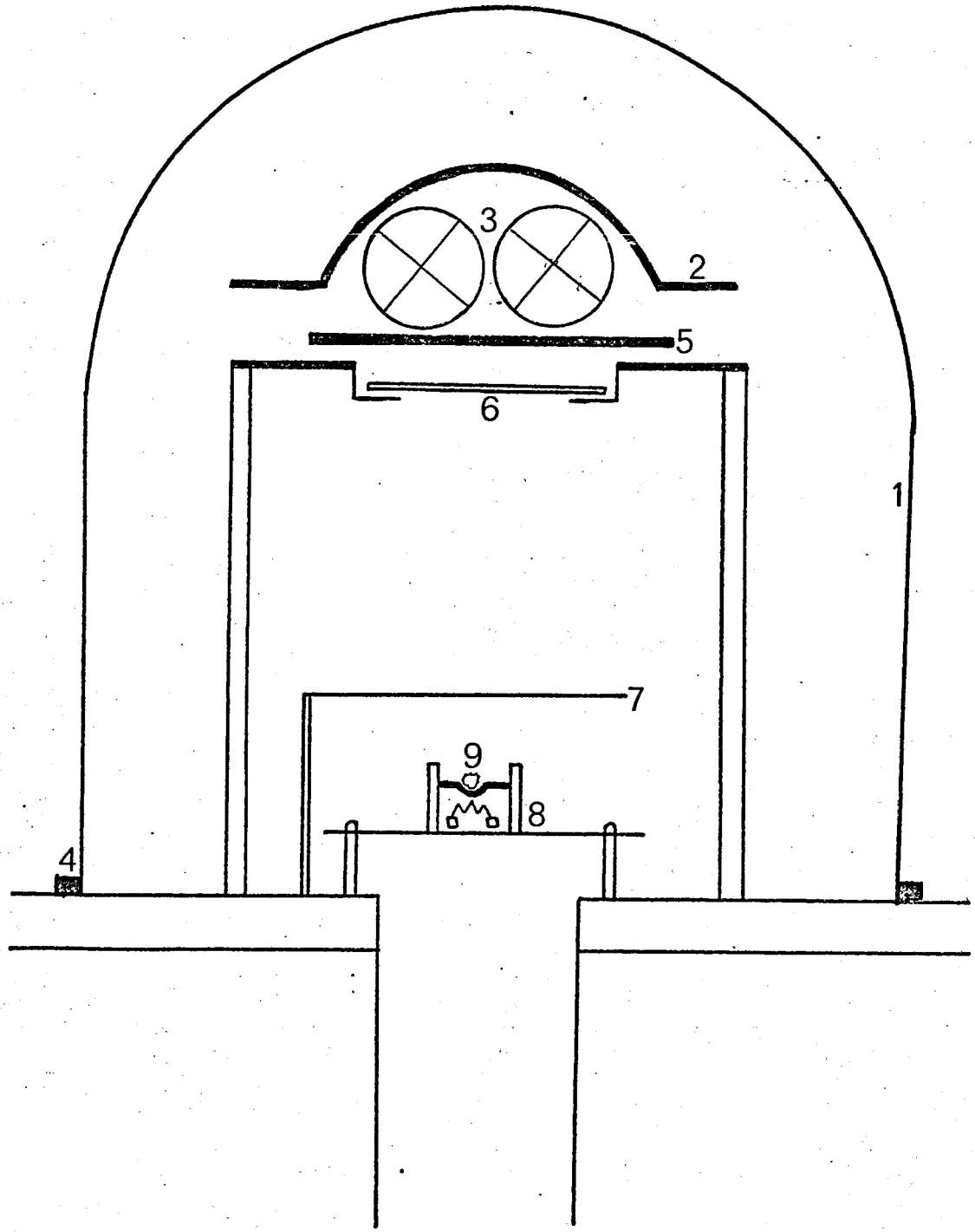

F i g . (2.1)

1. Standard 18" bell jar.
2. Reflector.
3. Quartz iodine lamps.
4. Rubber seal.
5. Stainless steel plate.
6. Substrate.
7. Shutter.
8. Electron gun.
9. Evaporating material.

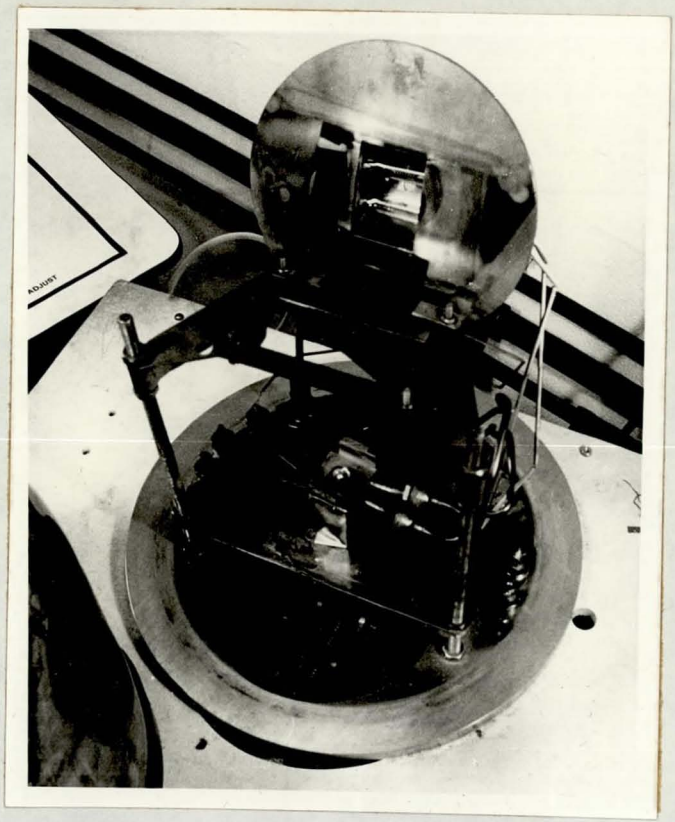

F i g. (2.2)

Evaporation chamber.

F i g. (2.3)

View of the evaporation unit with the power supply.

Substrates temperatures were measured by placing a chromal - alumel thermocouple on the upper surface of the substrate. This introduced a small but unknown error in determining the exact temperatures of the films which were deposited on the lower surface.

The thickness of the films was monitore d by observing their transmission - colour . In this way three sequences , of films were made , with increasing thickness. Each sequence consisting of 6 films.

The thickness,of some of the samples , was measured after evaporation and again after the experimental measurements using a Rank - Taylor - Hobson "Tallystep" , to verify no change of the thickness. But the thickness measurements of most of the films were made after the optical measurments , as will be explained later.

2.1.2 The Electron Beam Source

The electron beam evaporating source which was designed by Varian Associates Ltd. was of the type where the electron beam is bent 270^{o} before reaching the target by a magnetic field perpendicular to the direction of the beam.

The self accelerated type of gun , see Fig. (2.4) , uses the potential both to focus the beam and to accelerate the electrons to full velocity. The target material is contained in a hearth which is made of copper and is water - coole d. During evaporation a frozen layer of evaporated material is deposited across the copper surface , which insures total purity of the evaporant and avoids the highly corrosive characteristics of many elements when they are heated near their vapour temperature.

The power supply gave 5kV and was current limited at 500 mA . This

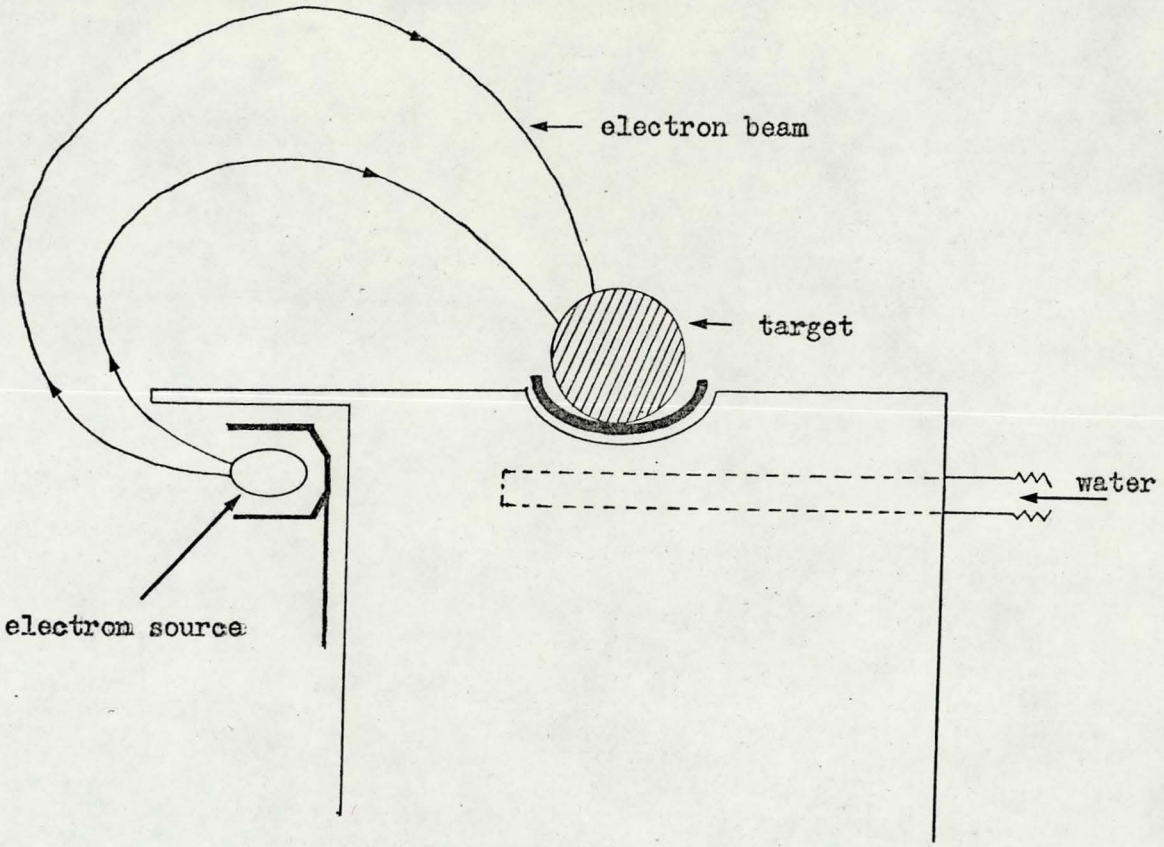

F i g . (2.4)

Beam orientation in the electron gun.

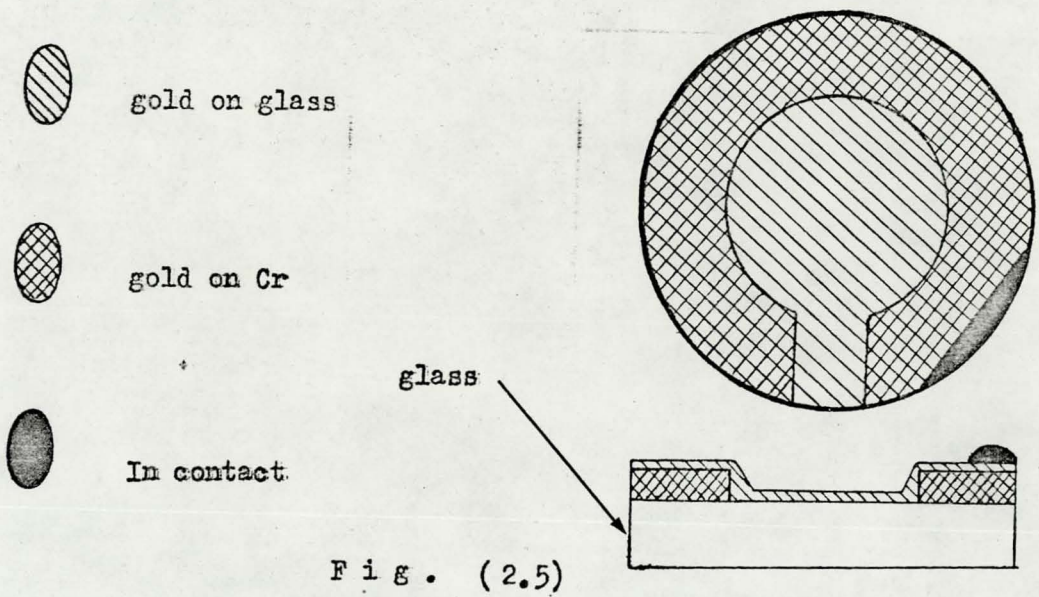

F i g . (2.5)

Sample construction.

gave a total of 2.5 kilowatts output in the beam. The source is capable of evaporating almost any material including refractory metals , and when the problems involved in using an electron gun have been understood , the system becomes a highly efficient evaporating unit ,which is easy to use and requires only nominal maintenance.

2.1.3 The Substrates

The substrates used in this work were 7059 Corning glass slides of 2.0 inch. diameter. They have a typical smoothness of less than 50 Angstroms and a volume resistivity at 500° C of at least 10^{8} ohm - cm.

Substrates were ultrasonically agitated and washed in deionised water and detergent Decon for ten minutes,rinsed three times in deionised water and isopropyl alcohol. When the vacuum chamber was pumped down to 10^{-5} torr , the substrates were de - gassed for fifteen minutes at a temperature 100° higher than the final operating temperature.

2.1.4 Film Fabrication

The deposition sequence was as follows :

1. A thick ring - shaped layer of Chromium deposited rapidly from a carbon crucible at a pressure less than 10^{-5} torr and a temperature 200° C.It had been found that if a film of Chromium is first deposited on the glass by a vacuum evaporation then the gold film which is deposited by vacuum evaporation on the Chromium undercoat is safely bonded on the glass substrate.

   The thick ring - shaped layer had an inner diameter approximately equal to the diameter of the O - rings used to seal the

windows of the electrolytic cell. That layer was necessary because it prevented the outer part of the gold film which was in contact with the O - ring , from destruction.

2. The cyclic piece of tantalum used to give the above ring shape was taken out at this stage.

3. An ultra thin layer of Chromium 3-5 Angstroms thick deposited very rapidly at 200° C and a pressure less than 10^{-5} torr.

4. The crucible with the chromium was taken out of the chamber.

5. A new pump - down followed and the temperature of the substrates was kept for 20 minutes at 200° C.

6. A slow deposition of the gold film followed , when the temperature of the substrate reached 30° C and the pressure 10^{-6} torr. The mean rate of deposition has been estimated at 10Å/ min. The gold was evaporated from a carbon crucible which was warmed up first , to very high temperature to release all the gases contained in it.

7. Annealing of the film was followed for 15 minutes , at 300° C.

8. When the temperature of the substrate was 30° C the chamber was opened and a ohmic contact was made on the surface of the film . After that the film was loaded on the electrolytic cell. Fig.(2.5) gives an idea of the materials distribution on the glass substrate. The same procedure was used for making all samples so that conditions would be as near as possible the same for each sample.

2.2 The Electrolytic Cell

The electrolytic cell is made of perspex and all electrodes are held in

position by neoprene O-ring seals. The electrolyte was a 0.1 molar solution of sodium sulphate in triple - distilled deionised water . The working - electrode was the film of gold of approximately 500mm^2 area , which had been made according to the described procedure.

Fig. (2.7) contains a cross section and Fig. (2.8) a photograph of the electrolytic cell and the whole optical system.

Electrical contact was made to the gold film by an indium soldered joint , which was not in contact with the electrolyte.

The counter - electrode was formed from a piece of platinum gauge of very high specific surface , with a total area of probably more than 100 cm^2 . Platinum electrodes are generally used in electrochemical work of this kind. The high surface area is required because a double layer structure also exists at the surface of this electrode, and the capacitance of this layer should be made large in comparison to that of the electrode to be studied.

A third electrode had also been included in the cell during the first ER measurements. This was a saturated calomel reference electrode , (SCE). Single electrode potentials can be measured if it is ensured that the third electrode maintains a constant potential during observation. The calomel electrode may be used only in conjunction with a high impedance electrometer to measure potentials and must not be allowed to take a current of more than 10^{-9} Amps.

There were two windows on the electrolytic cell , one on the front and one on the back. The thin gold film was evaporated on the inner - surface of the front window and a glass substrate consisted the back window. The counter - electrode had a cyclic cross - section so the light - beam was able to pass through the electrolytic cell for

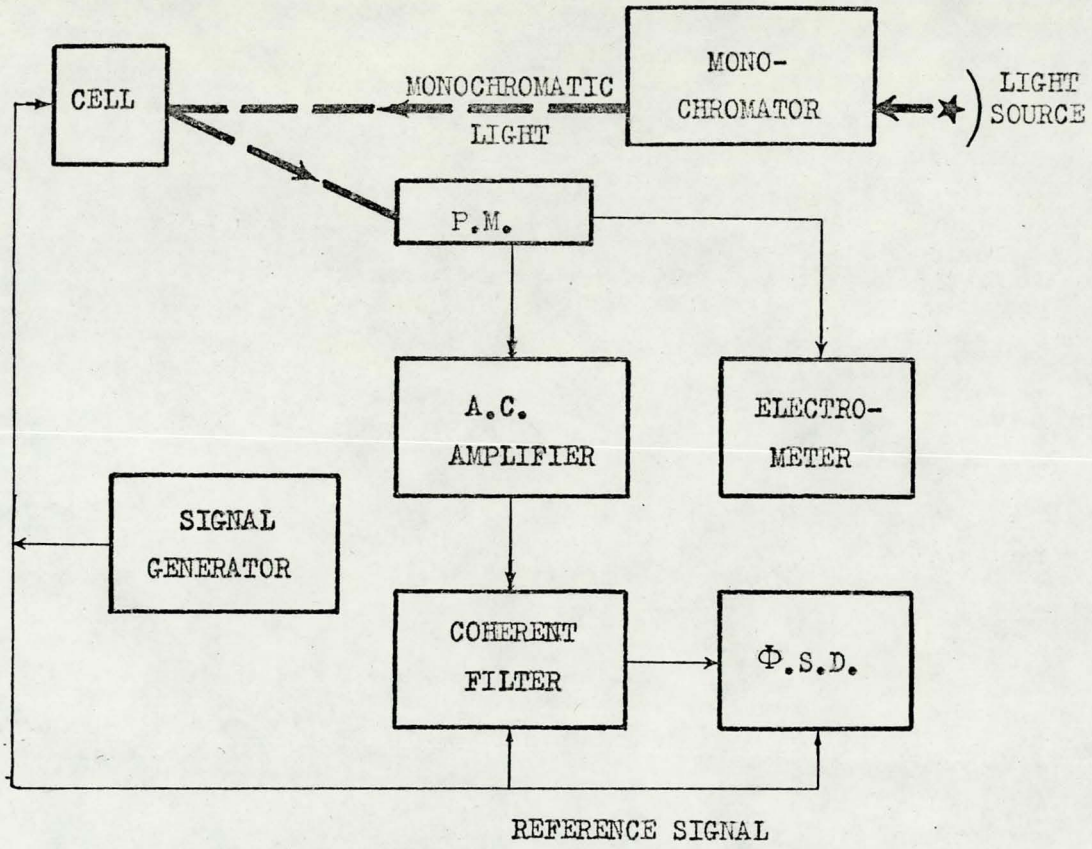

Fig. (2.6)

Schematic diagram of the optical and detection system.

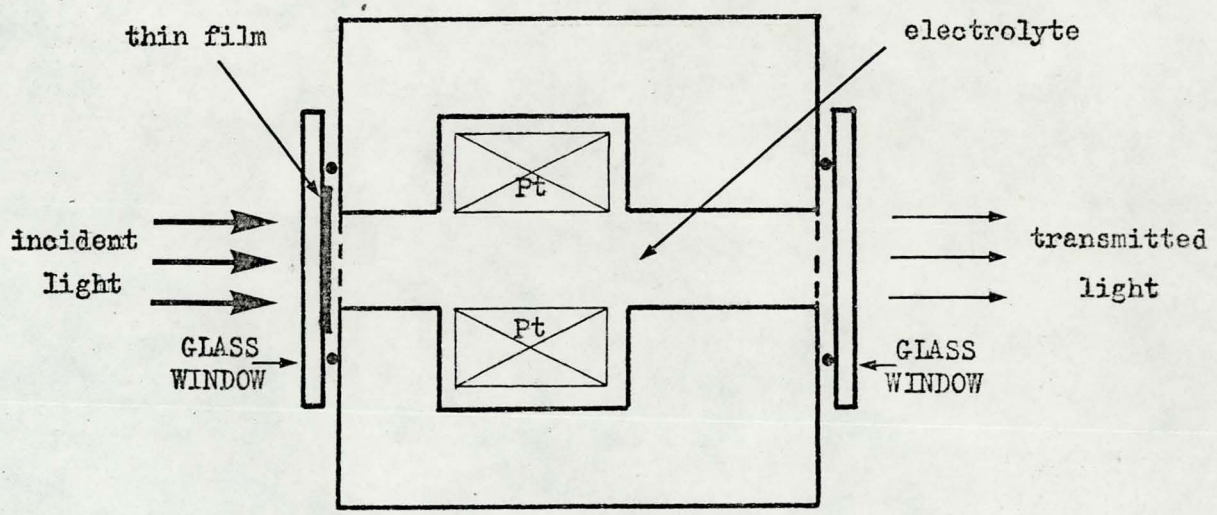

Fig. (2.7)

Cross - section of the electrolytic cell.

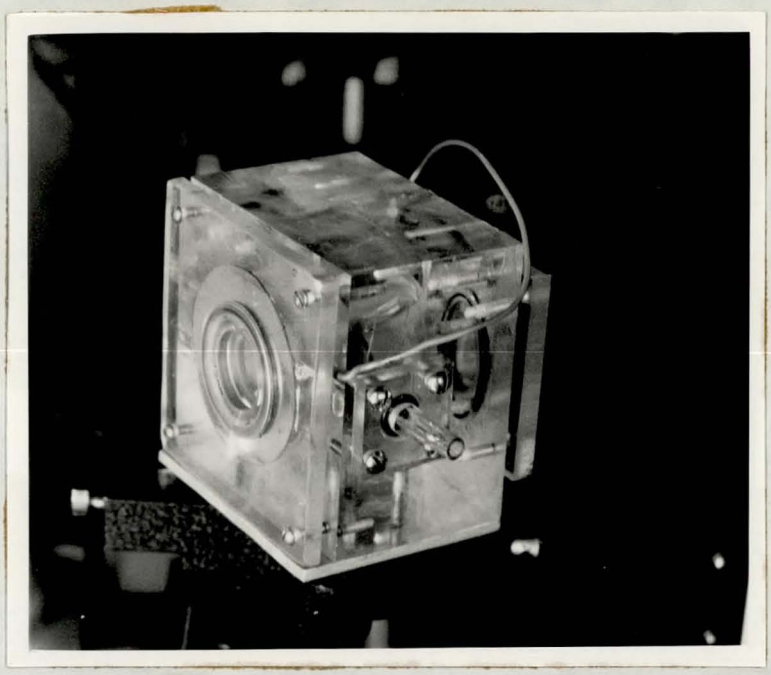

a) The electrolytic cell.

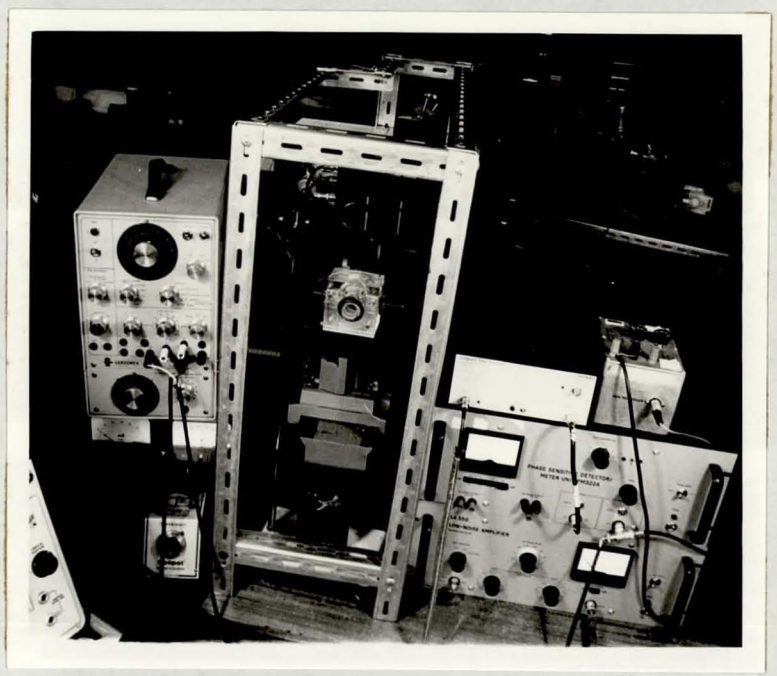

b) The electrolytic cell and part of the apparatus.

F i g. (2.8)

transmittance and electrotransmittance measurements.

Absorption , because of the electrolyte , accounted for a mean value of 2-3 % reduction of the intensity of the light beam. The transmittance spectrum of the electrolyte with the two windows was approximately flat over the working spectral region of the used optical system. Therefore no corrections were required for the transmittance and electrotransmittance measurements.

The total capacitance C_T of the cell may be written

$$\frac{1}{C_T} = \frac{1}{C_S} + \frac{1}{C_G}$$

where C_S and C_G are the capacitances due to double layer at the gold thin film and counter electrode respectively. C_G is much greater than C_S because of the large specific area of the gauge and its effect on the total capacitance may therefore be neglected.

The differential capacity of the cell C_T was measured at the beginning using a Marconi bridge. This unit has facilities which enable the oscillator frequency to be externally controlled , and a bias control to allow a standing voltage to be applied across the electrodes while measuring the capacitance.

Better results were achieved finally using a special system which shall be described next.

2.2.1 Capacitance Measurements

The electronic system /33/ which is represented in Fig. (2.9) was

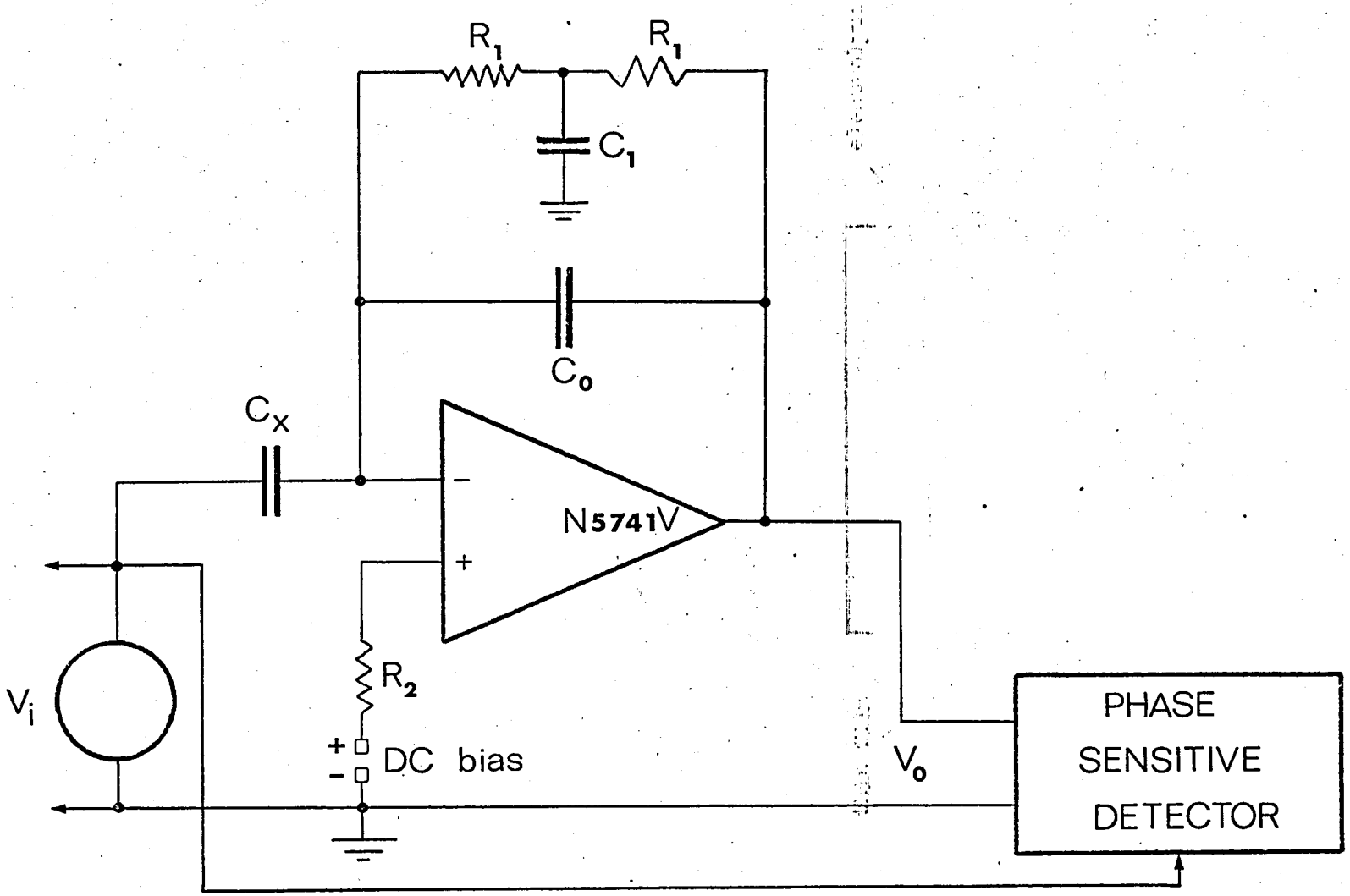

F i g. (2.9)

Circuit for capacitance measurements, (D.C. bias = 0V for the cell).

finally used for the capacitance measurements of the electrolytic cell and the Schottky diode.

The operational amplifier eliminates stray admittances and makes the capacitance reading independent of the frequency. The network R_1, C_1, R_1, provides D.C. negative feedback but negligible A.C. feedback at the measuring frequency provided that C_1 is sufficiently large.

Therefore the unknown capacity was calculated from the following formula

$$C_X = \frac{V_o}{V_i} C_o$$

A standard capacity was used for C_o. V_i was measured with an electronic volt-meter and V_o was read on the output of the phase sensitive detector. The value of C_o is usually adjusted to be approximately the same as the largest expected value of C_X. In the case of the capacitance measurements of the electrolytic cell the value of C_o was elected to be 100×10^{-6} F because it was found from the literature that the double layer differential capacitance measured with a mercury - electrode for different solvents does not exceed the value of 100×10^{-6} F, /38/.

Fig. (2.10) shows the variation of the capacity with the frequency in the frequency region 10 - 100 Hz. The capacity remains approximately constant in this frequency region. The value of 14 Hz was elected for the modulation frequency, because this was the frequency which gave the larger ER signal during the preliminary measurements.

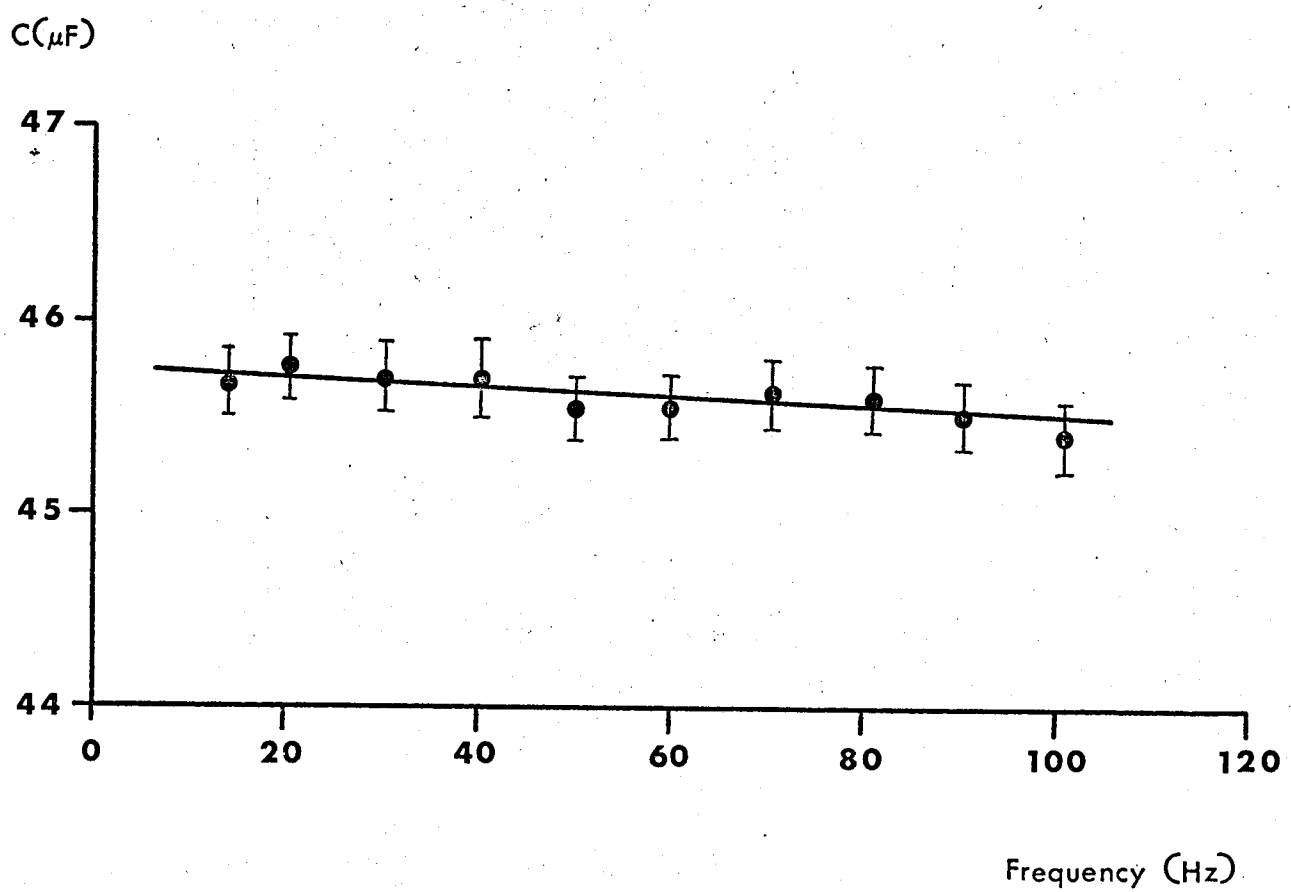

F i g. (2.10)

The capacitance of the electrolytic cell as a function of frequency.

It can be seen from Fig. (2.10) that the value of the capacity of the electrolytic cell is less at 100 Hz than at 14 Hz. This combined with the previous observation helps us to say that the value of the ER effect depends upon the double layer capacitance.

The capacitance of the electrolytic cell was measured with each film individually and the same approximately straight line was found representing the capacity as a function of frequency.

The volume of the used electrolytic - solution was 20 mlt. approximately. The distance between the two windows was about 2 inches long, which means that the light absorption , in the used spectral region , is very low.

Care was taken , not to create any stress on the film when the front window with the thin gold film was mounted on the cell.

The used electrolytic cell was gas - tight i.e. the concentration of the diluted gases in the electrolyte remained constant after the cell was sealed hermetically with the use of O - rings.

The temperature of the gold - electrode and the electrolyte was approximately 25^{o} C.

2.2.2 Purification of the Solution

The purification procedure was undergone each time the gold electrode was changed. The cell was connected to a special pump so the solution was able to circulate through a chemically purified charcoal-column for at least 40 hours.

The large purification time and high purity of the used solvants

was thought to guarantee the absence of adsorbable ions , in the solution.

It was necessary to keep all the electrochemical conditions the same and therefore to have only a simple capacitance effect at the gold-electrolyte interface in order to study changes in ER spectrum due to changes of film parameters.

The platinum gauge was purified once with H_2SO_4 and HNO_3 . It was cleaned in a stream of triple - distilled water and dried into an oven at about 300° C , for 5 hours.

As has been indicated in chapter 1 , the purification of the electrolyte is of great importance in the case of double layer studies and for studing effect related with the double layer capacitance. Even traces of adsorbable species , existing in the solution , will change the structure of the double layer and they will affect all the phenomena related to it.

2.3 Optical System

A projector lamp (12 V - 100 W) was used as light source. The light was focused on the entry slit of a HILGER & WATTS D330 Single Grating Monochromator. The monochromatic light coming out of the exit slit of the monochromator was focused again , with ordinary glass lenses onto the sample , which was on the front window of the electrolytic cell , at nearly normal incidence. The reflected monochromatic light felt on the cathode of a photomultiplier.

A stabilised power supply was used for the light source to give a steady light intensity.

The grating which was used in the monochromator had a grating ruling of 1,200 L/mm covering a wavelength range between 0.3 μ m –1.0 μm.

However the spectral region of the described optical system was limited , between 1.1 eV and 3.5 eV , because of the use of ordinary glass lenses.

The monochromator was calibrated , before any other measurement , with the aid of a Hg - source and a pen recorder. A pen recorder marker unit had been built up for this purpose and a contact was mounted into the mechanism which rotates the grating in the monochromator.

All the mentioned elements were mounted on a heavy optical bench which was electrically grounded.

The whole system was covered by a special black cloth supported on a metalic frame. So the electrolytic cell and the photomultiplier were always into dark. This was necessary for the photomultiplier because the room light increased dangerously the dark current. For better results the whole room was always in the dark.

2.4 The Detection System

One of the greatest problems was the detection of the ER signal , because it was superimposed on the top of a large D.C. signal. The problem was solved with the use of a photomultiplier , as optical transducer , which was not saturated because of the existence of the large background.

A photodiode was used at the begining without any success. A better detector was necessary because the output signal was very low and noisy.

The use of an E.M.I. 9524B photomultiplier was decidedon after that. But again its limited spectral region did not permit adequate measurements.

Finally the 9558B photomultiplierwas used with satisfactory results. The 9558B photomultiplier has a S – 20 photocathode and 11 venetian blind dynodes having CsSb secondary surfaces.

A special magnet was mounted near the photocathode of the 9558 B photomultiplier to reduce the dark current and a photomultiplier housing was made , for safety and to support the magne t. The permanent ring magnet assembly mounted against the end window of the photomultiplier tube changes the position of the effective photocathode. In other words the axial lines of the force deflect the electrons from unused cathode areas away from the dynode system so that they are not multiplied . Consequently a reduction in anode dark current of at least an order of magnitude is feasible by this method according to E.M.I.'s specifi-cations.

Special care was given to design the photomultiplier dynode chain , because one of the basic requirements was the ability to measure high light intensities. The current through the dynode chain was at least ten times the anode current so the dynode voltages remained the same. The per missible maximum mean current of the used photo-multiplier was 1 mA . The maximum used currents were less than 0.5 mA .

Fig. (2.6) is a diagramatic representation of the detection system. The D.C. output of the photomultiplier was connected to a Keithley high impedance electrometer to give the magnitude of the background

signal i.e. the D.C. reflectance. The A.C. output was connected to the input of an A.C. amplifier. The amplified A.C. signal i.e. the R signal was fed into the input of a phase sensitive detector through a coherent filter. The use of a coherent filter as an intermediate stage ,between amplifier and phase sensitive detector was absolutely necessary. Because the very low signal due to the modulation of the reflectivity of the gold - electrode was buried in noise .

Shot noise and Johnson noise were present on the output of the photomultiplier.

The Shot noise was due to the fluctuations in the rate of emission of electrons from the cathode.

Owing to the low values of the anode current of the photomultiplier met in practice ,it is necessary to use high values of load resistance which introduces an additional source of noise, due to the thermal fluctuations of charge density along the resistor. This is so-called Johnson noise.

The phase sensitive detector operates on the p rinciple that the in - coming signal is full wave rectified at the frequency of the reference signal, and all input signals except these having components at the reference signal are averaged to zero , the rest are full wave rectified and appear as a D.C. voltage propotional to the R.M.S. voltage of the buried signal. In this way the magnitude of repetitive signals which are buried in noise may be measured.

The Coherent Filter is a narrow - band filter. Its centre frequency is established by an external reference waveform which gives the ability to follow a frequency - unstable signal. It normally uses

the same reference as the P.S.D. Its narrow bandwidth and wide dynamic range (100 dB) enable the P.S.D. to penetrate over 100 dB below the noise level.

The Coherent Filter was Brookdeal model 467 , the P.S.D. Brookdeal model PM 322A and the A.C. Amplifier a Brookdeal model LA 350.

A Servomex 600 ohms output signal generator was used. The constant voltage output was used to give , through a 180^{o} phase shifter , the reference signal and the variable voltage output gave the modulating voltage for the electrolytic cell. The phase shifter was used because the two outputs of the generator were not in phase.

2.5 ER Measurements

The D.C. reflectivity and its induced change due to the modulating field , was measured for 54 wavelengths in the spectral region 1.5 - 3.1 eV . The value of ΔR was followed by the corresponding gain in dB. The data was processed by computer.

The light intensity remained constant during each experiment ; the light source was switched - on one hour before each experiment to help stabilise the system.

A light - chopper was used , at the beginning, for the measurement of the reflectivity of the gold films. But there was need to remove it from the light path each time the induced change in reflectivity was measured . A large error was involved , in this way , in the value of the ER because the position of the chopper was changed slightly after every replacement.

The removal of the light chopper during the measurment of ΔR was

necessary , because it was found that the chopping of the light beam introduced noise in ΔR signal even when the chopping - frequency was entirely different from the modulation frequency , used for the electrolytic cell.

Hence the use of a high - impedance voltmeter was decided for the measurements of R . The same technique , for the measurement of R, has been recently used by McIntyre.

It was found that the direct measurement of R , connecting an electrometer on the output load of the photomultiplier circuit eliminates a large number of possible experimental errors.

The ER effect in gold thin films was studied as a function of the film thickness. It was found that the ER spectrum was shifted to lower photon - energies as the thickness of the thin film was decreased.

Unsuccessful attemps were made to measure the ER spectrum of thin gold films , prepared according to the previously described conditions ,and having thickness less than 70 Angstroms. For film - thicknesses of about 70 Angstroms a very noisy and not reproducible signal was detected. For films thinner than 70 Angstroms it was impossible to measure any ER signal at the spectral region of the plasma edge , with the available detection - system.

A different deposition technique was tried , to examine the effect of the deposition conditions on the ER spectrum of thin gold films. The deposition was taking place when the substrate temperature was about 200^{o} C and not at 30^{o} C as previously. The films , which were obtained in this way had a bluish color in transmitted light.

This is because such small amounts of gold per unit area deposit as discontinuous "islands" rather than a continuous film /34/,/35/.

The films which had been prepared in this way did not exhibit any ER effect.

Thin gold films evaporated directly onto clean glass had a green colour in transmitted light. The ER spectra obtained from these films did not exhibit any differense from the ER specra of the films which had been deposited notdirectly onto glass but onto an Chromium undercoat about 5 Angstroms thick. This proves that the chromium undercoat does not affect the reflectivity and ER spectra.

It must be noticed that it has been reported by several authors /34/, /35/, /36/ that deposition of gold onto clean glass , with the object of making a thin film about 200 Angstroms thick results in a discontinuous film of very high resistance.

2.6 Reflectivity Measurements

The absolute reflectivity of each sample has been measured according to a simple technique.

A microscope slide was placed in a proper position between the monochromator and the film , so that a part of that light which was incident on the film was split directly on to the cathode of the photomultiplier. The rest of the beam , transmitted through the splitter , was reflected on the surface of the gold film and directioned onto the cathod of the same photomultiplier as in Fig. (2.11).

Two measurements were taken for each wavelength. One , X_{Au} , corresponding to the sum of the reflected light intensities from both film and splitter and a second one , Y_{Au} , corresponding to the light

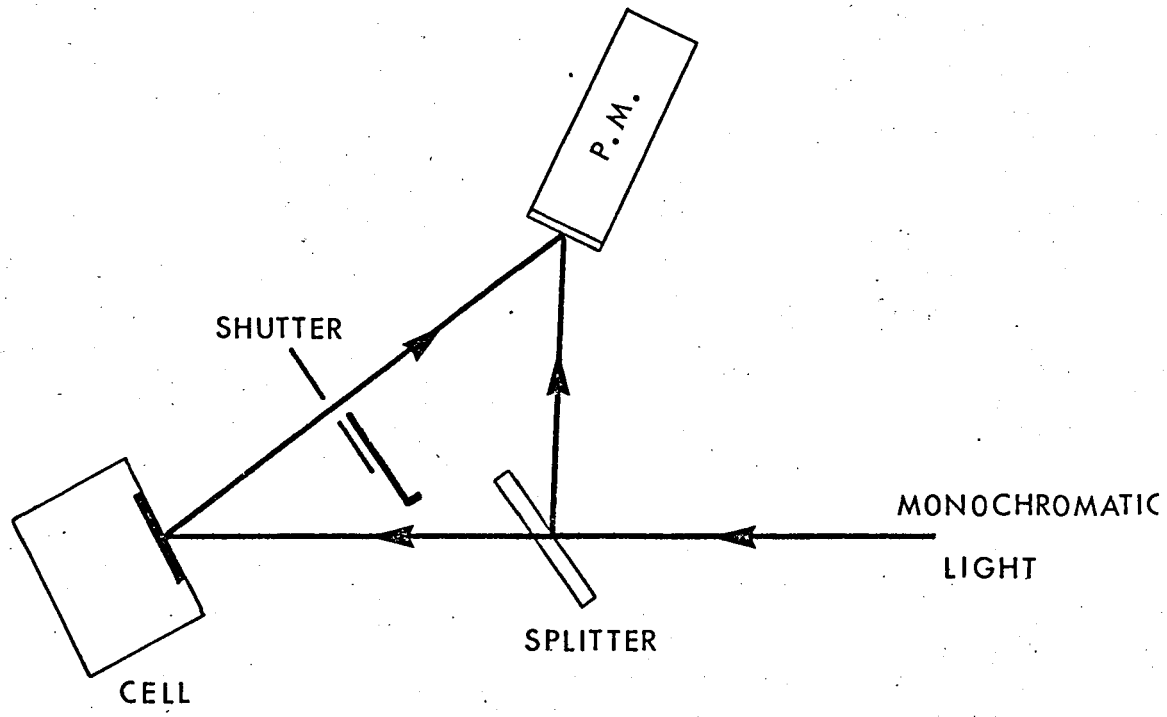

Fig. (2.11)

Experimental arrangement for the measurement of the reflectivity of gold films.

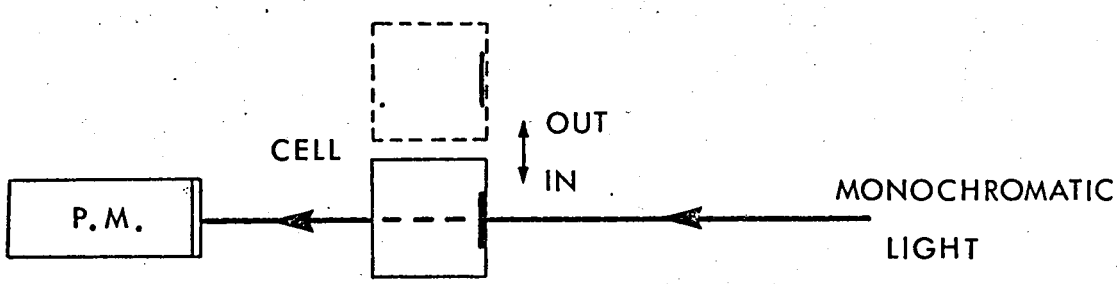

Fig. (2.12)

Experimental arrangement for the measurement of the transmittivity of gold films.

intensity reflected from the beam splitter.

So , in the case of a gold film

$$X_{Au} = aI + (1 - a)\cdot I R_{Au} \qquad (2.1)$$

$$Y_{Au} = aI \qquad (2.2)$$

where I is the intensity of the original light beam , aI the part of the light intensity which is reflected from the splitter and R_{Au} the reflectivity of the gold film i.e. the ratio of the reflected and incident light on the film.

The system of Eqs. (2.1) and (2.2) contains three unknown quantities , I , a , and R_{Au}. Therefore more relations must be found. The same procedure was employed for an aluminium mirror placed on the front of the electrolytic cell. One more relation can be written for aluminium.

$$X_{Al} = aI + (1 - a)\, I\, R_{Al} \qquad (2.3)$$

where the reflectivity of aluminium , R_{Al} , has been taken from the literature /32/ and X_{Al} is a measurable quantity. From Eqs. (2.1), (2.2) and (2.3) the reflectivity of a gold film can be calculated using the following formula

$$R_{Au} = \frac{X_{Au} - Y_{Au}}{X_{Al} - Y_{Au}} \cdot R_{Al} \qquad (2.4)$$

Computer calculations of R_{Au} gave adequate plots of the reflectivity

spectrum for each sample.

This technique gave quite good and accurate results, in the working range of the optical system.

It must be noticed that the dark current was negligible, because of all the precautions which had been taken for this purpose and mainly because of the use of the special shaped magnet on the top of the photomultiplier tube. Consequently there was no reason to take it into account, in the reflectivity calculations.

2.7 Electro - transmittance Measurements

Electrotransmittance measurements of thin gold films were taken, to help the interpretation of the ER data. The term Electrotransmittance (ET) is used here to describe the normalized induced change of the energy transmittance of a thin film, i.e. $\Delta T/T$. Where ΔT is the induced change and T the transmittance.

The electrolytic cell was placed between the monochromator and the photomultiplier. So, the light beam was falling onto the cathode of the photomultiplier after passing through the electrolytic cell. Care was taken to adjust the optical axis of the electrolytic cell to coincide with the light beam, Fig.(2.12).

The resolution of the monochromator was decreased during the ET measurements because the width of the front - slit of the monochromator was larger than in the case of ER measurements. This was necessary because the only available light - source was of low energy.

The electrolyte with the glass windows exhibited

an almost flat absorption spectrum over the entire spectral working region and the absorption was about 3 % . But the addition of a thin gold film on the front window increased the total absorption to about 60 % - 80 % , depending upon the thickness of the film and the wavelength of the incident light.

This introduced an error in the wavelength calculations. Although an error was involved in the determination of each wavelength ,comparative studies of ET or transmittance spectra for films with different thicknesses , eliminate the errors. This is due to the fact that the photon - energy axes of the spectra of the samples contain the same error at the corresponding wavelengths.

A Keithley electrometer was used for the measurement of the D.C. transmittivity and phase sensitive technique for the measurement of the ET.

2.8 Transmittance

The transmission spectrum of each of the samples was measured in conjunction with the ET measurements.

The adopted technique for the measurement of the transmittance spectrum was very simple but the obtained experimental transmission spectra were quite adequate. The ratio of the D.C. transmission with the light beam passing through the electrolytic cell to the D.C. transmission with the electrolytic cell removed from the way of the light beam , was plotted against photon energy.

A large number of experimental errors were eliminated by taking all the measurements in each wavelength with the electrolytic - cell in

and afterwards with the cell out of the way of the light beam. Fig. (2.12) shows the experimental arangement for the measurement of the transmittance spectra of the thin films.

The transmission spectra obtained for different films are shown in the same diagrams with the ET experimental results , for comparison purposes.

For gold films thicker than 300 Angstroms the measurement of the transmittance was quite difficult. The difficulty was due to the fact that the intensity of the monochromatic light should be very low otherwise the photomultiplier would be destroyed. Hence in the case of transmittance measurements the accuracy in the measurement of each wavelength was the same as in the case of electroreflectance measurements.

For films thinner than 300 Angstroms the above described technique was very satisfactory because it gave adequate results very fast and nothing special was needed.

Care was taken that when the cell was placed in the way of the light beam , all of the light was passed through the electrolytic cell. This was achieved by adjusting the position of the cell so that the maximum signal was taken at a certain wavelength. The diameter of the light beam was less than the diameter of the window of the cell at the point where the electrolytic cell was placed.

Consequently the reduction of the light intensity , when the beam was passed through the cell , was due solely to the absorption of the gold film and the electrolyte. The absorption due to the electrolyte was ignored because it was almost unique over the spectral region of the plasma edge of gold and also because it was 2% - 3% only.

2.9 Electrochemical Behavior of the Electrolytic Cell

Water can be reduced and oxidized electrolytically with the evolution of hydrogen and oxygen , respectively. When the electrode potential is made more cathodic than the equilibrium value , which is determined by the Nerst equation /37/, the evolution of hydrogen is thermodynamically possible. Conversely , hydrogen is oxidized , if it is present on the electrode , when the potential is made less cathodic than the equilibrium potential.

The same considerations are applicable to the equilibrium of oxygen - water.

Actually , the oxidation of water to oxygen generally requires an appreciable overvoltage , and the potential may be raised above +1.2V without causing any evolution of oxygen. The magnitude of the overvoltage greatly varies from one metal to another. Likewise , the evolution of hydrogen may involve relatively large overvoltages , and the area of actual stability of water extends more or less below - 0.8 V when the pH of the electrolyte is 7 as it was in our case.

When no reduction or oxidation occurs at the gold electrode , the currents observed with a continuously changing potential are solely due to the charging or discharging of the double layer capacity . Capacity currents are proportional to the differential capacity defined by dQ/dE. Where dQ is the change of the double layer charges when the potential difference between metal and electrolyte changes by dE. Consequently double layer phenomena can be studied in this way.

Current - voltage curves were taken for each sample individually ,

using a voltage wave having the shape of an isosceles triangle . Fig. (2.13) shows a typical current - voltage curve for a thin film of gold. The same curve exactly was repeated every 500 sec. The low currents during the anodic and cathodic sweep indicate the charging of the double layer capacitance.

An interesting experiment which verifies the fact that the differential double layer capacity remains approximately constant with the applied voltage , was the measurement of the charge of the double layer capacitance as a function of the applied voltage.

Fig. (2.14) shows the circuit with which the experiment was performed. A 600 ohms Helipot was used as potentiometer and a Keithley Electrometer was used to measure the charges.

The electrolytic cell capacity was charged at the desired voltage with the switch of the electrometer on the resistance range. So a resistance of 1000 ohms was involved in the charging circuit. When the voltage reached the desired value , the switch of the electrometer was turned to the coulomb range and the charge was measured as soon as possible , because the reading varied with the time.

The results obtained in this way , have been plotted in Fig. (2.15). It can be seen from this graph that the rate of the charge in the double layer capacitance with voltage remains approximately constant between -1 V and + 1V. In other words the double layer capacitance remains constant in that voltage region , since the capacitance is determined by the slope of the Q - V curve. A value of 10×10^{-6} F has been calculated from the slope of that curve. This value is four times less than the measured one , according to the paragraph 2.2.1.

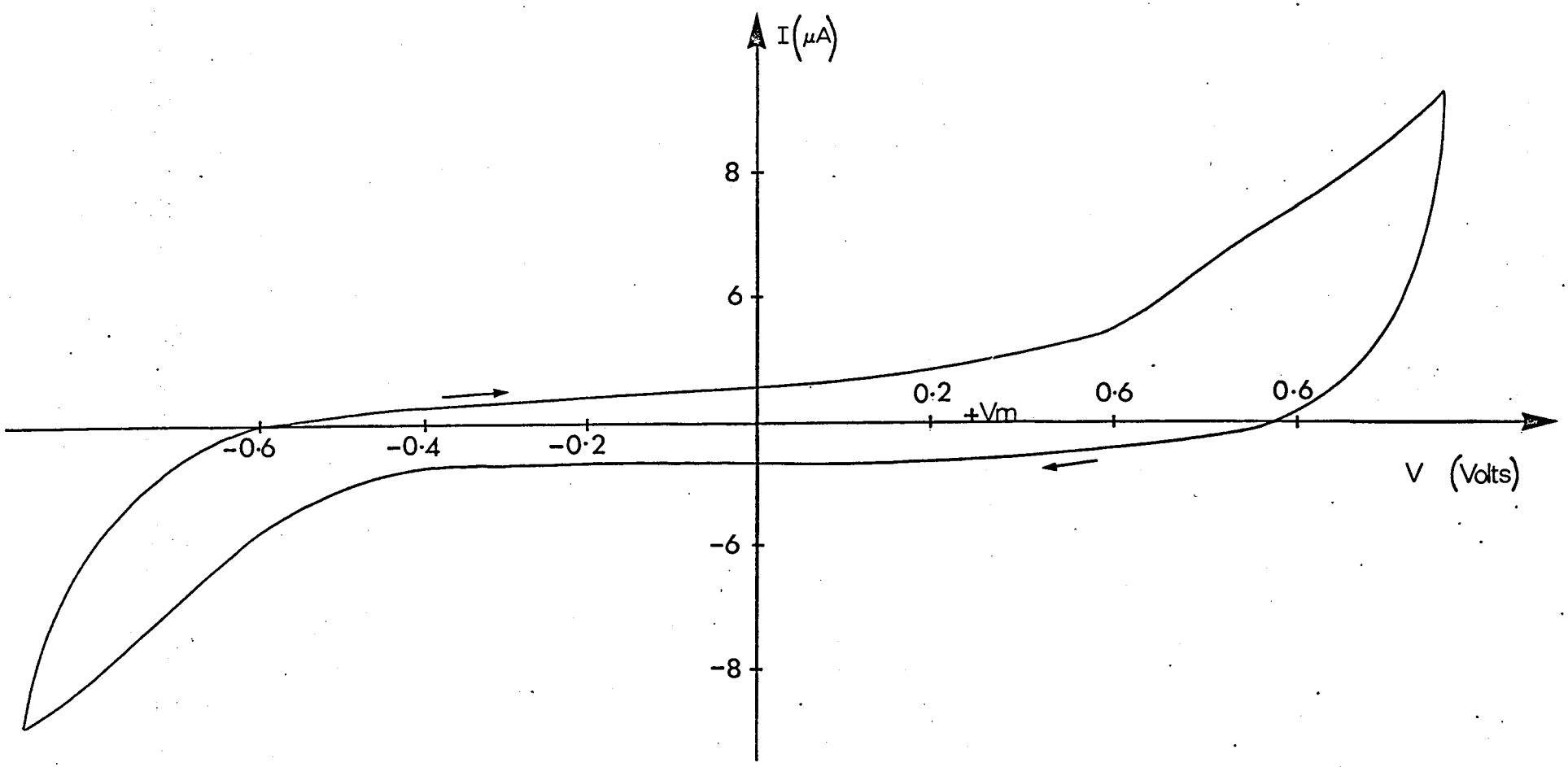

F i g. (2.13)

Electrochemical behavior of the electrolytic cell.

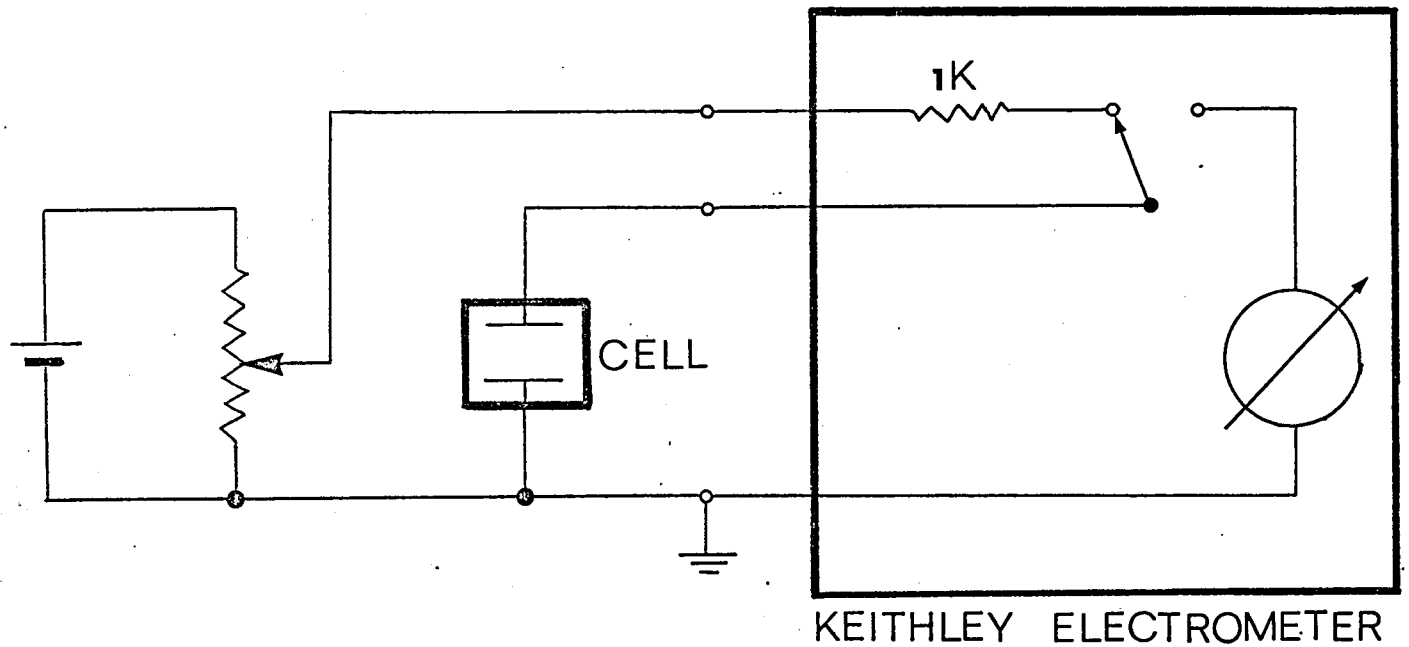

F i g. (2.14)

Circuit for the measurement of the charge of the electrolytic cell capacity.

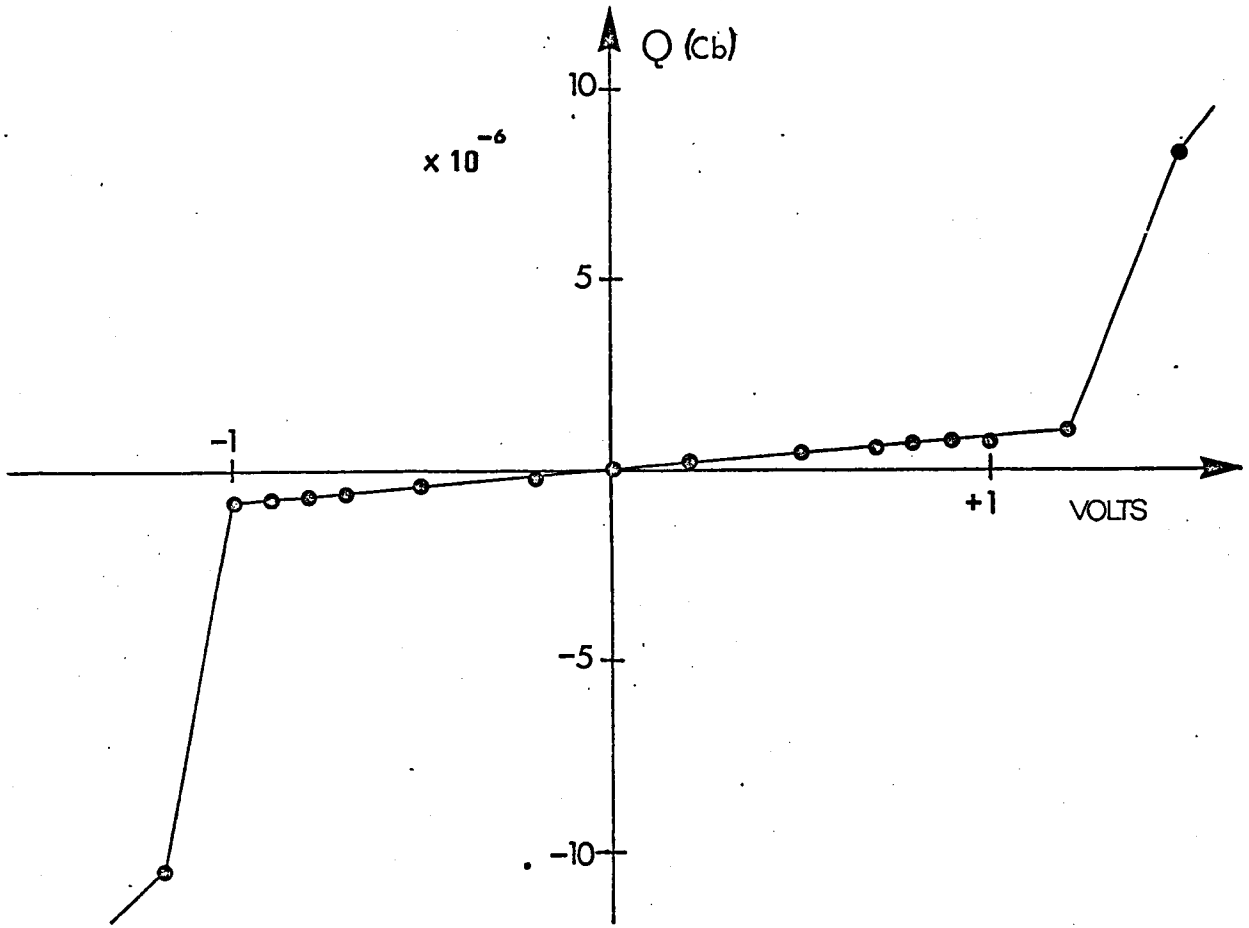

F i g. (2.15)

The charge of the capacitance of the electrolytic cell as a function of the applied voltage.

This discrepancy can be explained in terms of the fact that a large error was involved in the measured values of Q.

This simple experiment is of great importance because it determines the values of the voltages between which the value of the modulation voltage must be chosen when only capacitance - effects are desired, to accounty for the ER effect of the gold electrodes.

Also it shows that the double layer capacitance remains approximately constant between these limits.

2.10 Schottky Diode

Attempts made to measure the ER effect in very thin films , with a thickness of about 70 Angstroms , using the electrolytic technique, were unsuccessful. The signals were very low and very noisy.

A gold - silicon Schottky Diode was employed and better results were achieved. The Schottky Diode was placed on the position of the electrolytic cell so that the monochromatic light felt on the active area of the Schottky Diode and was then reflected onto the cathode of the photomultiplier.

The ER effect was measured for different reverse biasing voltages and for different values of modulating voltage , in the spectral region 1.5 eV to 3.0 eV . The signal due to the modulation of the reflectivity was small and noisy , a fact which introduced a large experimental error in the estimation of its magnitude at each wavelength.

The capacitance of the Schottky Diode was measured using the circuit of Fig. (2.9), as in the case of the electrolytic cell. The only

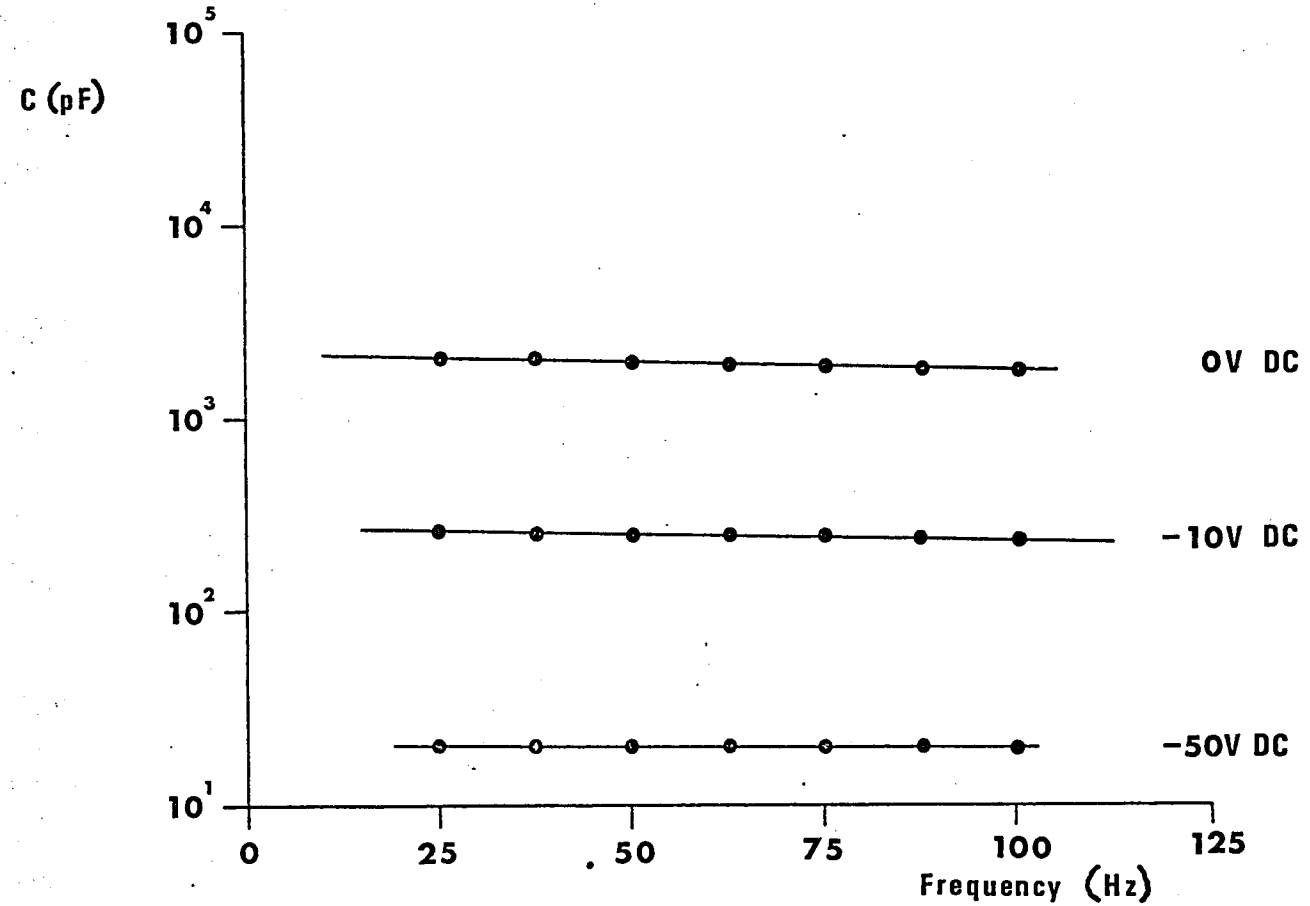

F i g. (2.16)

Schottky Diode capacity as a function of frequency and D.C. bias.

differences were that the value of C_o was changed to C_o = 2000 pF and a D.C. bias was used. Fig. (2.16) shows the variation of the capacitance with the applied D.C. bias and frequency.

It must be noticed that when the D.C. biasing voltage exceeded a value of about -10 V , the signal due to the modulation of the reflectivity decreased and it was very difficult to measure with the available detection system.

2.11 Thickness Measurements

The thickness of the thin gold films used were then measured using a Rank - Taylor - Hobson "Tallystep".

All the used samples were ultrasonically agitated and washed in deionised water so the remained solvent on the surface of the films was removed. Scratches were made on the surface of each film and the measurement of the depth of the scratches was tried at different positions on the surface of the film , to find an average thickness for each film.

A problem arose at this stage due to the fact that gold is a "soft" metal. The problem was solved by covering the scratched films with thin layer of silicon monoxide. The silicon monoxide was deposited on the gold films by evaporation of silicon monoxide from a carbon crucible , using the evaporation apparatus which has been already described.

The evaporation of silicon monoxide was very difficult and a minimum time of 30 minutes was necessary for the deposition of a silicon

F i g. (2.17)

"Talystep" trace.

monoxide film , about 20 - 30 Angstroms thick.

The thickness of each gold film was measured for three different positions. The three values were approximatelly the same.

A maximum relative error of $\pm$ 10% has been achieved for the estimation of the magnified depths of the scratches and will be assumed for all the values of thickness quoted.

Fig. (2.17) contains a typical trace from "Talystep". A line through the valleys has been taken as representing the true surface and gave a thickness of 500 Angstroms. The local spikes may represent dirt and droplets of silicon monoxide , on the surface of the gold film.

CHAPTER 3 - EXPERIMENTAL RESULTS

3.1 Reflectance and Electroreflectance

The experimental results of the measurements for the reflectance and ER of thin gold films taken according to the described techniques were plotted in the same graphs for comparison purposes. Figs . (3.1) , (3.2) , (3.3) and (3.4) contain the ER and reflectance spectra of four gold films with thicknesses 100 , 350 , 160 and 400 Angstroms respectively.

What can be easily seen is that the peaks of the ER spectra occur in the spectral region of the plasma edge of the gold films. Also it is obvious that the magnitude of the peaks of the ER spectra decreses with increasing thickness. It must be noticed that Internal Reflection Spectroscopy was used.

A more careful observation of the ER spectra will lead to the conclusion that the thickness affects the position of the peak of the ER spectrum. Fig. (3.5) contains the ER spectra of three gold films different only in thickness. It is obvious that the peak of the ER spectrum shifts to lower energies as the thickness decreases. The order of magnitude of each peak in Fig. (3.5) is as follows : for 190 Angstroms 2×10^{-4}, for 320 Angstroms 8.8×10^{-5} and for 420 Angstroms 2.9×10^{-5}. The three curves have been drawn in that way for demonstration purposes.

The corresponding plasma edges have been plotted in the same graph. Fig. (3.6) shows that the plasma edge of the gold films shifts to lower energies as the thickness of the films decreases.

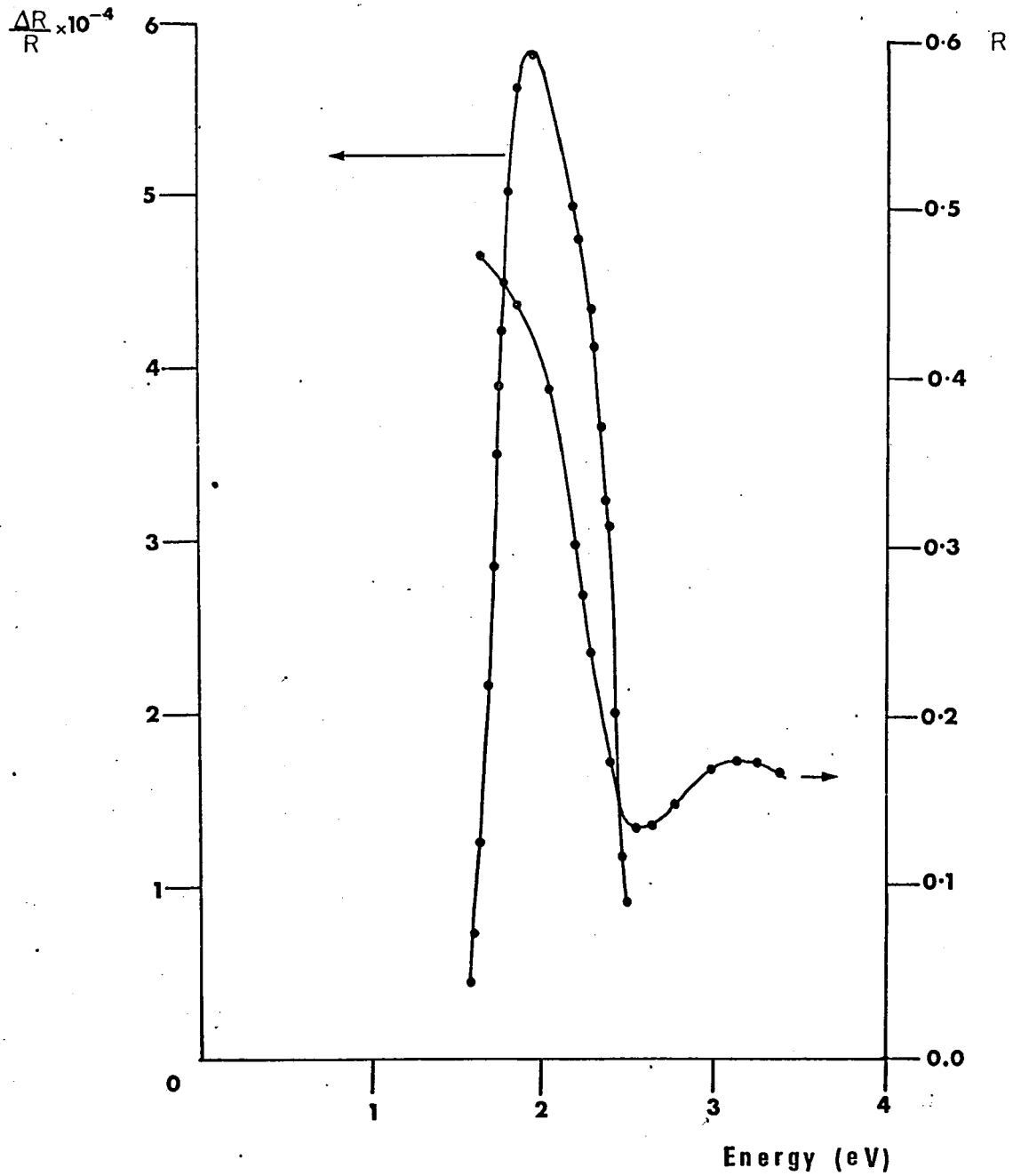

Fig. (3.1)

Reflectance and ER spectrum for a gold film 100 Å thick.

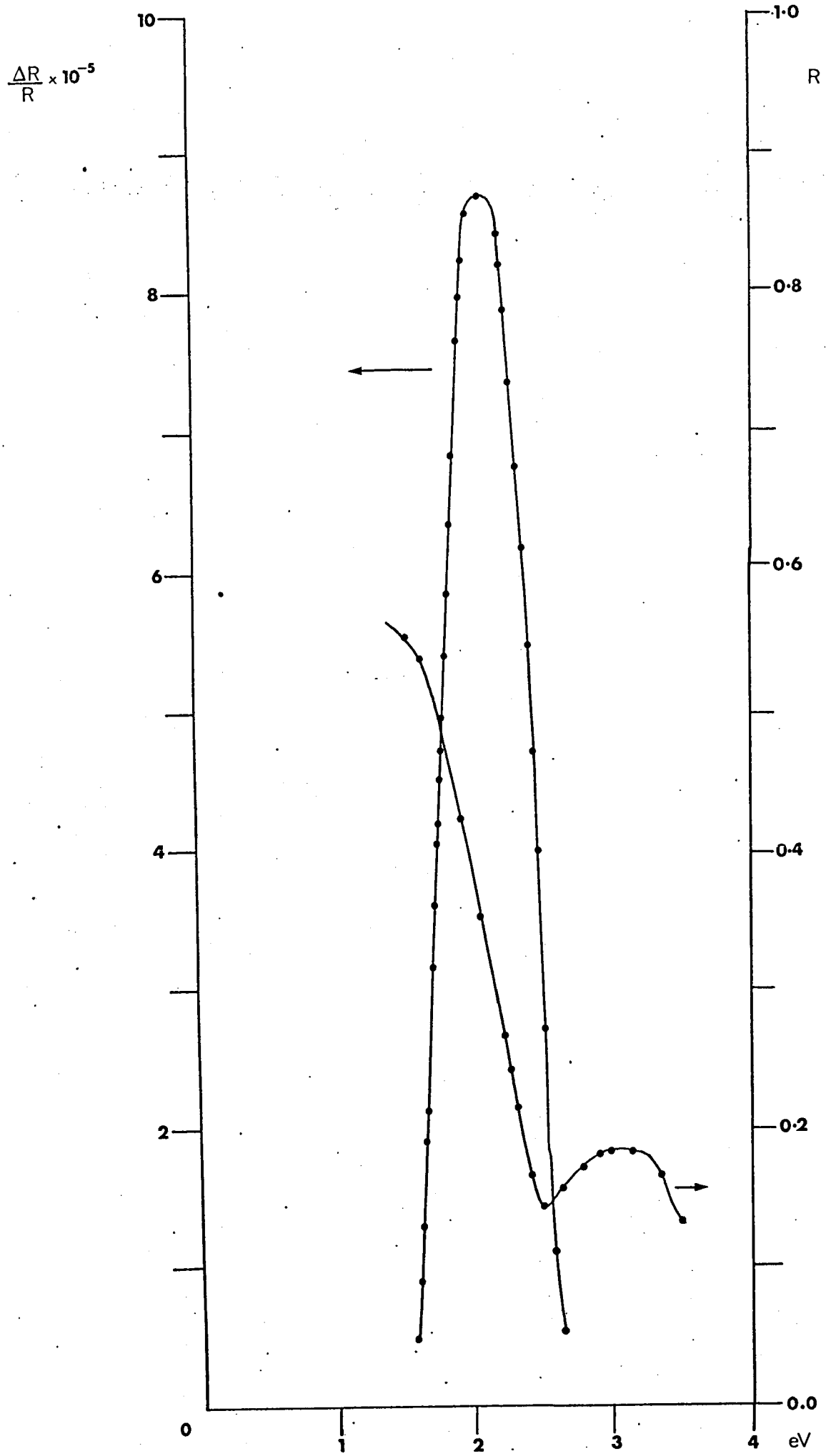

F i g. (3.2) Reflectance and ER spectrum for a gold film 350 Å thick.

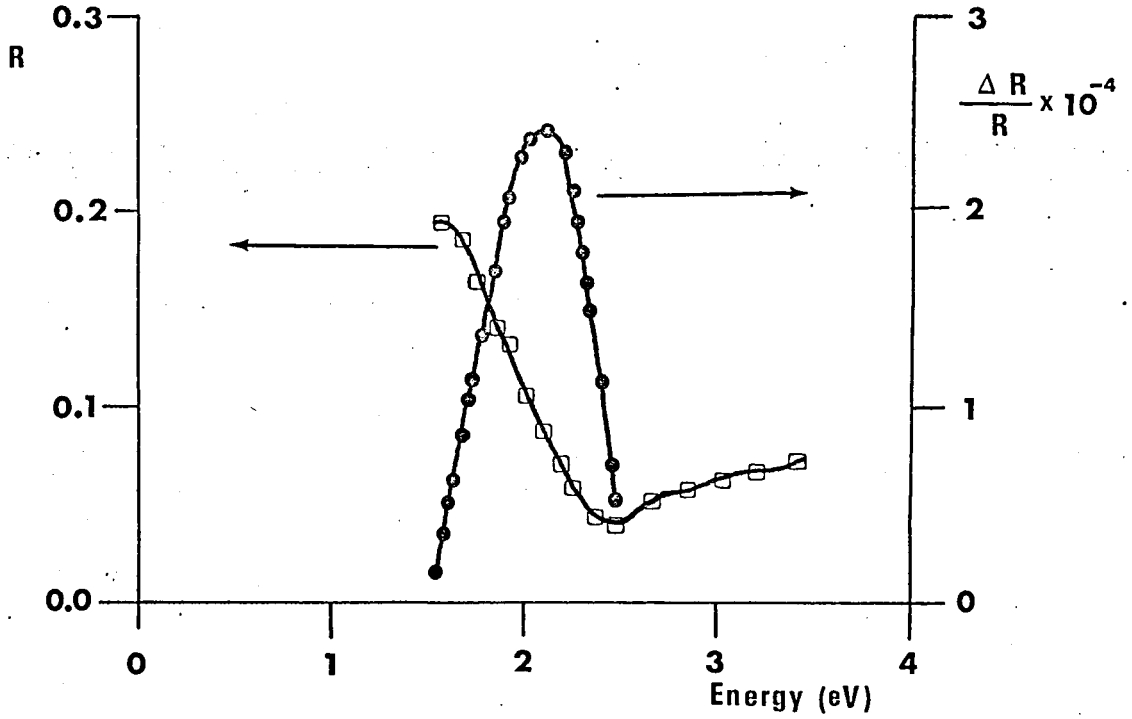

F i g. (3.3)

Reflectance and ER spectrum for a gold film 160 Å thick.

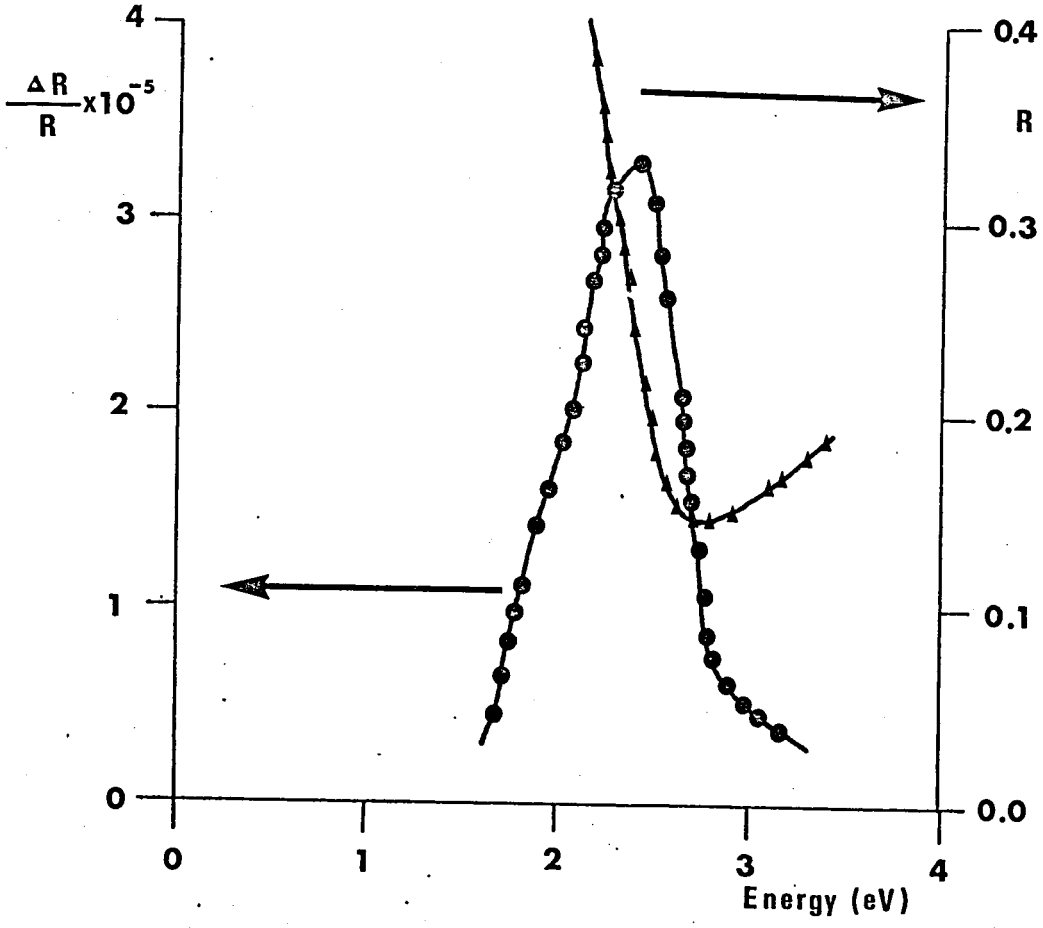

F i g. (3.4)

Reflectance and ER spectrum for a gold film 400 Å thick.

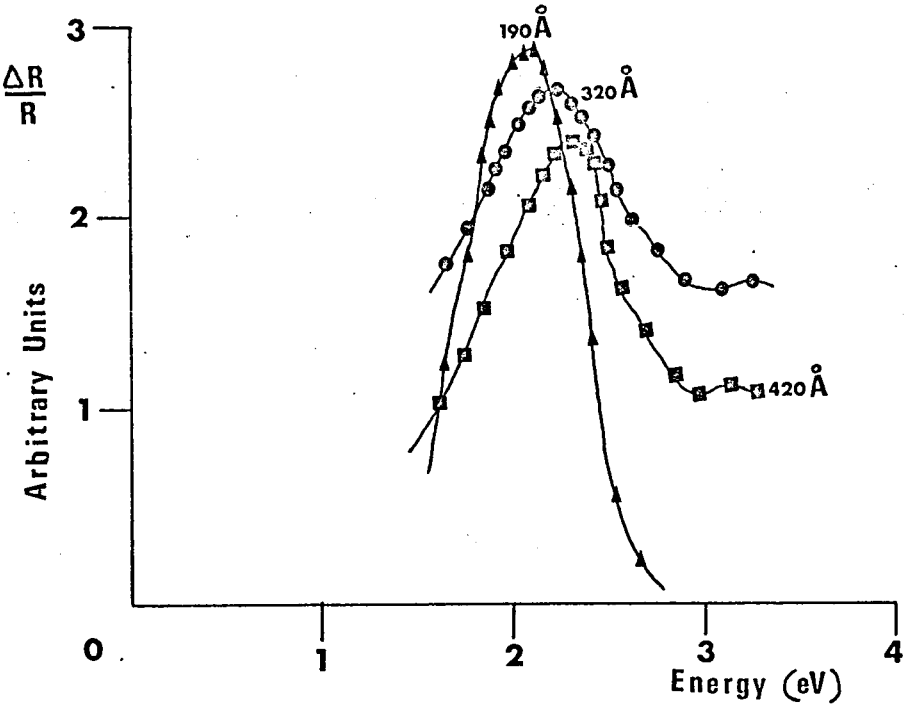

F i g. (3.5)

ER spectrum as a function of film thickness.

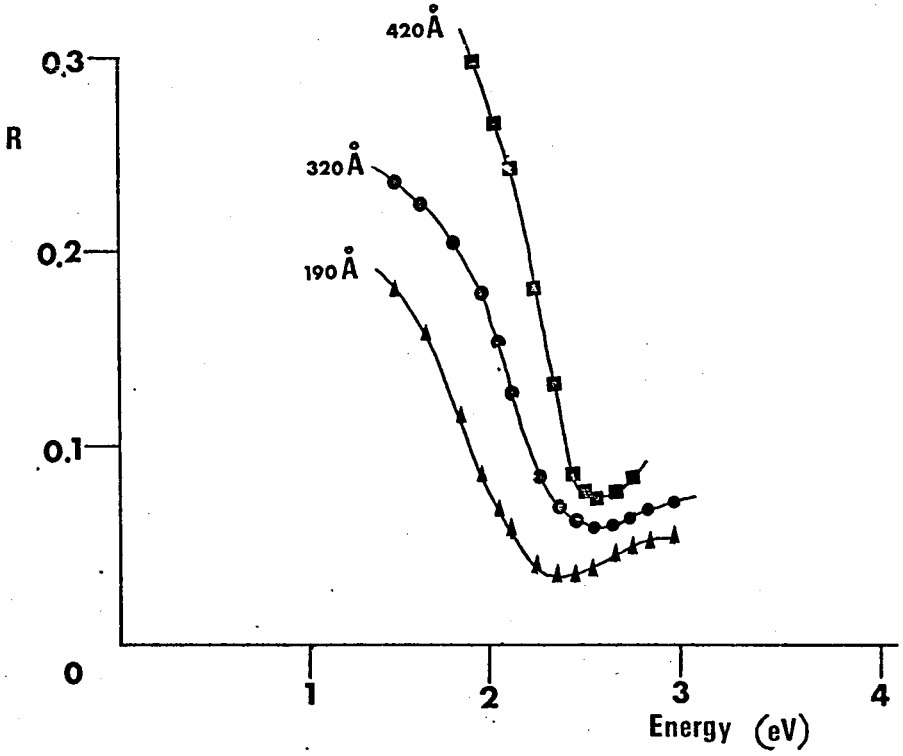

F i g. (3.6)

Reflectance spectrum as a function of film thickness.

An attempt was made to measure the ER effect as a function of the magnitude and the frequency of the modulating voltage. The results have been plotted in Figs. (3.7) and (3.8) respectively.

An important result arises from Fig. (3.7) ; that the magnitude of the ER effect increases linearly with increasing modulating voltage. The linear variation of the ER with modulating voltage occurs only between 0V and 1V peak. This is in accordance with previous measurements of the electrochemical behavior of the electrolytic cell.

Thus the magnitude of the ER effect varies linearly with the modulating voltage in the region where simple capacity effects are involved and account for the observed ER spectra of gold films.

The frequency dependence of the magnitude of the ER effect for three thin gold films is shown in Fig. (3.8). The magnitude of the ER effect remains approximately constant over a wide frequency region (10 - 1000 Hz).

3.2 Transmittance and Electrotransmittance

Figs. (3.9) , (3.10) and (3.11) show the transmittance and electrotransmittance spectra for three films with thicknesses 100, 160 and 350 Angstroms respectively. These are the same films of which the ER spectra have been discussed previously.

It can be seen , in these figures , that the electrotransmittance spectrum exhibits two peaks of opposite sign. A large negative peak occuring in low photon - energies and a small positive peak occuring at about 2.5 eV. The two peaks correspond to the two edges of the

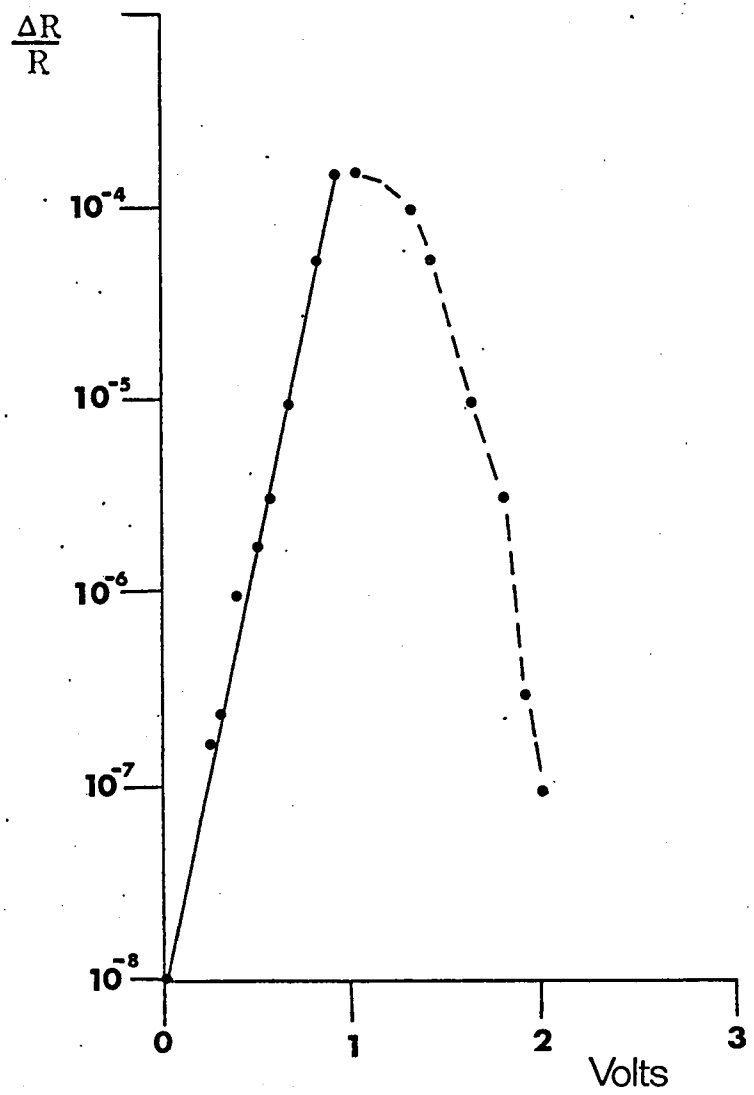

F i g. (3.7)

ER as a fumction of the magnitude of the modulating voltage .

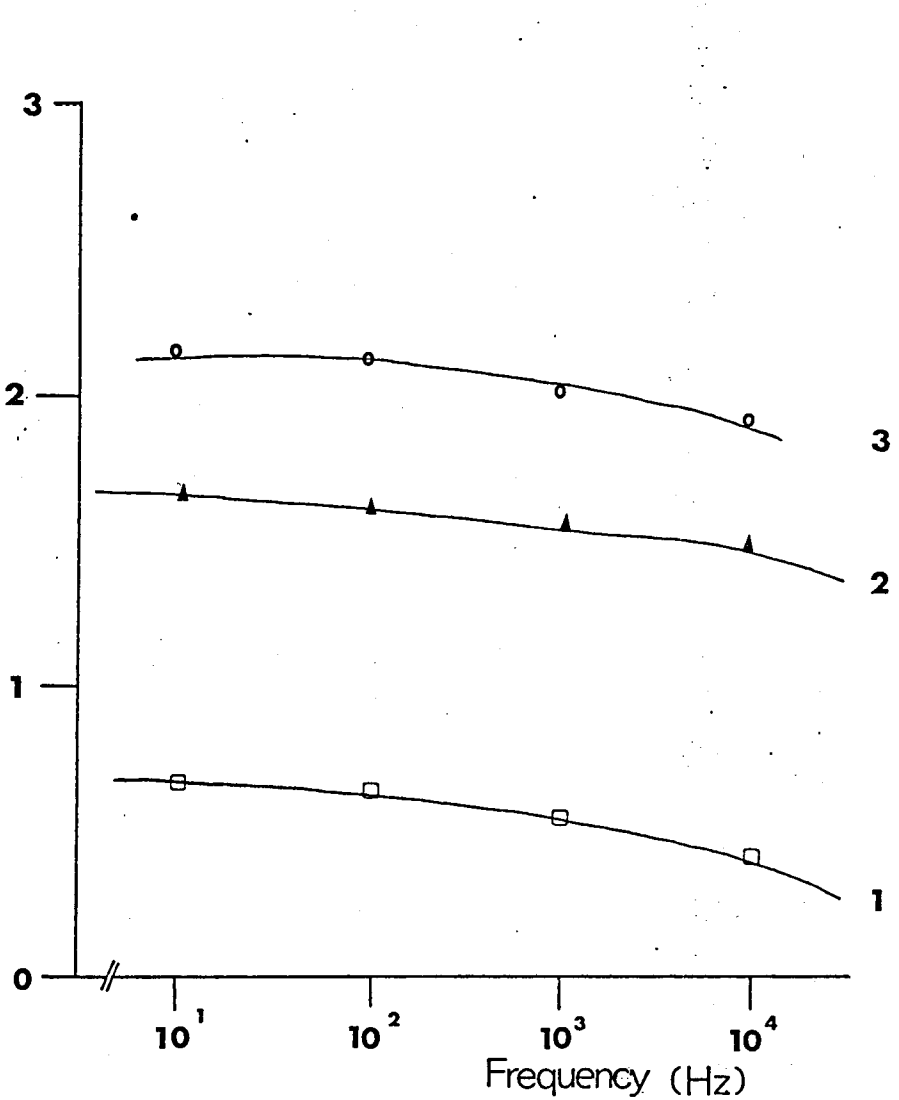

F i g. (3.8)

ER as a function of the frequency of the modulating voltage .

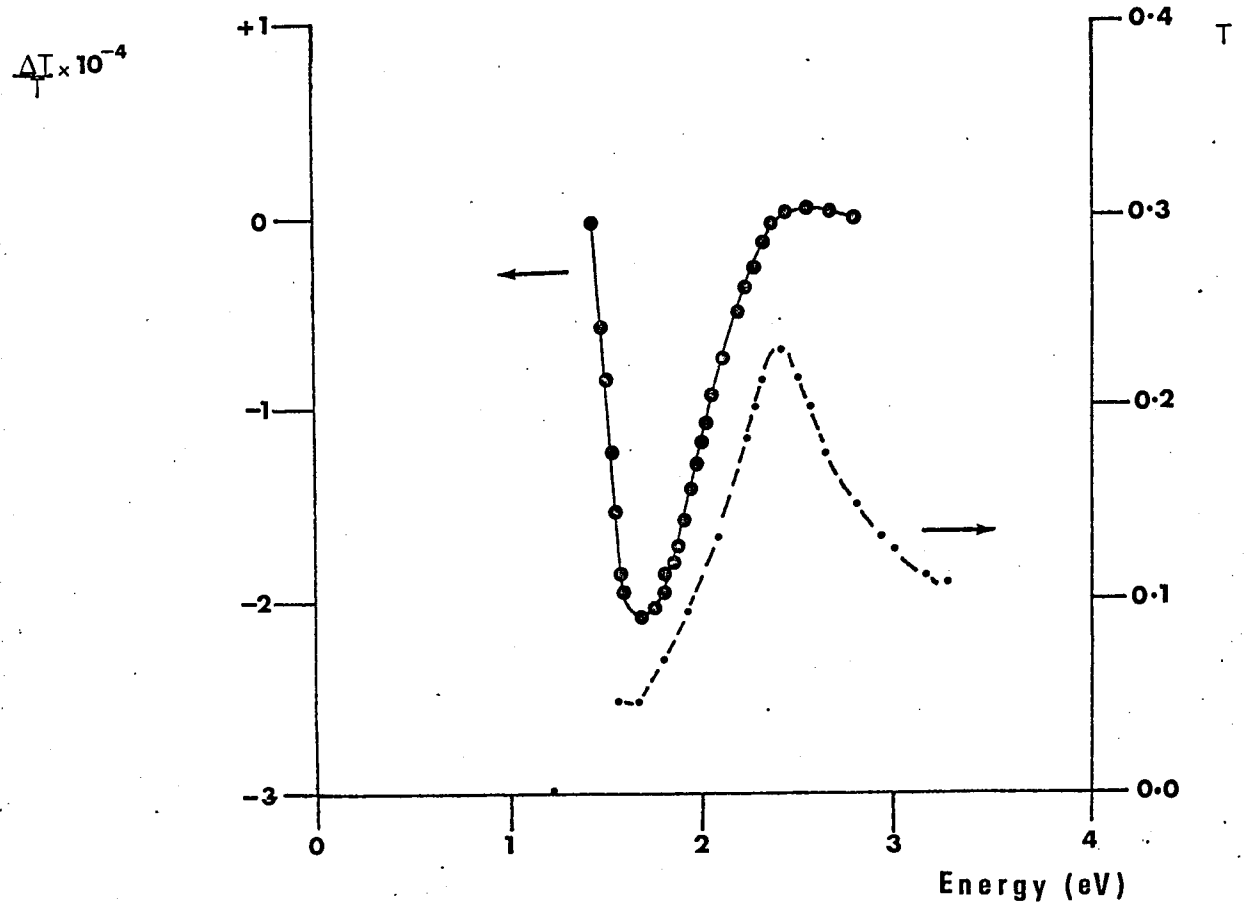

F i g. (3.9)

Transmittance and ET for a gold film 100 Å thick.

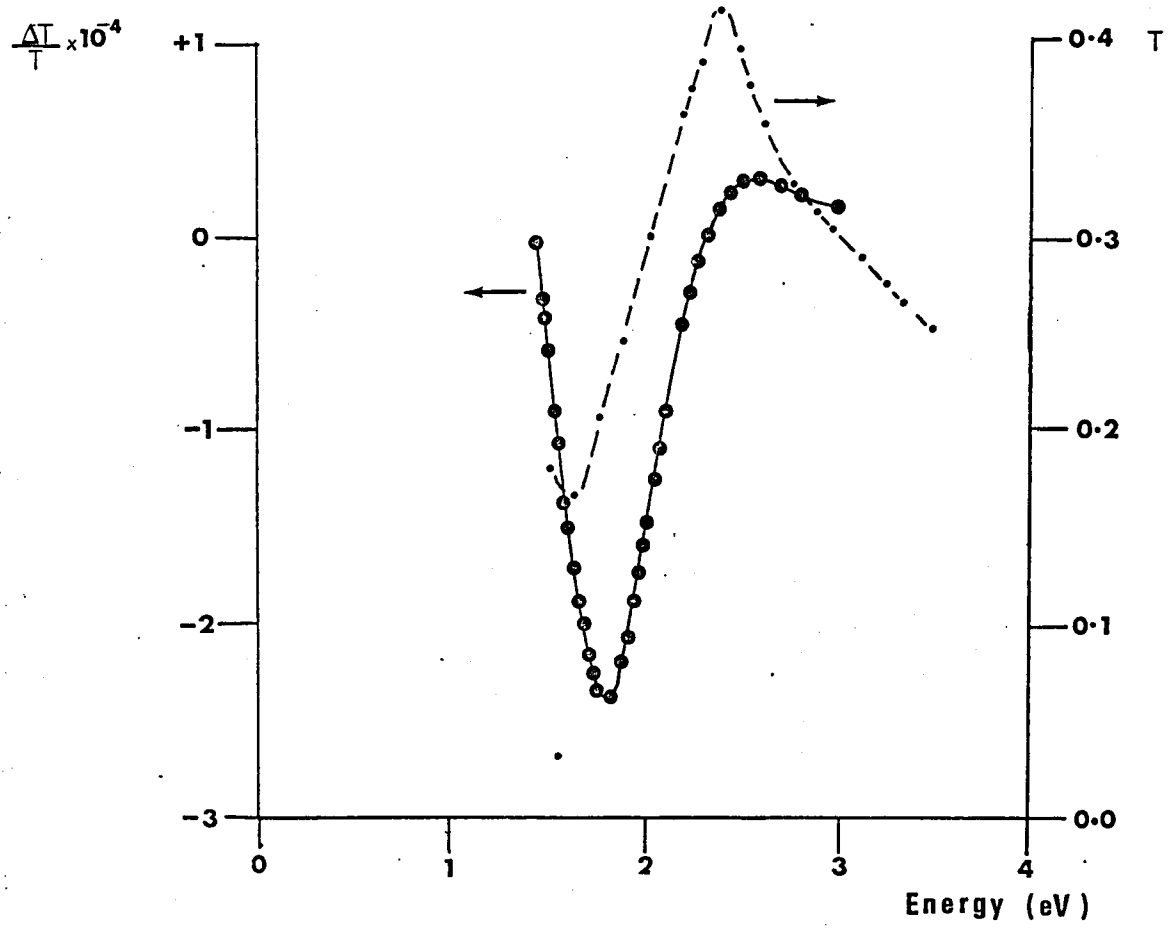

F i g. (3.10)

Transmittance and ET for a gold film 160 Å thick.

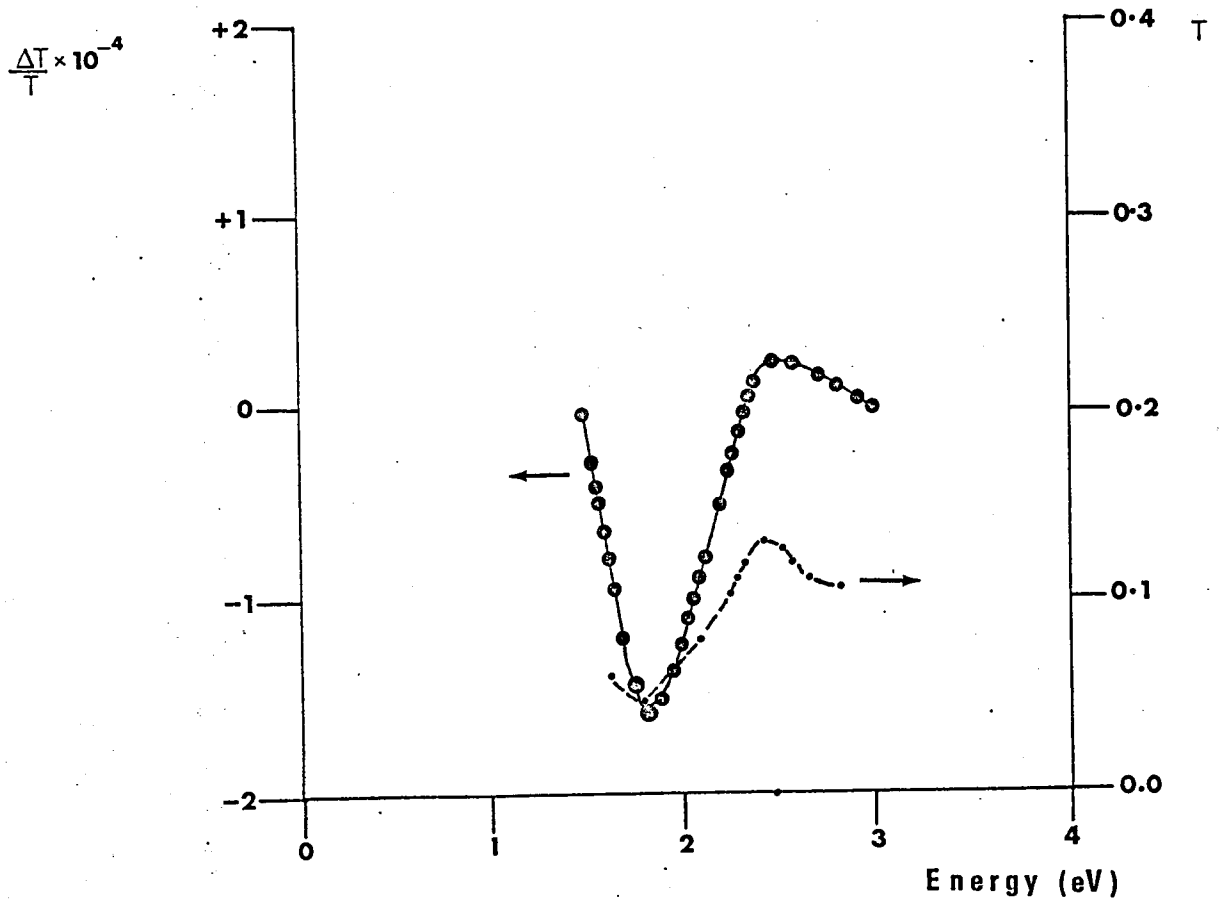

F i g. (3.11)

Transmittance and ET for a gold film 350 Å thick.

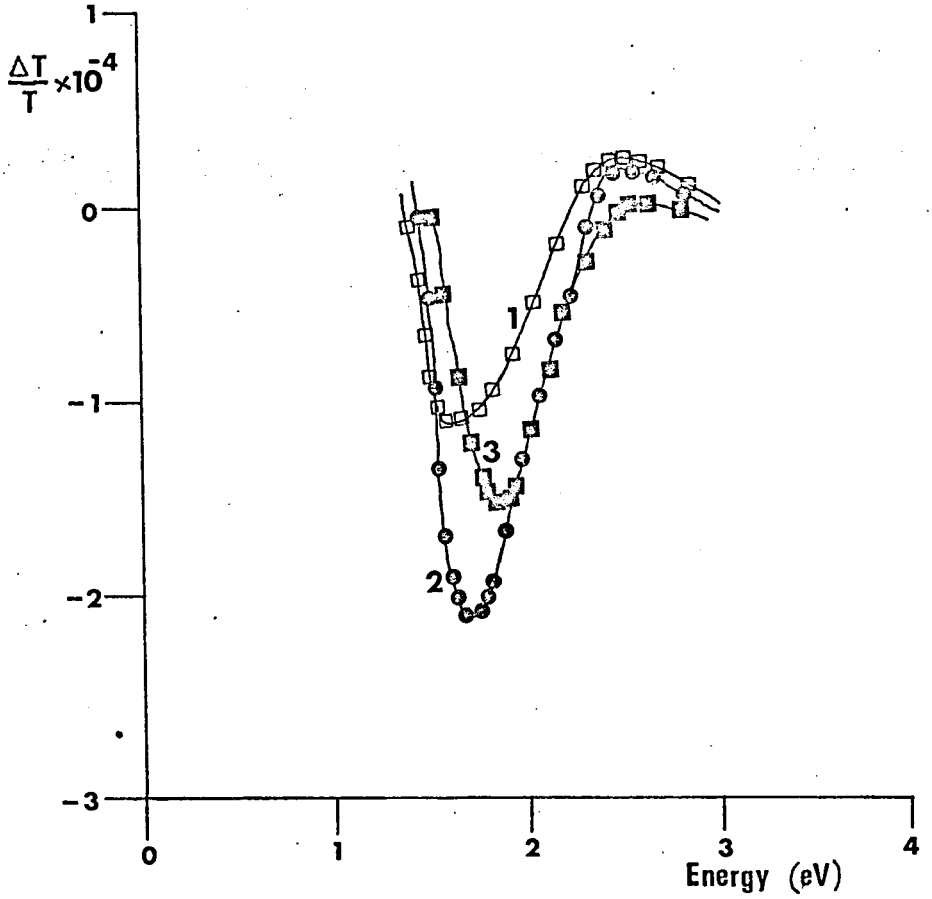

F i g. (3.12)

ET spectrum as a function of film thickness.

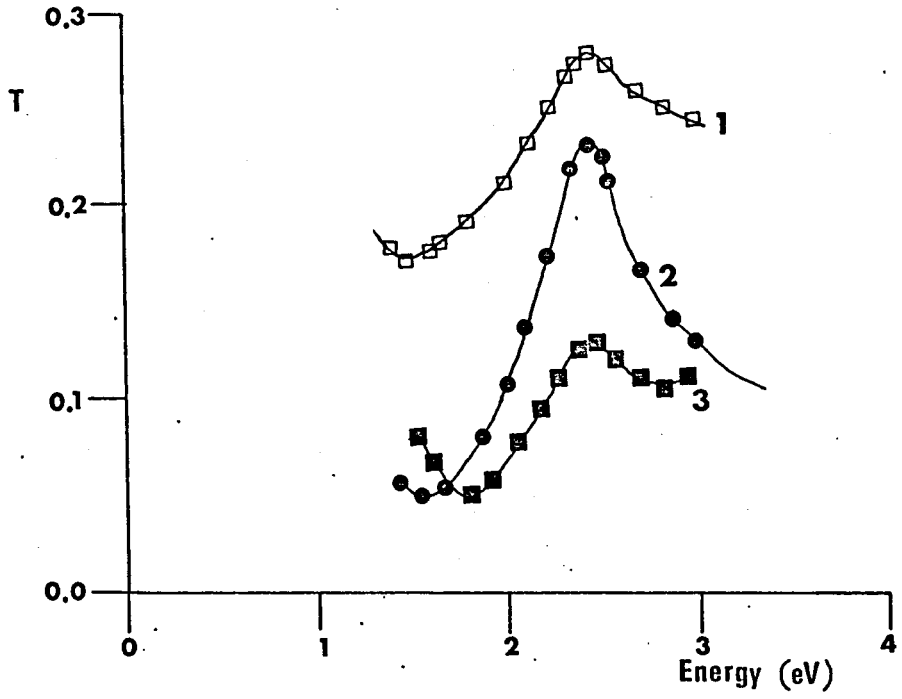

F i g. (3.13)

Transmittance spectrum as a function of film thickness.

transmittance spectrum.

The electrotransmittance spectra of three films have been plotted in the same graph of Fig. (3.12). Curves 1,2 and 3 correspond to films with thickness 320 , 420 and 190 Angstroms . In the case of electrotransmittance it seems that the negative only peak shifts to lower photon energies as the thickness of the film decreases. The position of the small positive peak does not seem to be affected from the thickness of the film.

Another interesting feature of the electrotransmittance spectrum is that the magnitude of the peak does not change very much with the thickness of the film , as happens in the case of electroreflectance.

Fig. (3.13) contains the transmittance spectra which correspond to the electrotransmittance spectra of Fig. (3.12). It is obvious that the peaks of the transmittance spectra do not shift with changing film thickness. However the two "edges" become less sharp as the thickness decreases and the points of the spectrum , where the transmission starts rising again , shift to lower and higher photon energies respectively.

In the case of very thick film , the transmission spectrum does not exhibit any substantial feature and the electrotransmittance signal is very weak , if not zero.

It must be noticed that the electroreflectance spectra of the same films exhibit only one positive peak at the spectral region of the plasma edge.

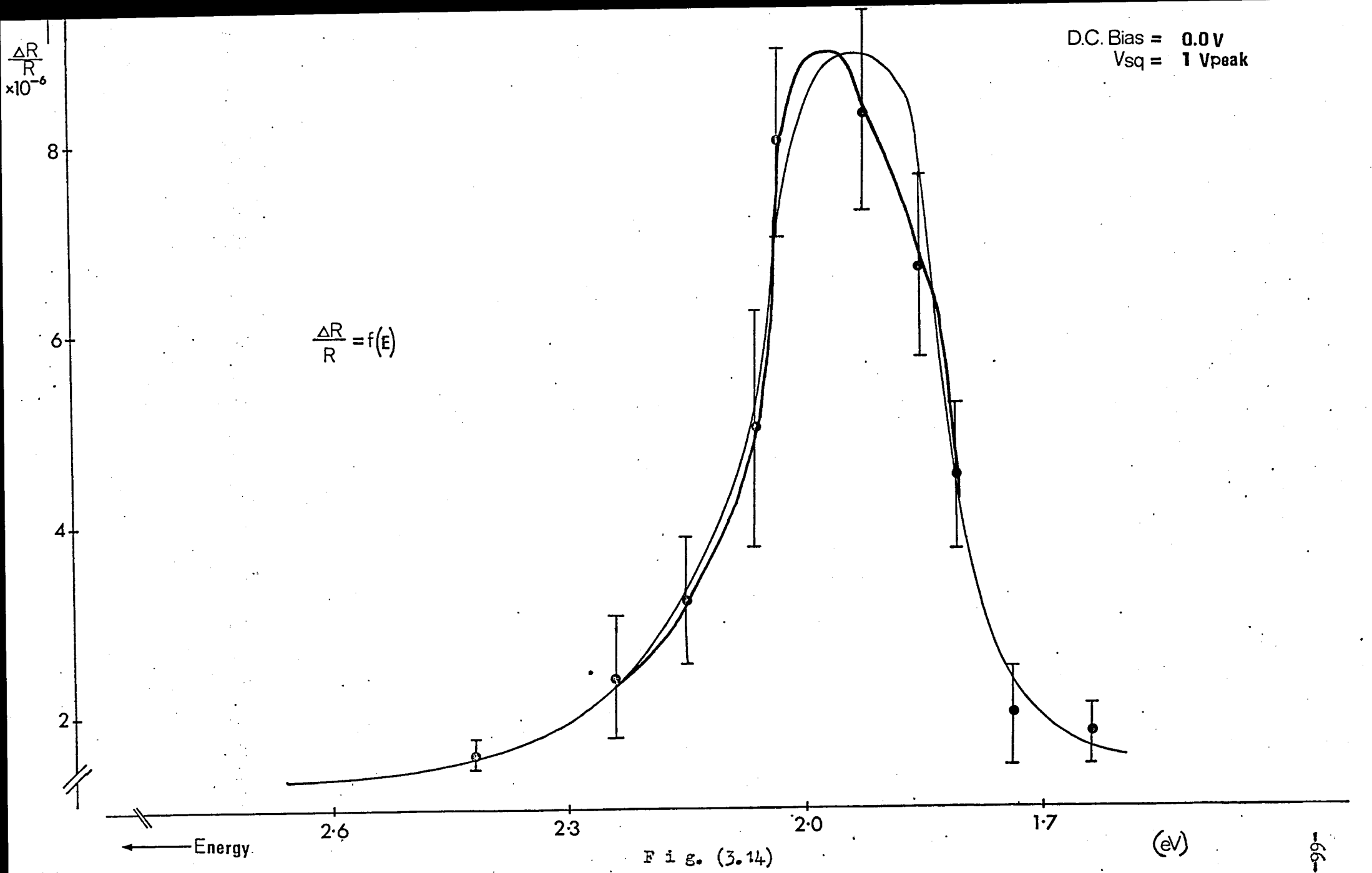

F i g. (3.14)

ER spectrum for the Schottky Diode with D.C. bias = 0 .

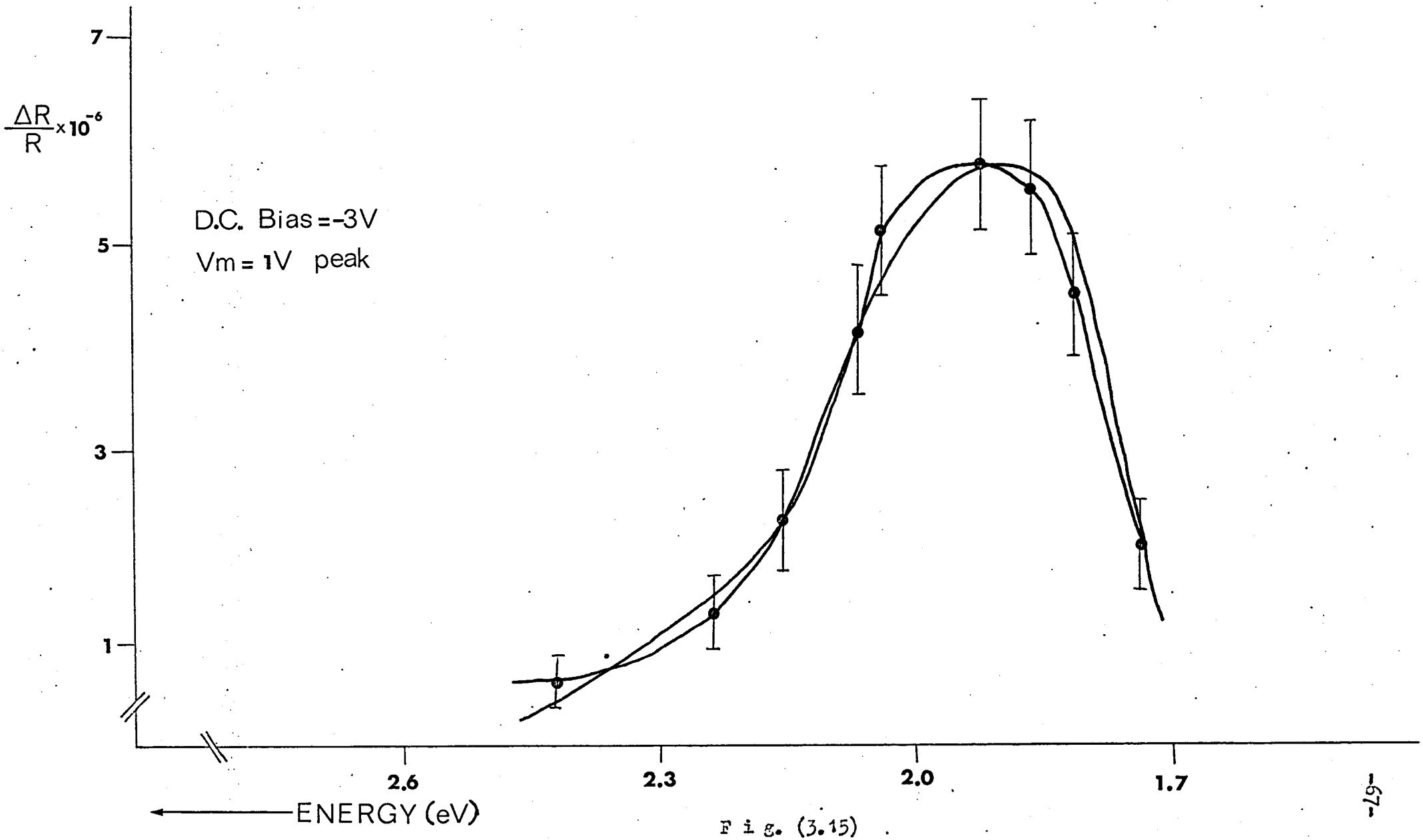

F i g. (3.15)

ER spectrum for the Schottky Diode with D.C. bias = -3V.

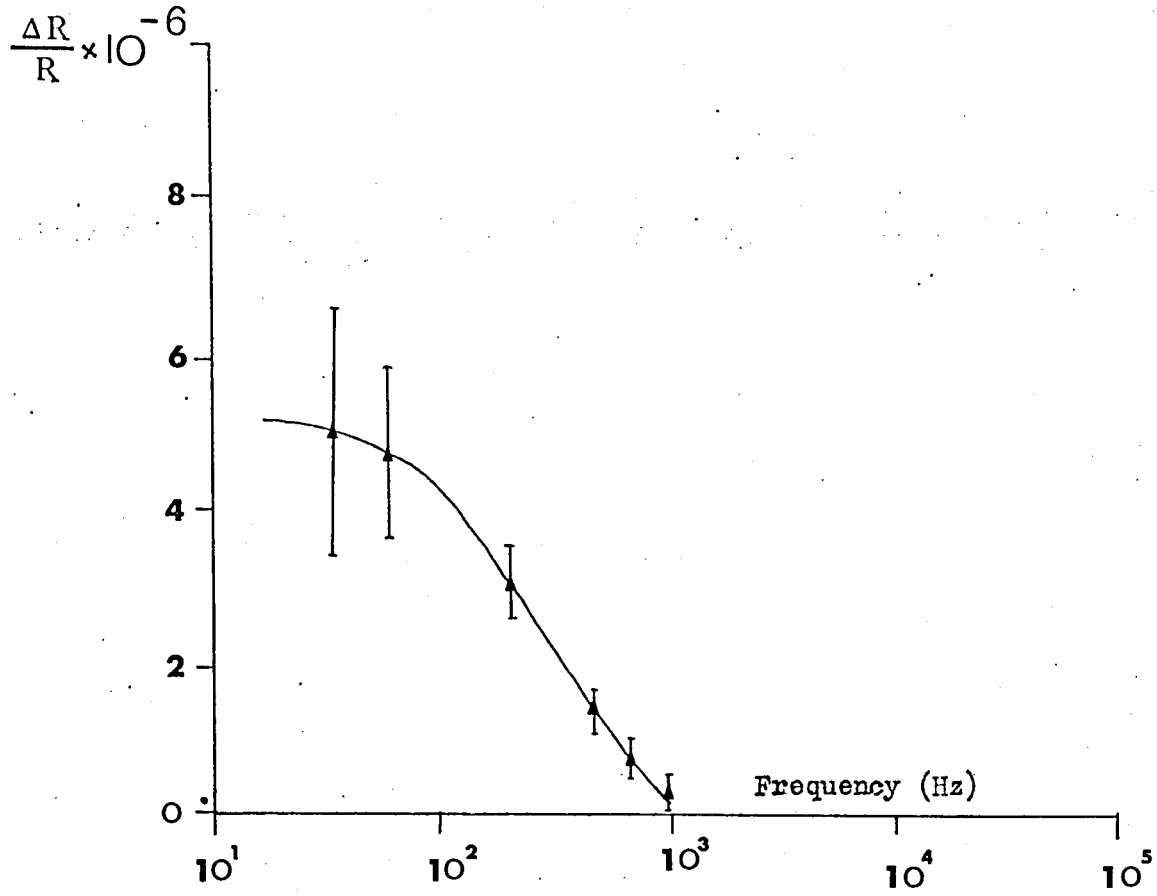

F i g. (3.16)

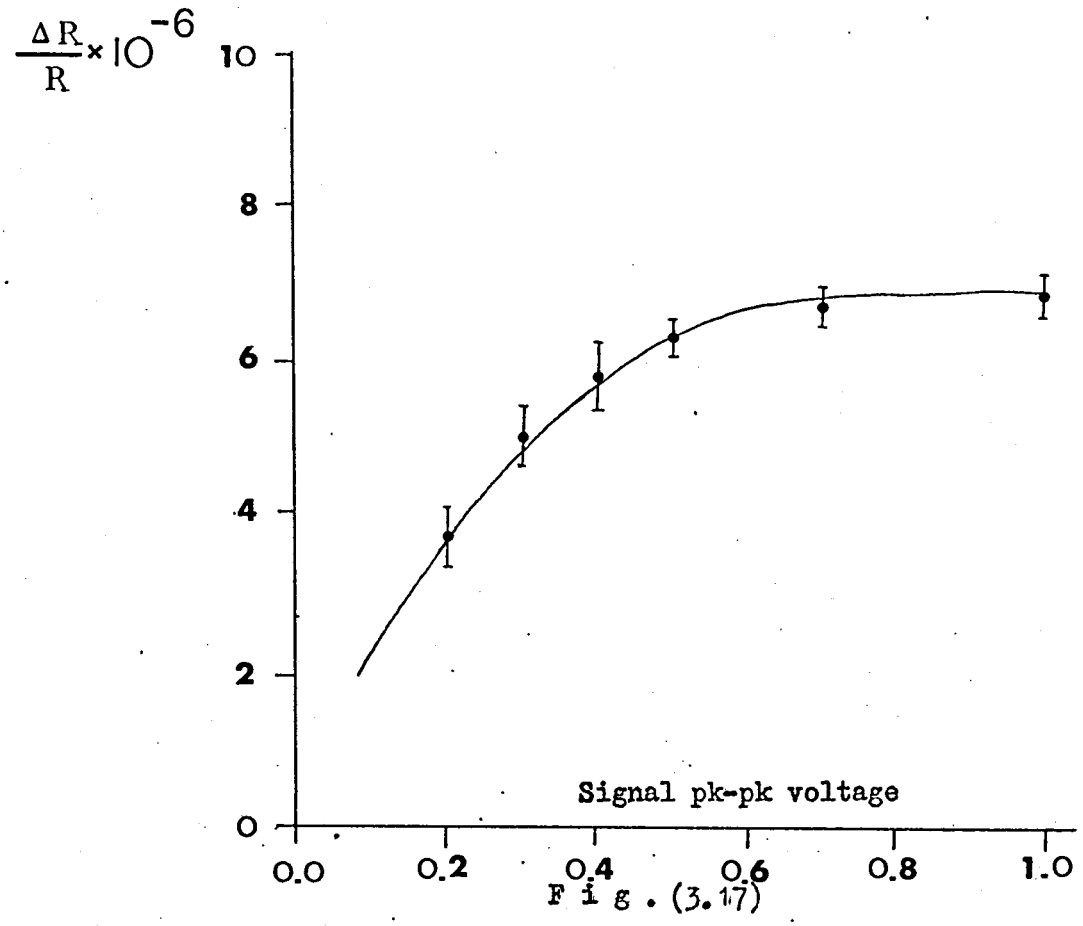

F i g . (3.17)

$\frac{\Delta R}{R}$ as a function of frequency and signal voltage for the Schottky diode.

3.3 Results From Schottky Diode

The ER spectrum of a thin gold film with a thickness of about 70 Angstroms is shown in Fig. (3.14). The peak of the ER spectrum occurs at about 2.0 eV when no reverse D.C. bias is applied on the Schottky Diode.

Fig. (3.15) shows the ER spectrum of the same Schottky Diode with a reverse D.C. biasing voltage of 3V applied on the diode. The peak is shifted to lower energies a fact which was expected. Something interesting can be seen ; the increase of the reverse biasing voltage reduces the magnitude of the peak of the ER spectrum. This is in accordance to Fig. (2.16).

The capacitance of the Schottky Diode remains constant over the frequency region 25-100 Hz , but its value decreases with increasing reverse D.C. biasing voltage a fact which affects the magnitude and the shape of the ER spectrum of the thin gold film.

Although a large D.C. bias was applied , the ER peak does not seem to shift very much to lower energies . This is because the Schottky barrier capacity decreases and consequently the electric field applied on the internal surface of the gold film does not change appreciably. Figs. (3.16) and (3.17) show how the magnitude of ER effect varies in the case of the gold - silicon Schottky diode, with the frequency and magnitude of the modulation voltage respectively.

A modulation signal of 1V peak - to - peak at 50 Hz was used to obtained the ER spectra of Figs. (3.14) and (3.15).

CHAPTER 4 - INTERPRETATION OF THE EXPERIMENTAL RESULTS

4.1 The Behaviour of Electromagnetic waves at an Interface

The transmission of visible light through a conducting medium and the behavior of such radiation at the interfaces between different media are aspects of the general behavior of electromagnetic waves which are governed by Maxwell's field equations.

A wave incident at an interface (a plane boundary between two phases) is partly reflected and partly transmitted. The Fresnel 's equations ensure contimity of the tangential components of the electric and the magnetic field at the interfaces and they give the ratios of the amplitudes of the incident , reflected and transmitted waves.

The Fresnel's formulas for the complex reflection and transmission coefficients at an interface between two homogeneous isotropic media j and k for perpendicular polarization and perpendicular incidence are /17/, (light being incident from phase j),

$$\bar{r}_{jk} = \frac{\bar{n}_j - \bar{n}_k}{\bar{n}_j + \bar{n}_k} \qquad (4.1)$$

$$\bar{t}_{jk} = \frac{2\bar{n}_j}{\bar{n}_j + \bar{n}_k} \qquad (4.2)$$

The magnetic permeabilities of the media are taken as unity for the visible region of the spectrum. $\bar{n}_j$ and $\bar{n}_k$ are the complex indexes of refraction of medium j and k respectively and are generally defined as

$$\bar{n} = n - jk.$$

where n is its real part and k the extinction coefficient.

The above quantities can be expressed in polar form as

$$\bar{r}_{jk} = |\bar{r}_{jk}| \exp(j\delta_{jk}) \tag{4.3}$$

$$\bar{t}_{jk} = |\bar{t}_{jk}| \exp(j\delta'_{jk}) \tag{4.4}$$

where δ_{jk} and δ'_{jk} represent the phase changes on reflection and transmission respectively for perpendicular polarised light.

The phase changes on reflection and transmission will be always positive ($0 \leqslant \delta_{jk} \leqslant 2\pi$), because we assume the time dependence of the field as exp $(+j\omega t)$, and they are given by the following relations

$$\delta_{jk} = \tan^{-1}\left[\frac{\mathrm{Im}(r_{jk})}{\mathrm{Re}(r_{jk})}\right] \tag{4.5}$$

$$\delta'_{jk} = \tan^{-1}\left[\frac{\mathrm{Im}(t_{jk})}{\mathrm{Re}(t_{jk})}\right] \tag{4.6}$$

with the aid of Fresnel's coefficients we can calculate the energy reflectance and transmittance at an interface as

$$R_{jk} = |\bar{r}_{jk}|^2 = \bar{r}_{jk} \cdot \bar{r}^*_{jk} \tag{4.7}$$

where $\bar{r}^*_{jk}$ is the complex conjugate of $\bar{r}_{jk}$.

4.2 Reflectance and Transmittance in a Thin Film

Consider a system consisting of two interfaces 1 and 2. This is the case of a thin film with a complex refractive index $\bar{n} = n - jk$ mounted on a substrate with refractive index n_o. The electromagnetic wave falls on to interface 1 coming from the phase with a refractive index n_o, Fig(4.1).

Multiple reflections take place at the surfaces of the film. The amplitude of the directly reflected wave is given by ar_1, where a is the amplitude of the incident wave. Internal reflection complex coefficients at the top and bottom surfaces respectivelly, are given by r'_1 and r_2. The transmission complex coefficient into the top surface is given by t_1 and the transmission complex coefficients out of the top and bottom surfaces by t' and t_2 respectively. The phase-change on one traversal of the film is $B/2$. Where

$$B = 2\omega dn/c - 2j\omega dk/c$$

Hence the amplitude of the reflected beam relative to the incident beam is

$$r = r_1 + t_1 t' r_2 \exp(-jB) + t_1 t' r_2^2 r'_1 \exp(-2jB) + \ldots$$

$$= r_1 + \left[t_1 t' r_2 \exp(-jB)\right]\left[1 - r_2 r'_1 \exp(-jB)\right]^{-1} \qquad (4.8a)$$

similarly for transmission

$$t = t_1 t_2 \exp(-jB/2) + t_1 t_2 r_2 r'_1 \exp(-3jB/2) + t_1 t_2 r_2^2 r_1'^2 \exp(-5jB/2) + \ldots$$

$$= t_1 t_2 \exp(-jB/2) \left[1 - r_2 r'_1 \exp(-jB) \right]^{-1} \qquad (4.9a)$$

According to Fig. (4.2)

$$r_1^2 + t_1 t' = 1$$

$$r_1 + r'_1 = 0$$

i.e.

$$t_1 t' = 1 - r_1^2$$

$$r_1 = - r'_1$$

Substitution of the last two relationships into Eqs (4.8a) and (4.9a) gives

$$r = \frac{r_1 + r_2 \exp(-jB)}{1 + r_1 r_2 \exp(-jB)}$$

$$t = \frac{t_1 t_2 \exp(-jB/2)}{1 + r_1 r_2 \exp(-jB)}$$

where r is the complex coefficent for the reflectance and t is the complex coefficent for the transmittance and r_1, r_2, t_1 and t_2 are given by

$$r_1 = \frac{n_o - \bar{n}}{n_o + \bar{n}} \qquad \text{and} \qquad r_2 = \frac{\bar{n} - n_L}{\bar{n} + n_L}$$

$$t_1 = \frac{2n_o}{n_o + \bar{n}} \qquad \text{and} \qquad t_2 = \frac{2\bar{n}}{\bar{n} + n_L}$$

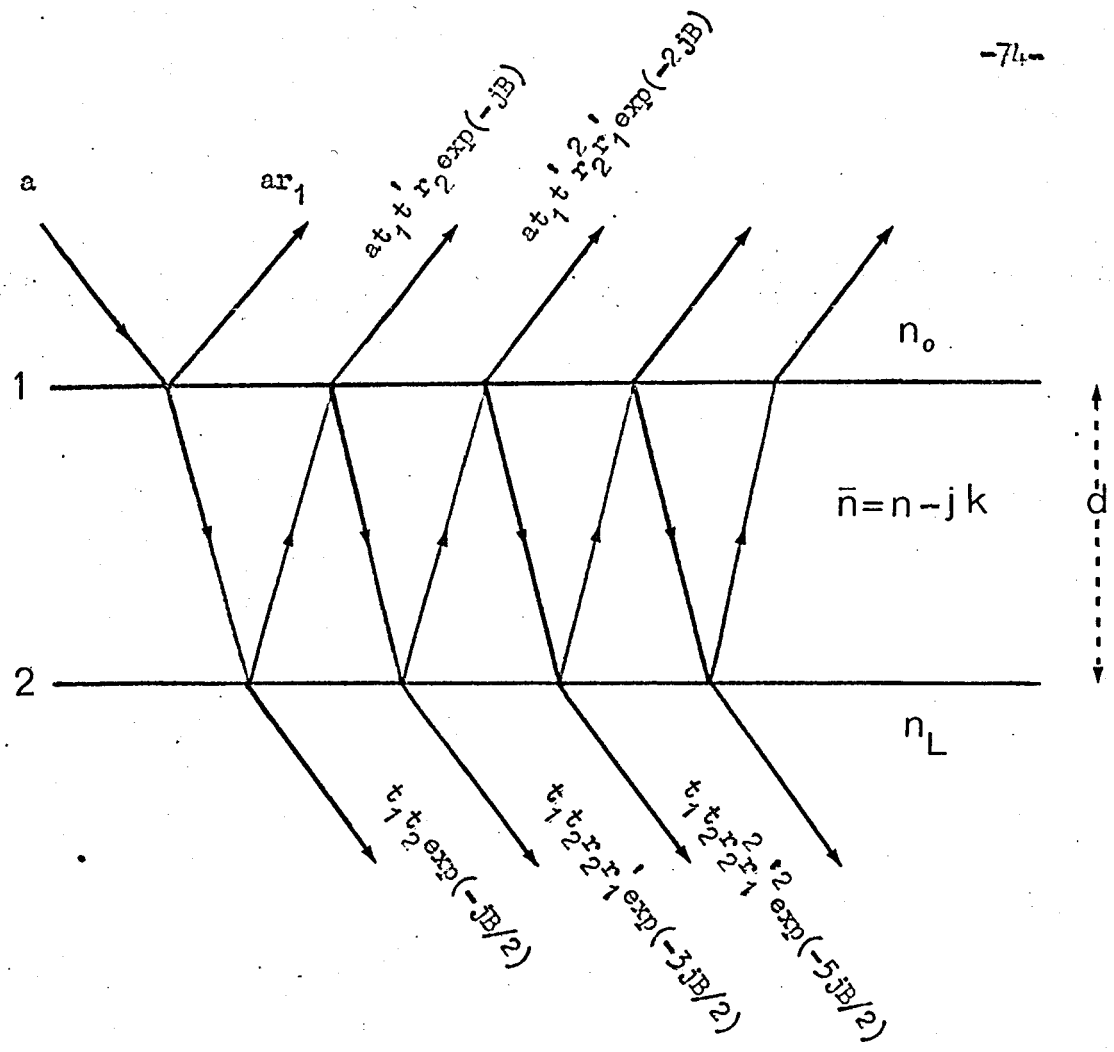
a
ar_1
$at_1t'r_2\exp(-j\beta)$
$at_1t'r_2^2r_1'\exp(-2j\beta)$
n_o
1
$\bar{n}=n-jk$
d
2
n_L
$t_1t_2\exp(-j\beta/2)$
$t_1t_2r_2r_1'\exp(-3j\beta/2)$
$t_1t_2r_2^2r_1'^2\exp(-5j\beta/2)$

F i g . (4.1)

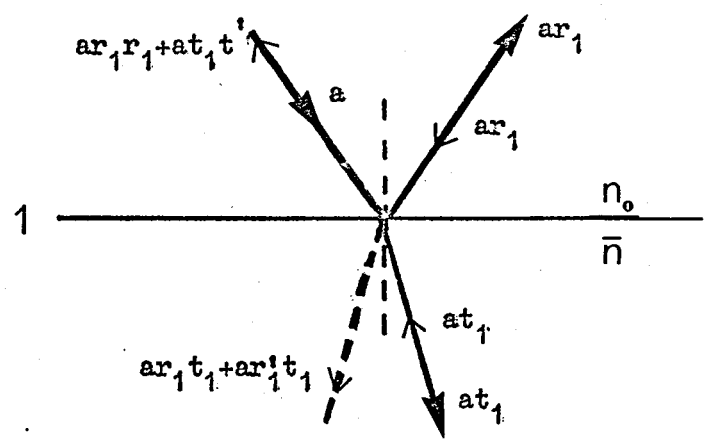
$ar_1r_1+at_1t'$
a
ar_1
ar_1
n_o
1
$\bar{n}$
at_1
$ar_1t_1+ar_1't_1$
at_1

F i g . (4.2)

Phases 1 and 3 have been assumed non - absorbing , so that

$$t_1 t_2 = \frac{2\, n_o}{n_o + n_L} \left(1 + r_1 r_2 \right)$$

Hence for a three phase system

$$r = \frac{r_1 + r_2 \exp\left(- jB \right)}{1 + r_1 r_2 \exp\left(- jB \right)} \qquad (4.8b)$$

$$t = \frac{2n_o}{n_o + n_L} \quad \frac{1 + r_1 r_2}{1 + r_1 r_2 \exp\left(-jB\right)} \quad \exp\left(-jB/2\right) \qquad (4.9b)$$

The energy reflectance , R , is

$$R = r\, r^* = |r|^2$$

The energy transmission , T , is

$$T = \frac{n_L}{n_o} \cdot t \cdot t^* = \frac{n_L}{n_o} |t|^2$$

Hence ,

$$R = \left| \frac{r_1 + r_2 \exp\left(-jB\right)}{1 + r_1 r_2 \exp\left(-jB\right)} \right|^2 \qquad (4.8)$$

$$T = \frac{4 n_L n_o}{\left(n_o + n_L\right)^2} \left| \frac{\left(1 + r_1 r_2\right) \exp\left(-jB/2\right)}{1 + r_1 r_2 \exp\left(-jB\right)} \right|^2 \qquad (4.9)$$

where r_1 and r_2 are the Fresnel's complex coefficients for

the interfaces 1 and 2 respectivelly , and $B = 2\omega d(n - jk)/C$.
Where d is the thickness of the film. Expanding (4.8) and (4.9)

$$R = \frac{|r_1|^2 + 2|r_1||r_2|\exp(-\beta)\cos\Phi + |r_2|^2 \exp(-2\beta)}{1 + 2|r_1||r_2|\exp(-\beta)\cos\Theta + |r_1|^2|r_2|^2 \exp(-2\beta)} \qquad (4.10)$$

$$T = \frac{4n_o n_L}{(n_o + n_L)^2} \quad \frac{1 + 2|r_1||r_2|\cos\Phi' + |r_1|^2|r_2|^2}{1 + 2|r_1||r_2|\exp(-\beta)\cos\Theta + |r_1|^2|r_2|^2 \exp(-2\beta)} \exp(-\beta) \qquad (4.11)$$

where $\beta = 2\omega kd/c$, is an absorption constant . d is the thickness of the film . $|r_1|$ and $|r_2|$, the moduli of the Fresnel amplitude reflection coefficient are given by

$$|r_1| = \left[\frac{(n_o - n)^2 + k^2}{(n_o + n)^2 + k^2}\right]^{\frac{1}{2}} \qquad (4.12)$$

$$|r_2| = \left[\frac{(n - n_L)^2 + k^2}{(n + n_L)^2 + k^2}\right]^{\frac{1}{2}} \qquad (4.13)$$

Φ and Θ are given by

$$\Phi = \delta_2 - \delta_1 - \Delta \qquad (4.14)$$

$$\Phi' = \delta_2 - \delta_1$$

$$\Theta = \delta_2 + \delta_1 - \Delta \qquad (4.15)$$

where δ_1 , δ_2 the phase angles at interfaces (obtained from the appropriate Fresnel coefficient) are given by

$$\delta_1 = \tan^{-1}\left[\frac{2n_o k}{n_o^2 - n^2 - k^2}\right] \qquad (4.16)$$

$$\delta_2 = \tan^{-1}\left[\frac{2n_L k}{n_L^2 - n^2 - k^2}\right] \qquad (4.17)$$

and

$$\Delta = 4\pi n \nu d / c \qquad (4.18)$$

where ν is the frequency of the incident wave.

4.2.1 The Phase Angles

Compared to the incident light, the phase change Δ in equations (4.14) and (4.15) is clearly a lag, since physically it is introduced by the finite time which the light takes, to traverse the film twice.

However the phase changes δ_1 and δ_2 are ambiguous since equations (4.12) and (4.13) both have two solutions. In order that the correct values be assigned to δ_1 and δ_2 in equations (4.14) and (4.15), it is necessary to consider carefully the reflections at each face of the film.

For simplicity numerical solutions of equations (4.14) and (4.15) are restricted to values between 0 and π.

To determine if δ_1 lies between 0 and π, it is convenient to make k small and investigate the effect of making $n<n_o$ and $n>n_o$. The reflection coefficient is defined in these circumstances as

$$r_1 \exp(j\delta_1) = \frac{n_o - n}{n_o + n} \qquad (4.19)$$

Therefore if $n<n_o$ one would expect $\delta=0$, i.e. zero phase change,

and if $n > n_o$ one would expect $\delta = \pi$. For absorbing materials it has been shown that

$$\tan \delta_1 = \frac{2kn_o}{(n_o - n)(n_o + n) - k^2} \qquad (4.20)$$

When k is small and $n < n_o$, then $\tan \delta_1$ is small and positive, it is expected to have a value near to zero, and δ_1 must therefore lie in quadrant A of Fig. (4.3a). If $n > n_o$ than $\tan \delta_1$ is small and negative, it is expected to have a value near to π and it must therefore lie in quadrant B of figure (4.3a). It is clear

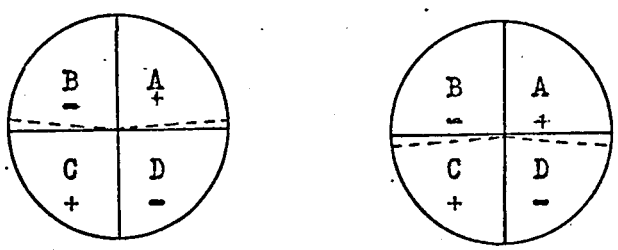

F i g. (4.3)

The quadrants in which lie (a) the phase shift δ_1

(b) the phase shift δ_2

from this argument that δ_1 lies between 0 and π.

$$\tan \delta_2 = \frac{2 n_L k}{(n_L - n)(n_L + n) - k^2} \qquad (4.21)$$

and

$$r_2 \exp j\delta_2 = \frac{n - n_L}{n_L + n} \qquad (4.22)$$

Using the same argument as before , one would expect $\delta = \pi$ if $n_L > n$, and $\delta = 0$ if $n_L < n$. However in this case when $n < n_L$ $\tan \delta_2$ lies in quadrant D , and when $n > n_L$ $\tan \delta_2$ lies in quadrant C of figure (4.3b). In this case therefore δ_2 lies between π and 2π . Since all phase angles are required to lie between 0 and π it is necessary to add π to δ_2 to satisfy this condition.

Therefore put

$$\delta_1 = \delta_1 \qquad (4.23)$$

$$\delta_2 = \delta_2 + \pi \qquad (4.24)$$

in equation (4.14) and (4.15) . The reflectance of an absorbing film is therefore given by Eq. (4.10) with

$$\Phi = \delta_2 - \delta_1 - \Delta + \pi \qquad (4.25)$$

$$\Theta = \delta_2 + \delta_1 - \Delta + \pi \qquad (4.26)$$

4.2.2 Comp utation

Computer calculations for the reflectance and transmittance of a gold

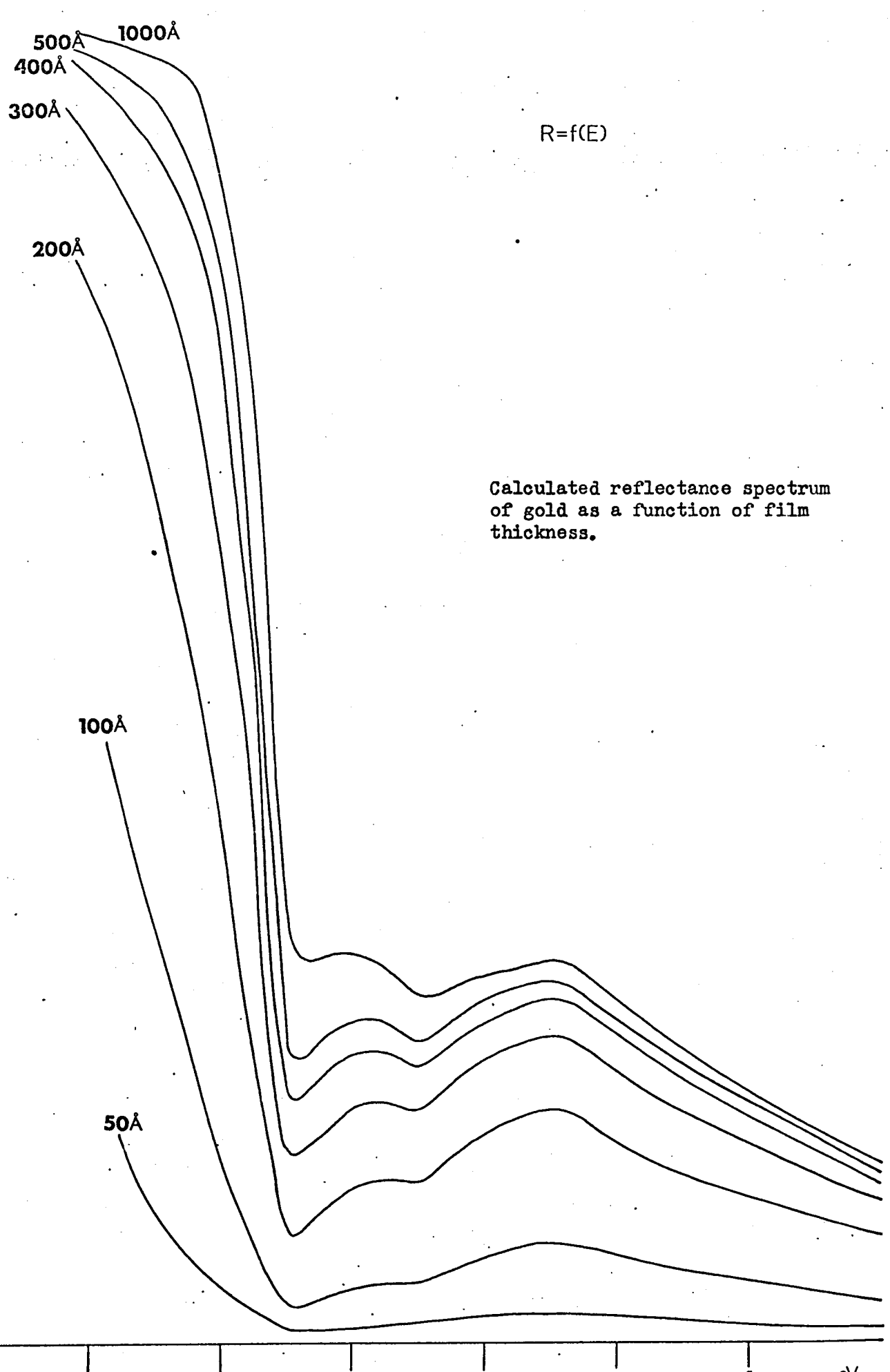

Calculated reflectance spectrum of gold as a function of film thickness.

Fig. (4.4)

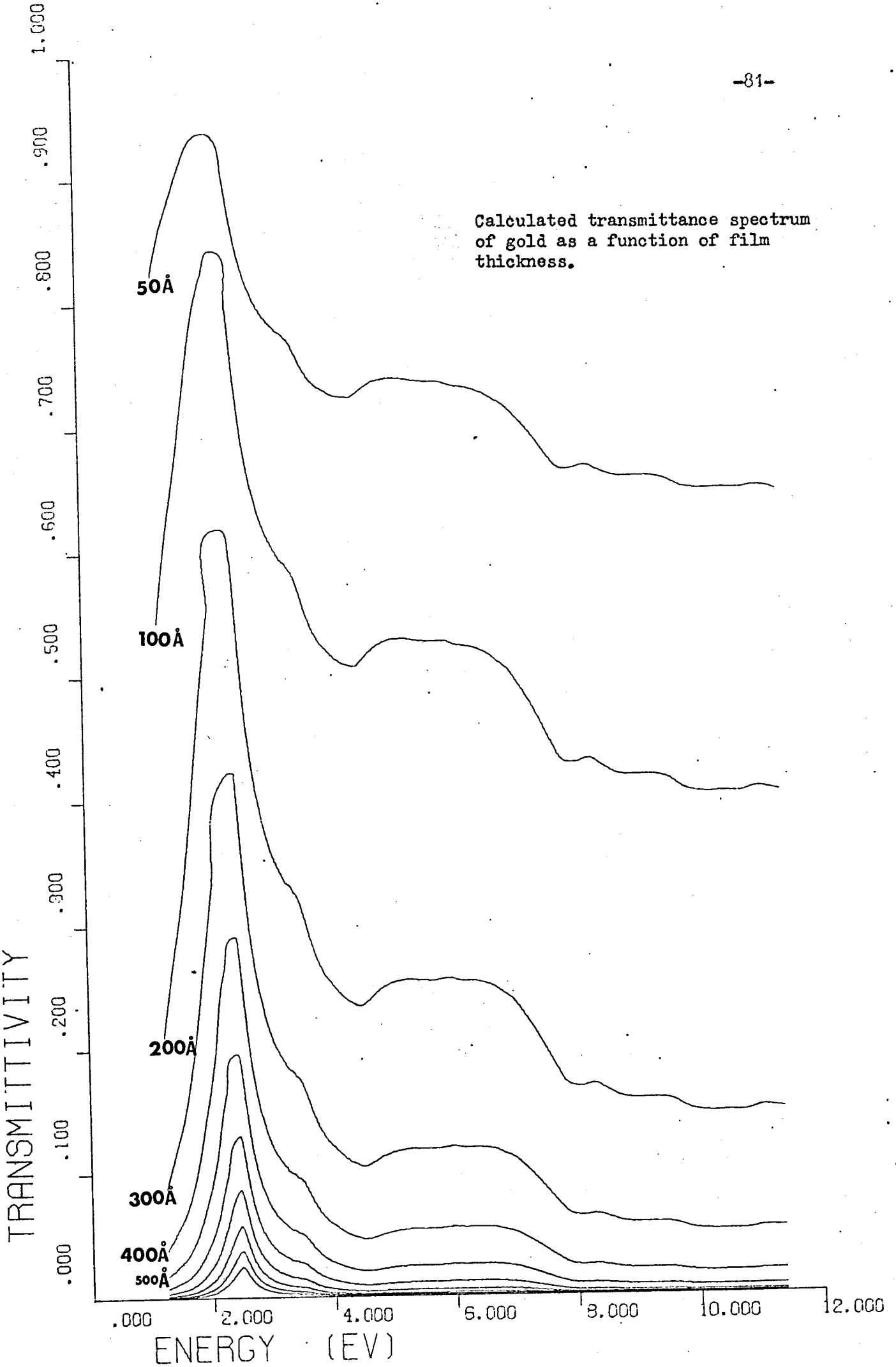

Calculated transmittance spectrum of gold as a function of film thickness.

Fig. (4.5)

film gave the curves of Figs. (4.4) and (4.5).

Fig. (4.4) shows the reflectances changes with photon - energy and film - thickness , and Fig. (4.5) shows how the transmittance changes with photon - energy and film thickness.

The thickness of the film affects very strongly the reflectance and transmittance spectra. As the thickness decreases from 1000 Angstroms to 50 Angstroms the plasma edge of the gold film becomes less sharp and moves to lower photon energies.

This is in very good agreement with the experimental results.

As the thickness of the film increases from 50 Angstroms to 1000 Angstroms the transmittance becomes lower. What is interesting to note in this case is that the position of the peak of the transmittance spectrum does not change with the thickness. Only the part of the edge which lies at the low photon - energy region shifts to lower energies as the thickness of the film decreases. This again is in very good agreement with the experimental results.

The values of the refractive index and extinction coefficient used were taken from /19/. See Fig.(4.6).

4.3 Optical Properties of Gold

In the previous chapters we have derived relationships which connect directly measurable quantities with optical constants . The optical constants n and k describe optical properties of a material. The refractive index n determines the phase velocity of a monochromatic light beam propagated in a medium , because $n = c/u$,

where c is the velocity of light in free space and u the phase velocity in the medium.

On the other hand the extinction coefficient k accounts for the energy - losses of the propagated light and determines the absorption of the material . Fig. (4.6) shows how n and k change with energy.

These two macroscopic quantities are related to microscopic properties of the materials. In the case of a good conductor n and k can be expressed as a function of the free collision time of the electrons the lattice dielectric constant and the electron density. The Drude model , /29/ , relates n and k with the above mentioned quantities. It is applicable to free - electron metals and includes intraband transitions. Where an intraband transition is taken to mean the transition corresponding to the optical excitation of an electron from below the Fermi energy to another state above the Fermi energy but within the same band. There is no threshold energy for such transitions.

The critirion which determines whether a metal behaves like an ideal free - electron metal or not is the exhibition of a sharp decrease in reflectance at the plasma frequency fact which identifies the plasma resonance.

In the context of optical studies , the plasma resonance refers to an externally forced collective oscillation. However plasma resonance involves the motion of many electrons moving in phase.

The name "plasma resonance" arises by analogy with ionized gases , in which the same phenomenon occurs. Indeed within the free electron

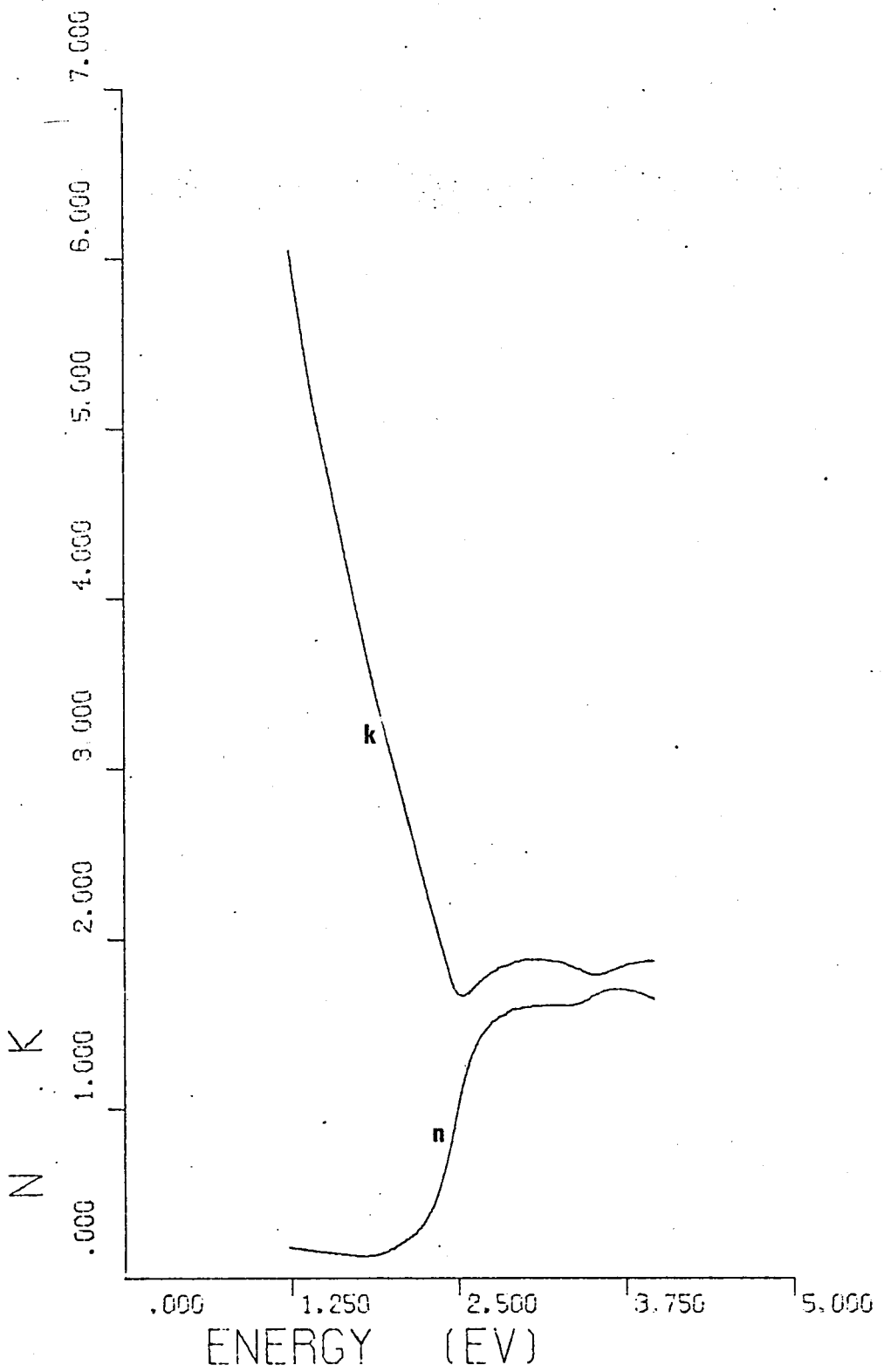

F i g. (4.6)

Optical constants of bulk gold as a function of photon-energy.

approximation electrons in a metal are an electron gas embeded in a material of dielectric constant ε_L .

This is not a true plasma oscillation because it dies when the external electromagnetic driving force vanishes.

The true plasma oscillation is a cooperative collective oscillation that persists even after the external field is removed.

Gold exhibits the characteristic decrease of reflectance (i.e. plasma edge) at the plasma frequency. So the Drude model is applicable in this case.

The predictions of Drude's model for the interaction of radiation with free charge carriers are that the real and imaginary parts of the free electrons dielectric constant $\bar{\varepsilon}_f$, are given by

$$\text{Re } \bar{\varepsilon}_f = n^2 - k^2 = \varepsilon_L \left[1 - \frac{Ne^2}{m^* m \varepsilon_o \varepsilon_L} \cdot \frac{1}{\omega^2 + \tau^{-2}} \right] \qquad (4.27)$$

$$\text{Im } \bar{\varepsilon}_f = 2nk = \frac{Ne^2}{m^* m \varepsilon_o \varepsilon_L} \cdot \frac{1}{\omega^2 + \tau^{-2}} \cdot \frac{1}{\omega \tau} \qquad (4.28)$$

where

$$\frac{Ne^2}{m^* m \varepsilon_o \varepsilon_L} = \omega_p^2$$

Where ε_L may differ from unity because of local field effects and core polarization. Band structure effects are included by using an effective mass , m^* , in these equations , rather than using the free - electron mass , m .

With the aid of these two relationships if n and k are known, the free collision time and the lattice dielectric constant can be found.

Eqs. (4.27) and (4.28) give

$$\left[n^2 - k^2\right] = \varepsilon_L - \tau\left[2 n k \omega\right]$$

Fig. (4.7) shows the behavior of $n^2 - k^2$ against $2nk$. The optical constants for gold are taken from /19/. The intersection of the straight line with orizontal axis gives $\varepsilon_L = 20$ and the slope of the straight line gives $\tau = 1.5 \times 10^{-14}$ sec. These values will be used to make approximations in the derivation of the mathematical expression of our model.

These extrapolated values can be used in the visible part of the electromagnetic spectrum where the plasma edge of gold exists. However, these values are only approximate because the optical constants used have been measured for a thick film of gold. But they still can be used for comparative studies of thin gold films prepared under certain conditions as described in section (2.1.4)

4.3.1 Plasma Edge

The plasma frequency of gold lies in the visible, spectral region, where $\omega\tau \gg 1$. Consequently from Eq. (4.27)

$$\text{Re}\ \bar{\varepsilon}_f = n^2 - k^2 = \varepsilon_L \left(1 - \frac{\omega_p^2}{\omega^2}\right) \qquad (4.29)$$

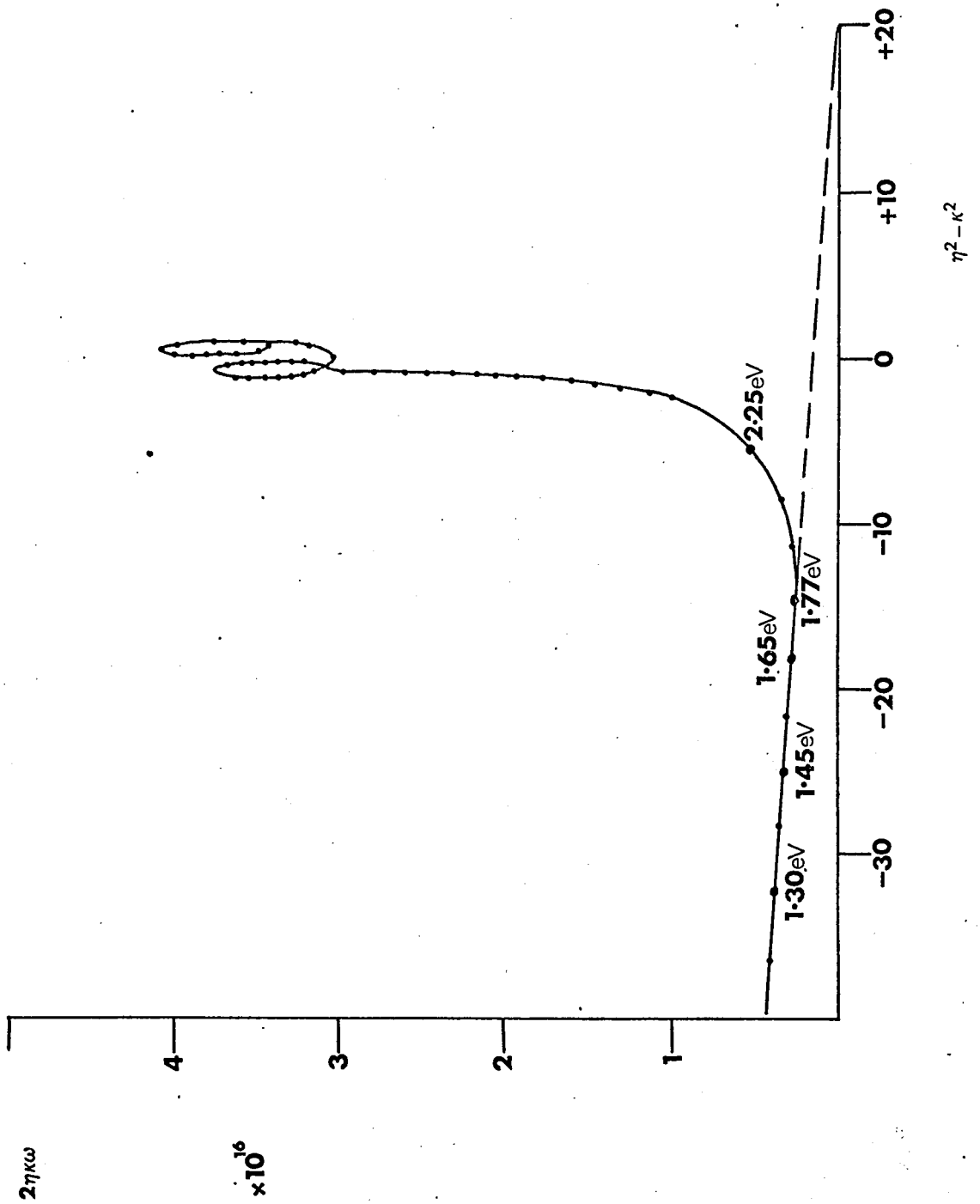

F i g. (4.7)

Calculation of ε_L and τ.

The plasma frequency is defined by

$$n^2 - k^2 = 0$$

and

$$2nk \ll 1$$

From Eq. (4.29) $n = 0$ when $\omega = \omega_p$. Thus at the plasma frequency, $n = 0$ which indicates an infinite phase velocity and an infinite wavelength. For an infinite wavelength many of the electrons may be oscillating in phase. However, there is no polarization charge density as with a true plasma oscillation.

Since the phase angle between the E and H vectors, given by $\tan^{-1}(k/n)$, is now 90°, the Poynting vector is zero, and no energy is propagated into the material. As we have assumed no losses, this clearly means that the reflectivity is unity.

The reflectivity of a gold ambient interface is given by

$$R = \frac{(n - n_o)^2 + k^2}{(n + n_o)^2 + k^2} \qquad (4.30)$$

where n_o and $n - jk$ are the refractive indices of the ambient material and the gold respectively.

Substituting $n = 0$ Eq. (4.30) gives

$$R = 1$$

Hence at the plasma frequency the energy reflectance is 1. From

Eq. (4.30) it can be seen that

$$R = 0$$

when bith $n = n_o$ and $k = 0$. Substituting these values of n and k in Eq. (4.29) we find that the reflectance becomes zero when the frequency of the incident electromagnetic radiation is

$$\omega_o = \left(\frac{\varepsilon_L}{\varepsilon_L - n_o^2} \right)^{\frac{1}{2}} \cdot \omega_p \qquad (4.31)$$

As $n_o^2 \ll \varepsilon_L$, $\omega_o > \omega_p$ and the frequency, for which the reflectance is zero, is approximately the plasma frequency.

So as the frequency of the incident electromagnetic radiation increases from ω_p to ω_o the reflectance falls from 1 to 0. This sharp decrease of the reflectance, near the plasma frequency, determines the plasma edge of the gold, Fig. (4.8).

It must be noted that plasma resonance, unlike resonance absorption, has a finite frequency width even when no energy loss mechanism is involved. From Eq. (4.31), the change from zero to 100 % reflection takes place in a frequency internal

$$\Delta\omega = \left[1 - \left(\frac{\varepsilon_L}{\varepsilon_L - n_o^2} \right)^{\frac{1}{2}} \right] \omega_p \qquad (4.32)$$

As a consequence plasma resonance effects due to electrons in a completely filled energy bend can be observed even though such

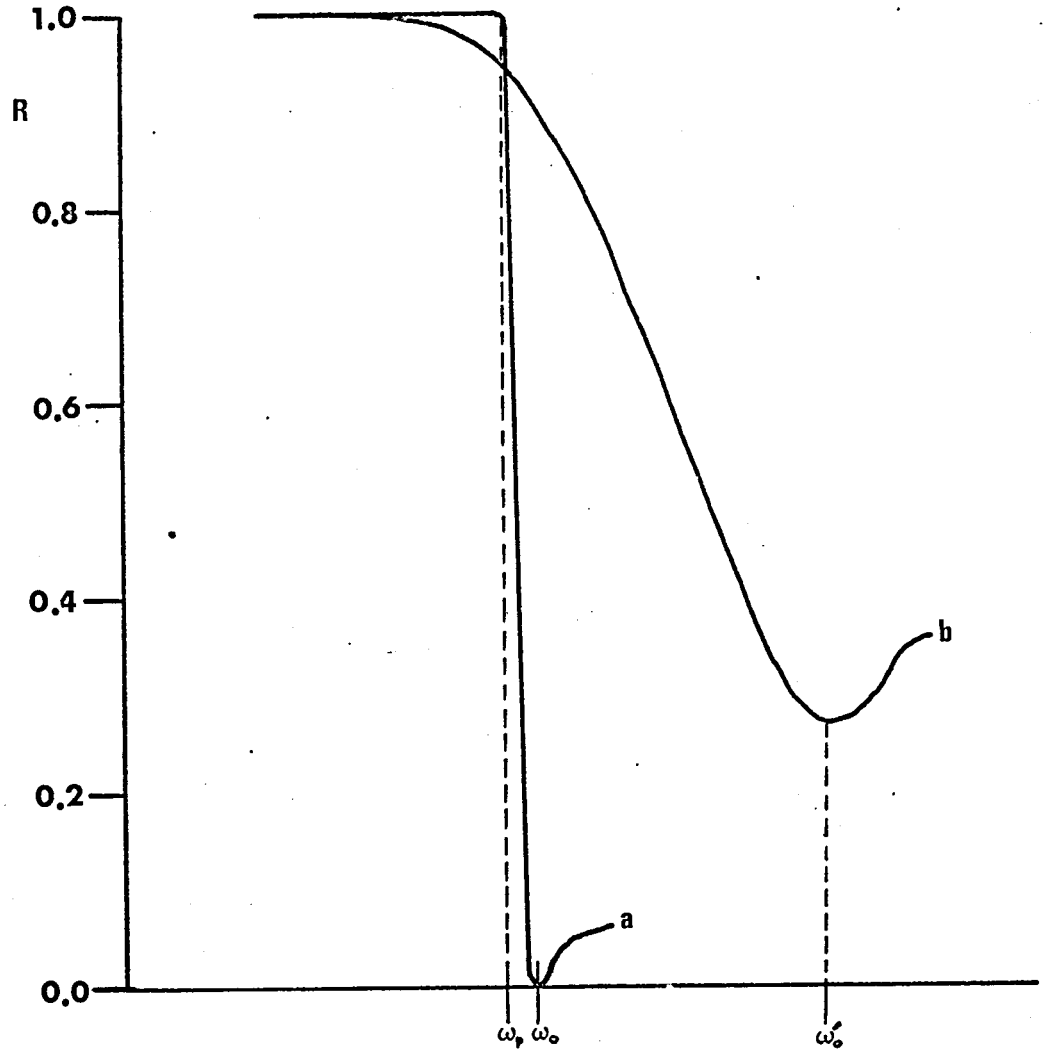

F i g. (4.8)

(a) The plasma edge of an ideal free electron metal .

(b) The plasma edge of a real metal .

electrons cannot contribute to the D.C. conductivity of the material.

For a glass substrate having a refractive index of about 1.5 the reflectance should rise from zero to unity for a change in wavelength of only 3% giving a sharpe characteristic reflection edge.

In practice the reflectivity never reaches unity as n never goes to zero , and it is therefore not possible to determine the plasma frequency directly. However , the refractive index goes through unity and even in lossy materials there is a fairly sharp reflection minimum which may be used to evluate the plasma frequency.

This is of course the ideal case when there is no damping term. In the presense of the damping term , i.e. in the presense of the mean free time between electron collisions , the plasma edge is determined again by the plasma frequency and the frequency where the reflectance falls to a minimum.

The difference is that the plasma edge in this case has a smaller absolute slope. It is not nearly vertical as in the ideal case we have examined . Curve (b) of Fig. (4.8) represents the plasma edge when the mean free time between collisions is taken into account. In this case the minimum of the reflectance occurs above the plasma frequency.

The use of plasma edge reflectance measurements in the past has been confined mainly to the determination of carrier concentration, effective mass at the surface of a metal or semiconductor speciment or the scattering time, /18/ , /28/ , /29/ and /30/ .

As it has been shown the ER spectrum is based on the reflectance spectrum

and specially on the plasma edge. So the detailed study of the plasma edge of gold will enable a better understanding of the nature of the ER spectrum.

4.3.2 The Classical Skin Effect

The equations given above are invalid if the mean free path of the electron (which is determined by the mean free collision time) becomes greater than the skin depth. Under these conditions the electrons interacting with the radiation field have sufficient collisions to remain in thermal equilibrium with the bulk of the electrons or the lattice.

The classical skin depth can be calculated from Eq. (3.18) and Eq. (3.19) with the assumption that at sufficient low frequencies and high purity the lifetime is determined by electron - phonon scattering. In other words the classical skin depth is expressed in terms of the ordinary D.C. electrical conductivity, when $\omega\tau \ll 1$.

For $\omega\tau \gg 1$ it is not correct to use the D.C. electrical conductivity. The use of the D.C. electrical conductivity . The use of the D.C. electrical conductivity implicitly assumes that the electric field acting on an electron is constant for several life times. That is , Ohm's law requires equilibrium . Equilibrium is established by electron - phonon collisions , and it requires several of these events during the period of one oscillation of the electric field.

Deriations from Ohm's law that occur when the electric field varies appreciably during a time τ , that is when $\omega\tau > 1$, are easily handled . At this frequency region Ohm's law must be modified.

A complex conductivity must be used which is related to the D.C. conductivity according to

$$\bar{\sigma} = \sigma_0 / (1 - j\omega\tau) \qquad (4.33)$$

The electrons now move according to the electric field of the incident radiation but they "remember" the electric field at earlier times. That is, the inertia of the electrons leads to relaxation effects.

Drude's model of metals incorporates these relaxation effects into the model by means of the damping term τ.

The nature, then, of the interaction between photons and electrons in metals changes with increasing frequency and electron free collision time.

At the high frequencies inertial effects of the electron become important. This is the relaxation region. Here, the electron suffers many collisions within the skin depth, but the electric field of the incident electromagnetic radiation also oscillates many times between collisions.

As the radiation frequency increases the electrons respond to the oscillating electric field as free - electrons, only occasionally undergoing a collision. Thus the electrons act to screen the external field, so the reflection is high and the absorption is negligible. It must be noted that absorption here refers to the fraction of the incident light absorbed, not to the absorption coefficient.

At very high frequencies, the reflectance drops and transmission is

dominat. We have seen already that transmission takes place above the plasma frequency. Then there is no longer a skin effect. Transmission also occurs below the plasma frequency if $\omega \gg \omega_p^2 \tau$. This follows from Eqs. (4.27) and (4.28) if $\omega\tau \gg 1$, for then, $n^2 - k^2 = 1$ and $2nk = 0$ so that the reflectance and absorption approach zero.

4.3.3 Computation

The theoritical reflectance curves predicted by Howson /18/ have been recomputed over a different frequency range 3.0×10^{14} Hz — 9.7×10^{14} Hz corresponding to the photon - energy region 1.24eV-4eV.

N/m^* was given values of 1,3,5,8 all $\times 10^{28}$ m^{-3} and was given values 1.5 , 3.0 , 7.0 all $\times 10^{-14}$ sec.

A lattice dielectric constant of 20 was assumed which corresponds to gold.

The film was assumed 50 Å , 150 Å , 300 Å thick and to have a non-absorbing substrate of refractive index 1.5. The refractive index of the non - absorbing anbient was assumed 1.33.

Given in Figs.(4.9) are curves of reflectance variation with the above parameters. These curves are similar to those given by Howson /18/ although the frequency region is different.

A rise in the value of N/m^* for the material has the effect of shifting the reflectance minimum to higher frequencies i.e. to higher energies.

A decrease in the value of the mean free collision time has the effect

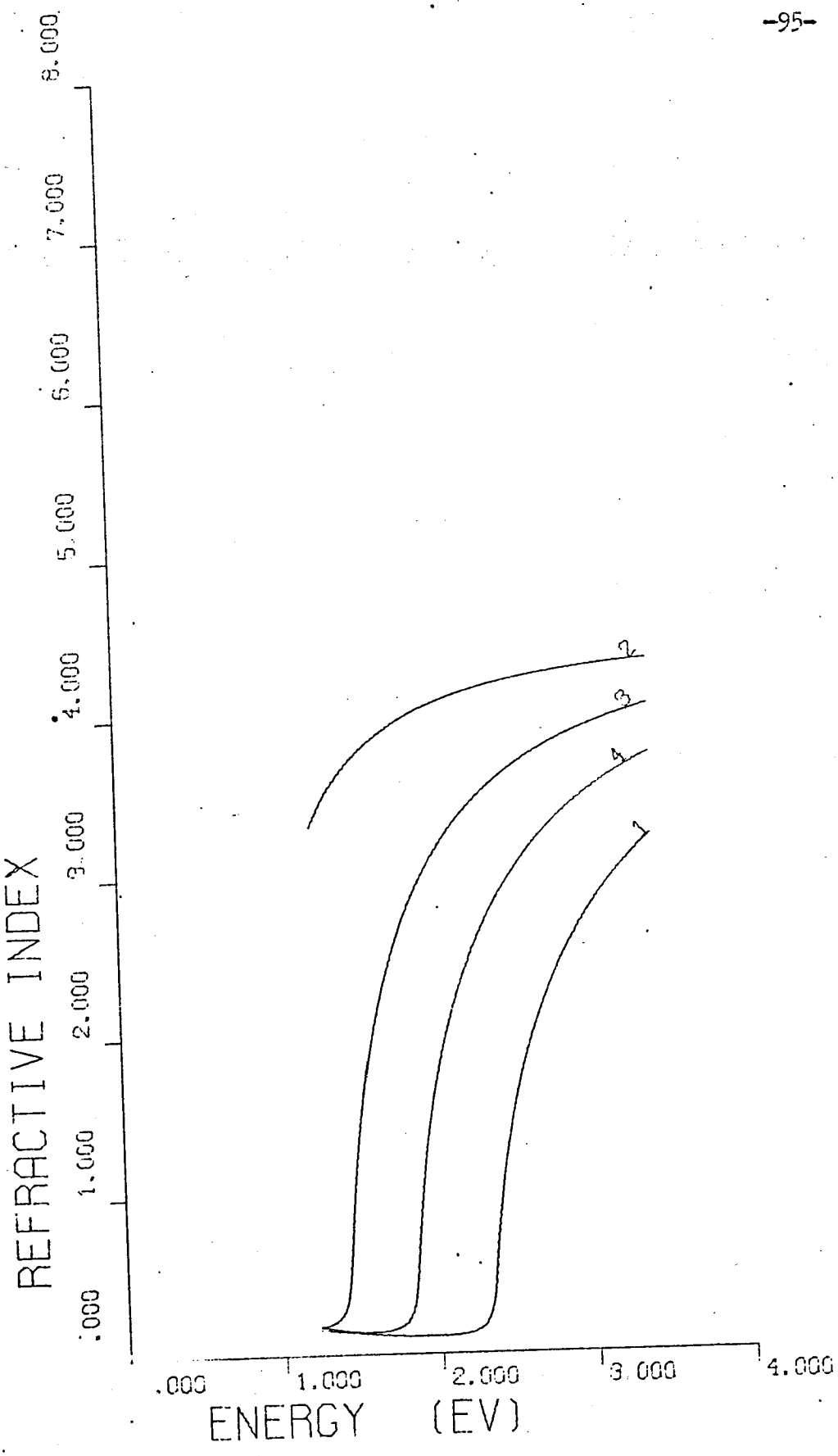

F i g.(4.9 - A)

Computed values of the real refractive index for values of N/m* of 1, 8×10^{28} m^{-3} ; 2 , 1×10^{28} m^{-3} ; 3 , 3×10^{28} m^{-3} ; 4 , 5×10^{28} m^{-3}, shown as a function of frequency for a value of τ of 1.5×10^{-14} .

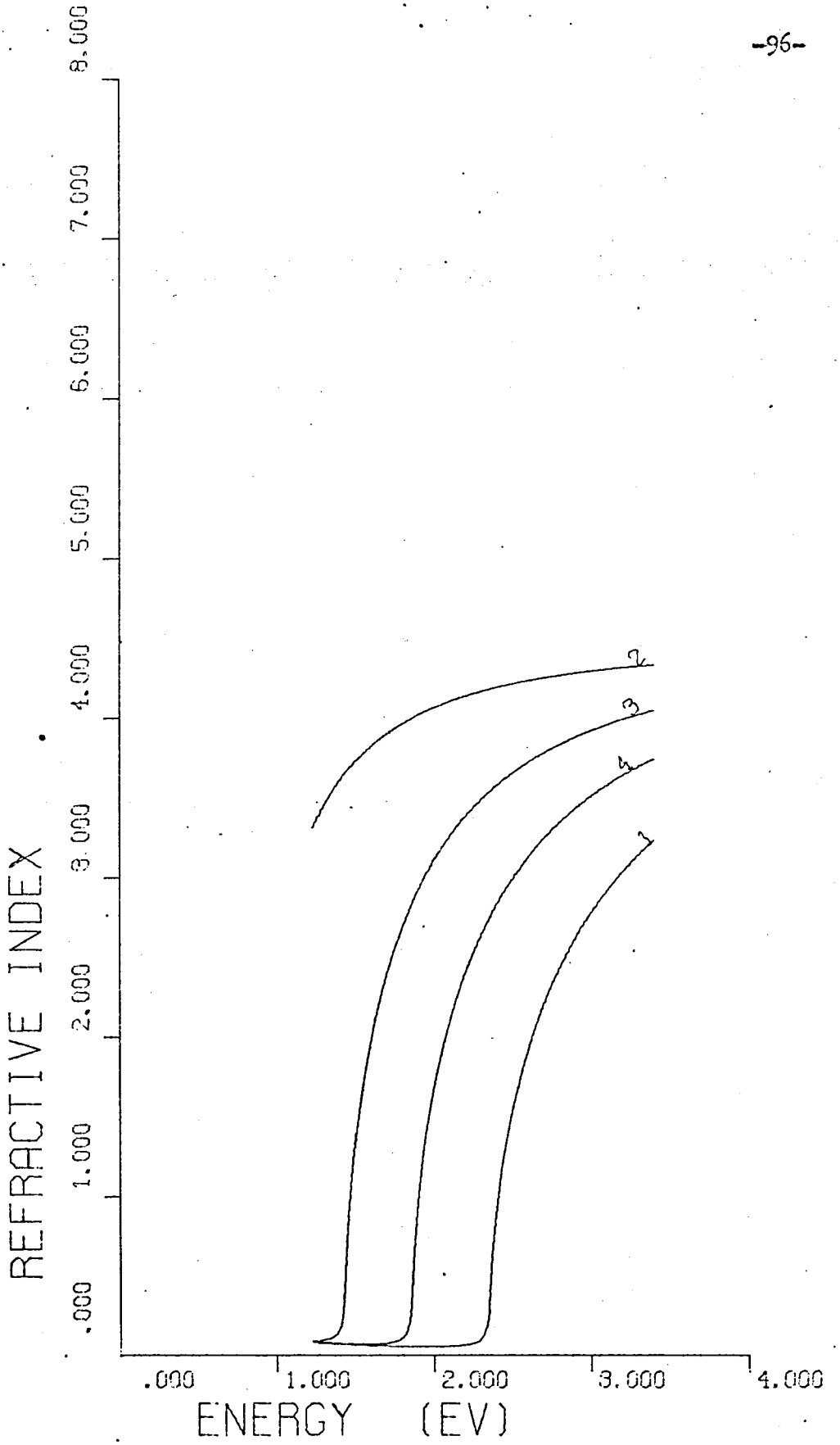

F i g. (4.9 - B)

Computed values of the real refractive index for values of N/m^* of 1 , 8×10^{28} m^{-3} ; 2 , 1×10^{28} m^{-3} ; 3 , 3×10^{28} m^{-3} ; 4 , 5×10^{28} m^{-3}, shown as a function of frequency for a value of τ of 3×10^{-14}.

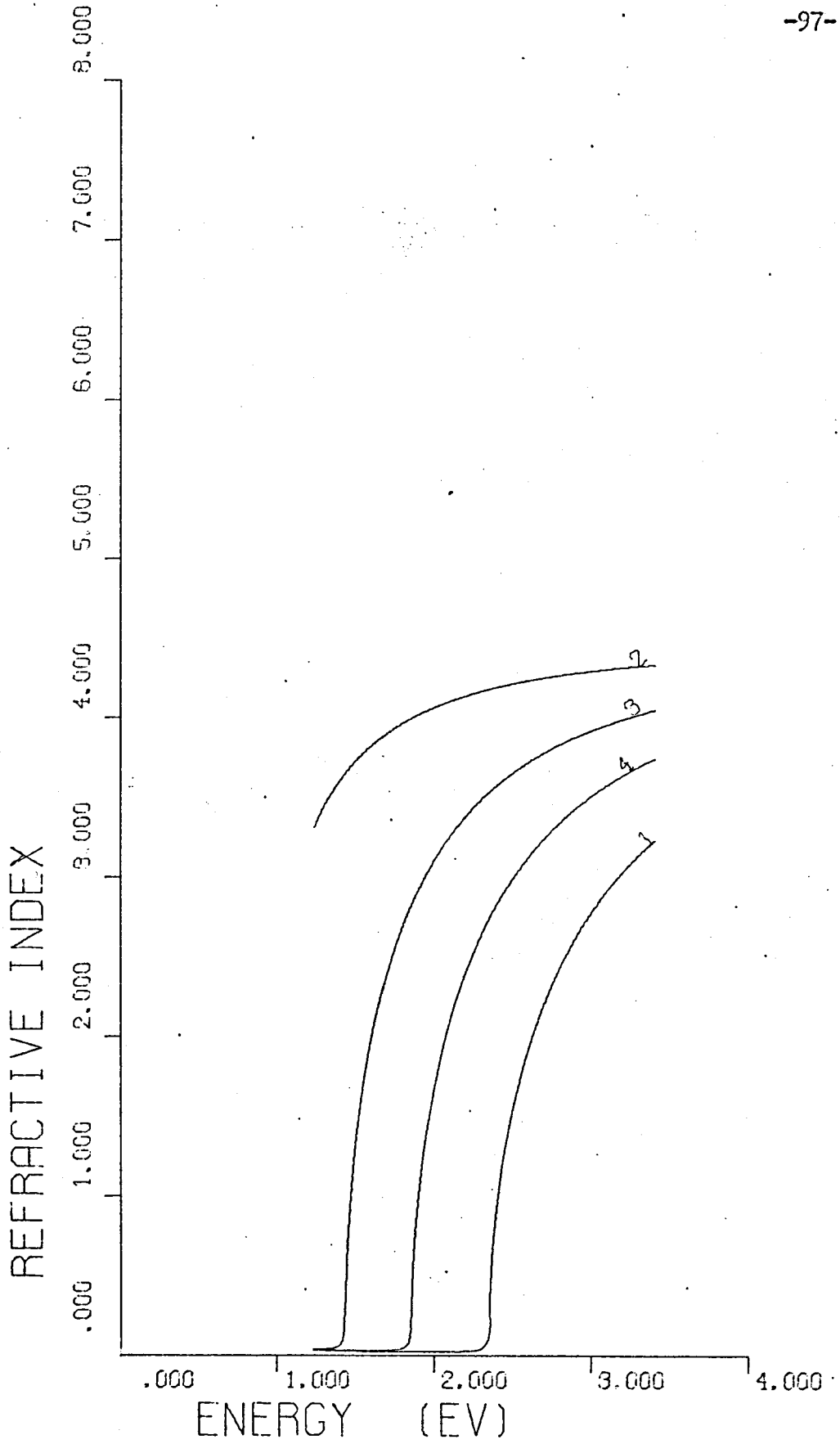

F i g. (4.9 - C)

Computed values of the real refractive index for values of N/m* of 1, 8×10^{28} m^{-3} ; 2 , 1×10^{28} m^{-3};3,3 $\times 10^{28}$ m^{-3} ; 4 , 5×10^{28} m^{-3} , shown as a function of frequency for a value of α of 7×10^{-14}.

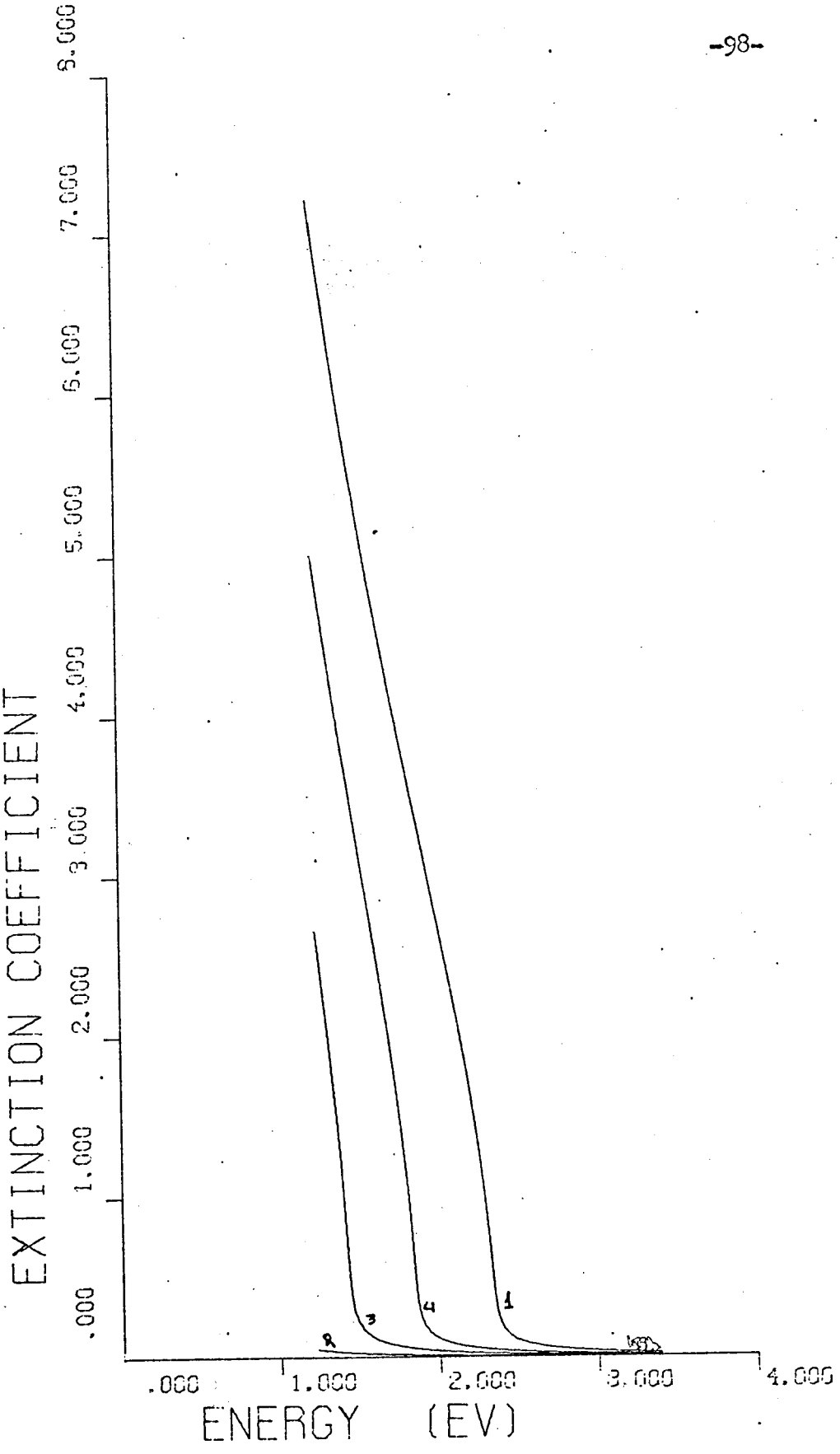

F i g. (4.9 - D)

Computed values of the extinction coefficient for the range of N/m* and κ used for the refractive index in Fig. (4.9-A) and using equivalent indentifying symbols.

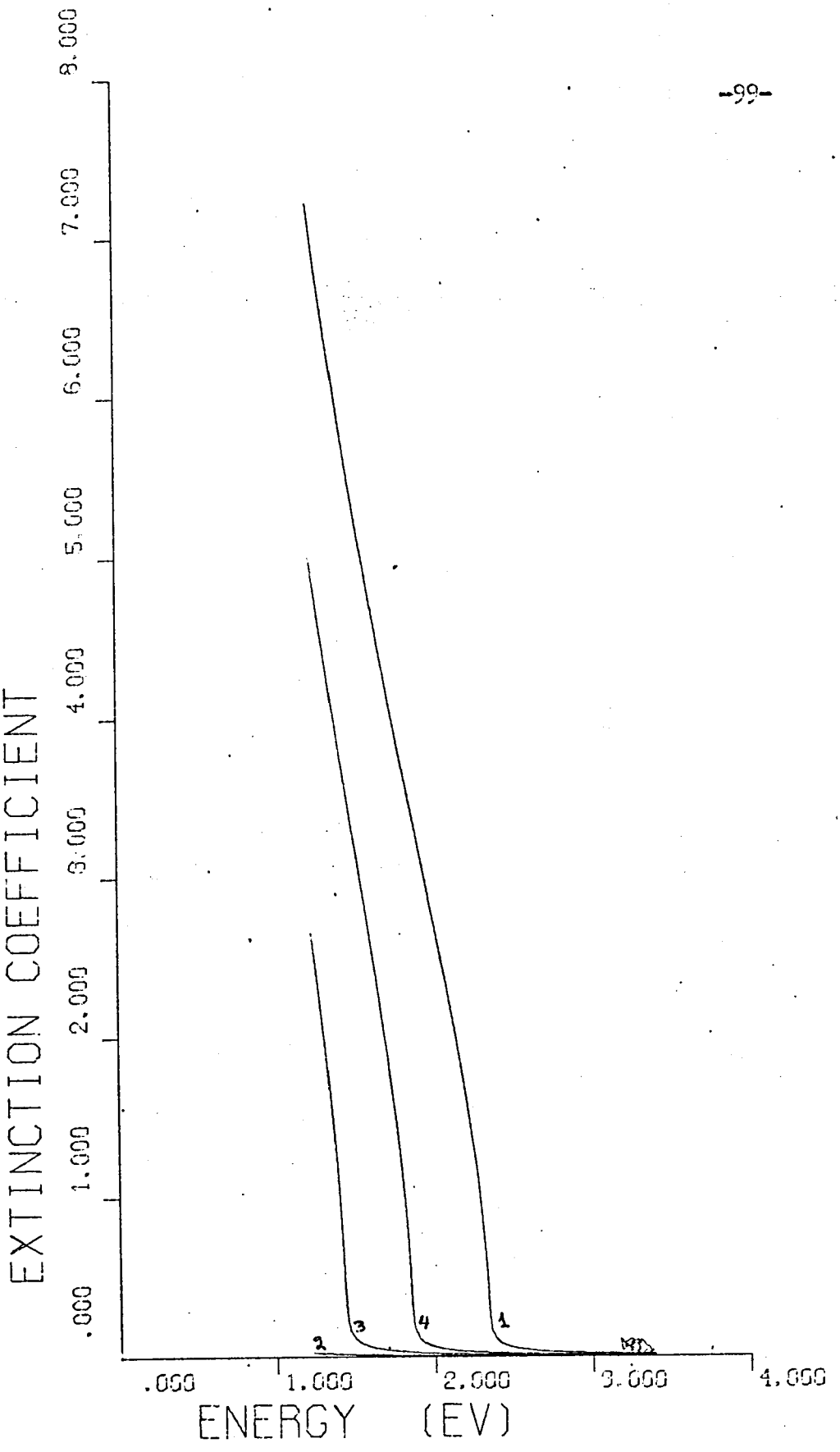

F i g. (4.9 - E)

Computed values of the extinction coefficient for the range of N/m* and α used for the refractive index in Fig.(4.9-B) and using equivalent indentifying symbols.

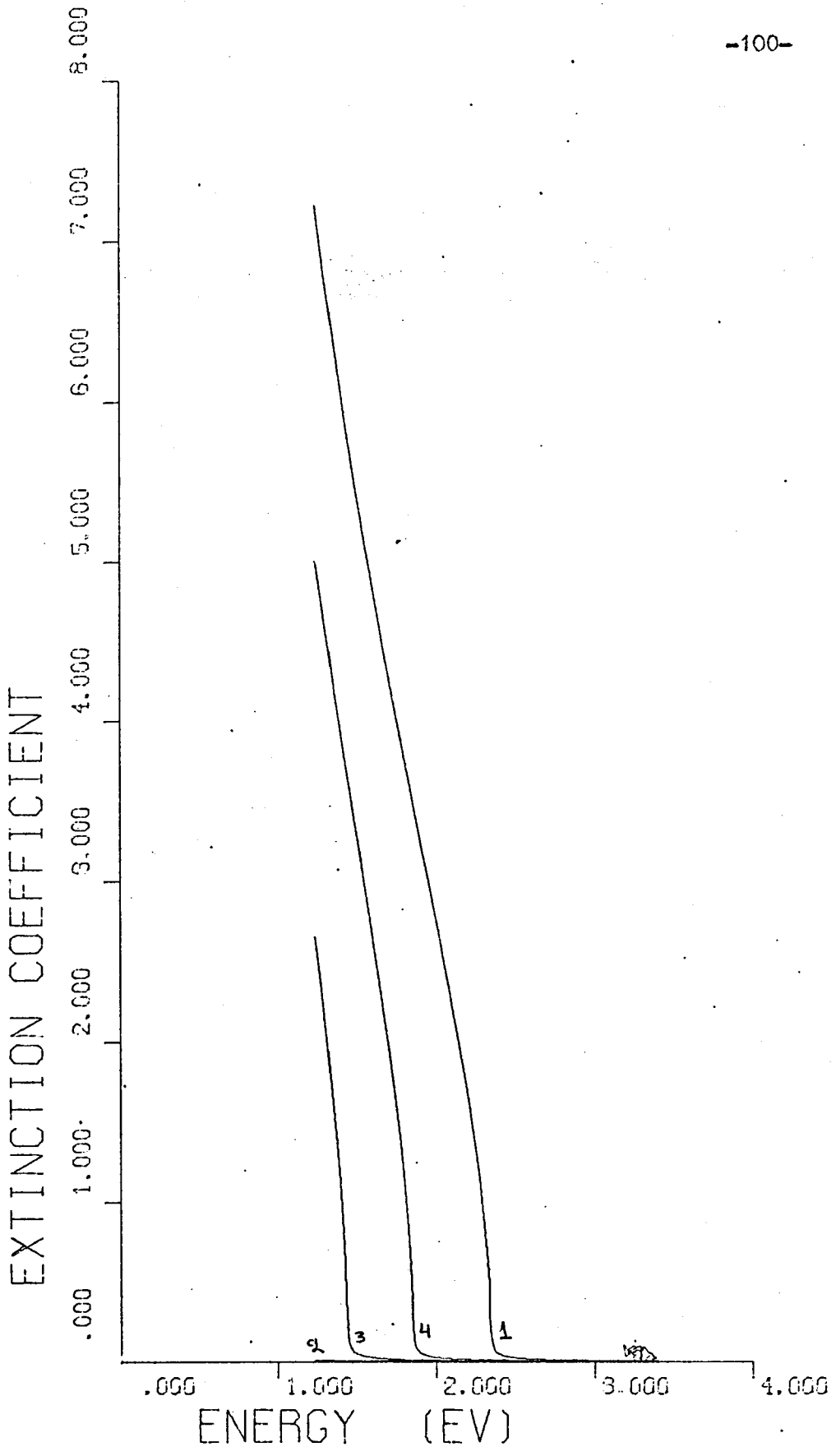

F i g. (4.9 - F)

Computed valucs of the extinction coefficient for the range of N/m* and τ used for the refractive index in Fig.(4.9-C) and using equivalent indentifying symbols.

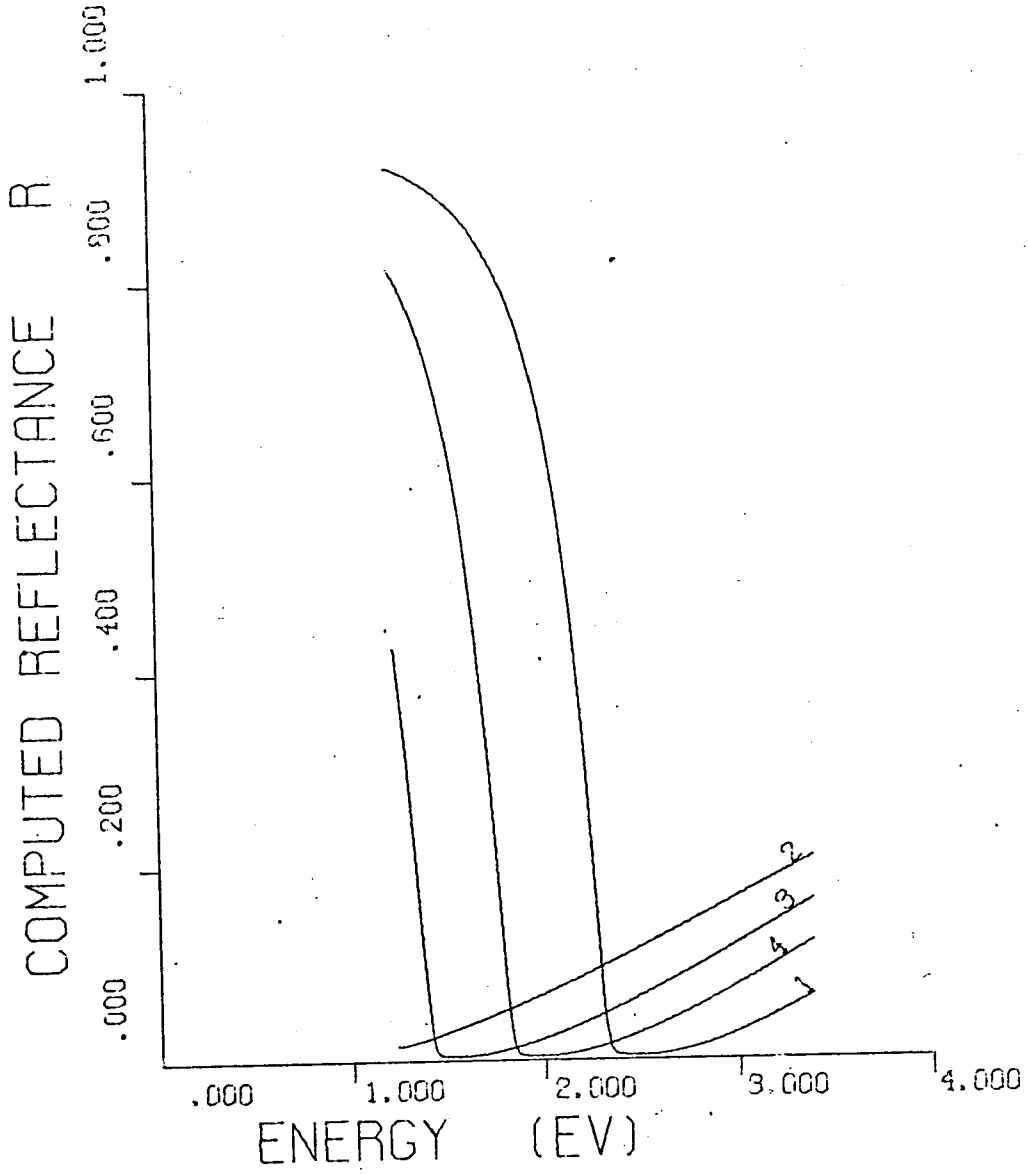

F i g. (4.9 - G)

Reflectance resulting from the computed values of the refractive index and extinction coefficient , given in Fig. (4.9 - A) for film thickness of d = 50 Å .

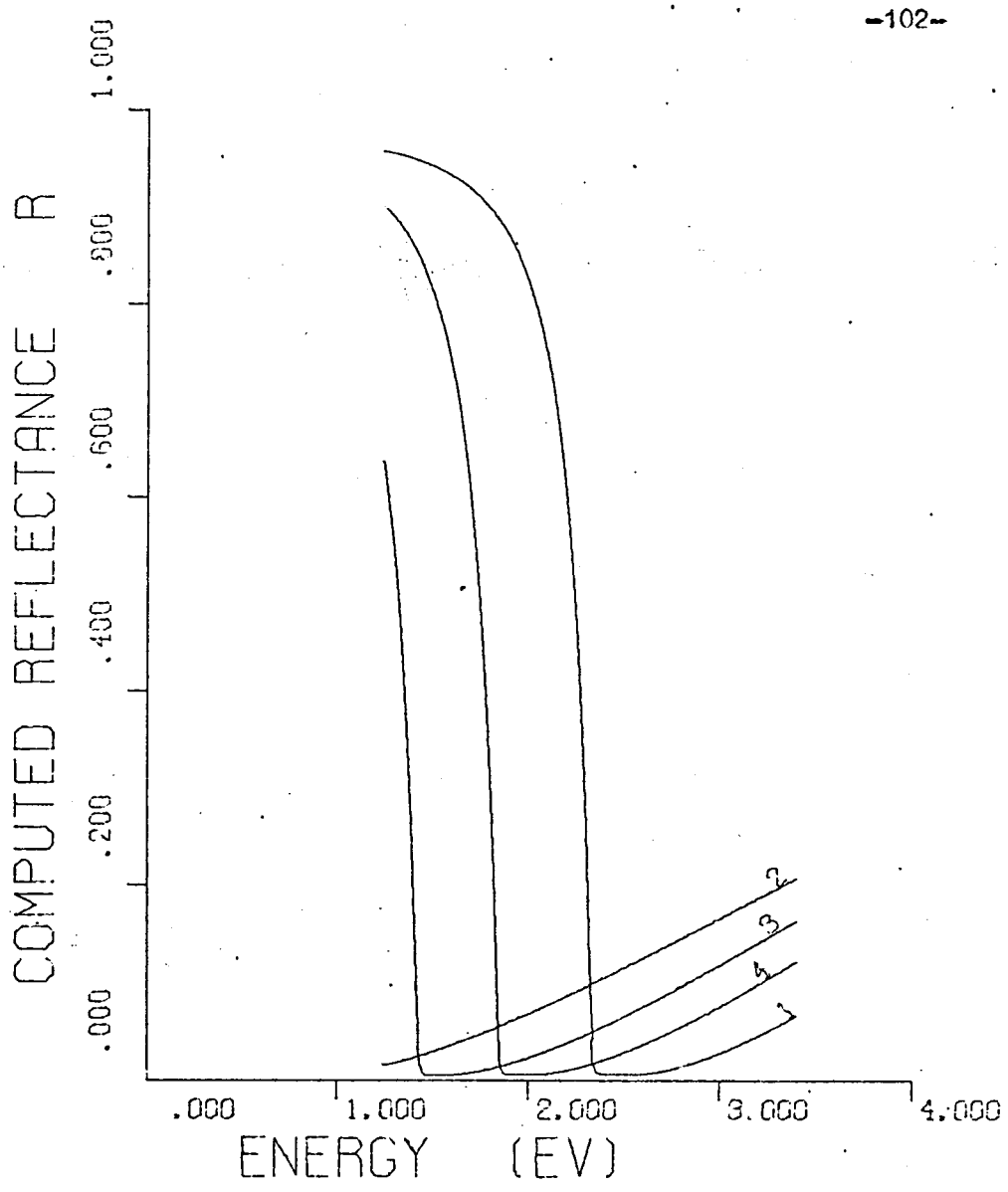

F i g. (4.9 - H)

Reflectance resulting from the computed values of the refractive index and extinction coefficient ,given in Fig.(4.9-B) for film thickness of d = 50 Å .

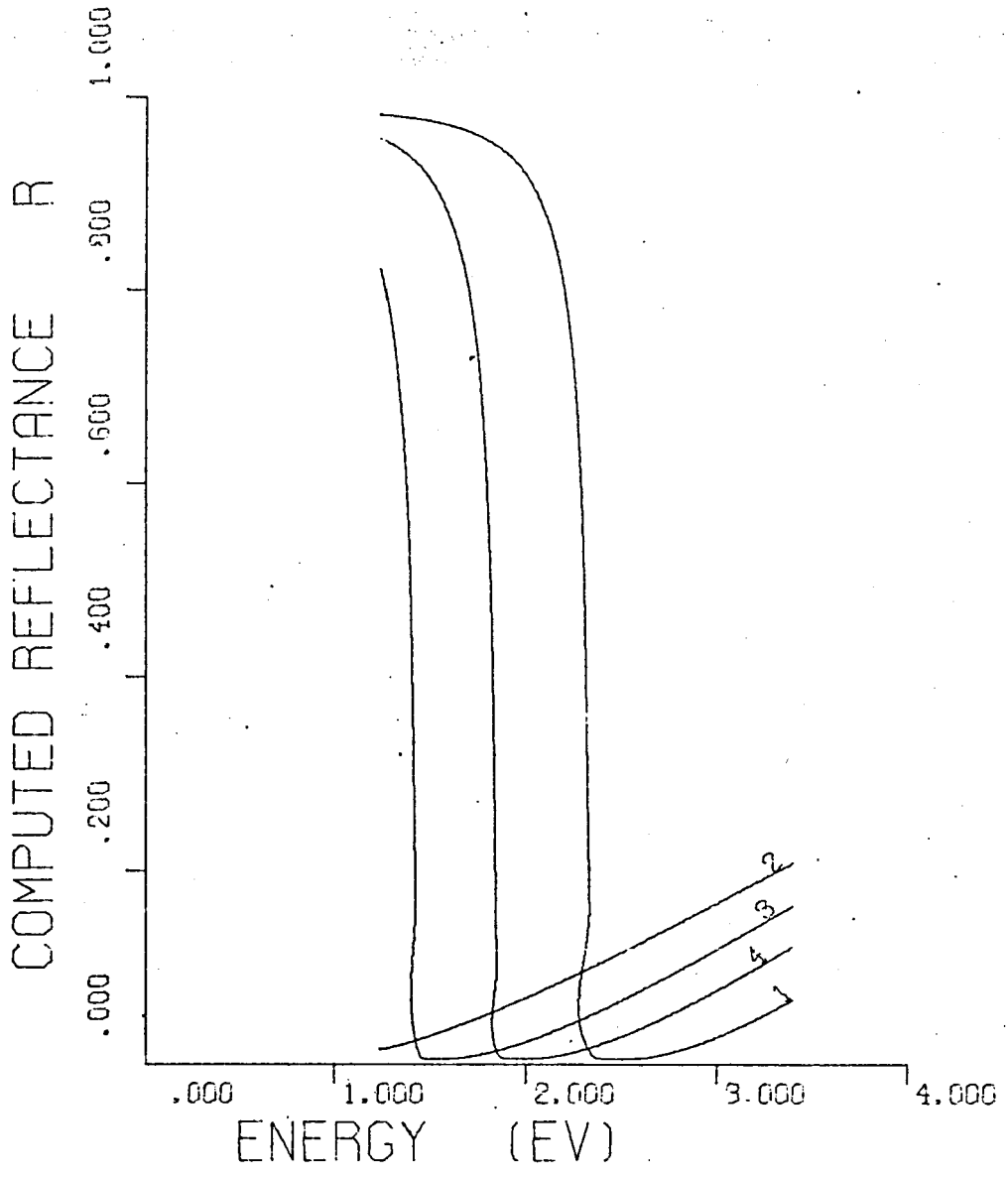

F i g. (4.9 - I)

Reflectance resulting from the computed values of the refractive index and extinction coefficient , given in Fig. (4.9-C) for film thickness of $d = 50$ Å .

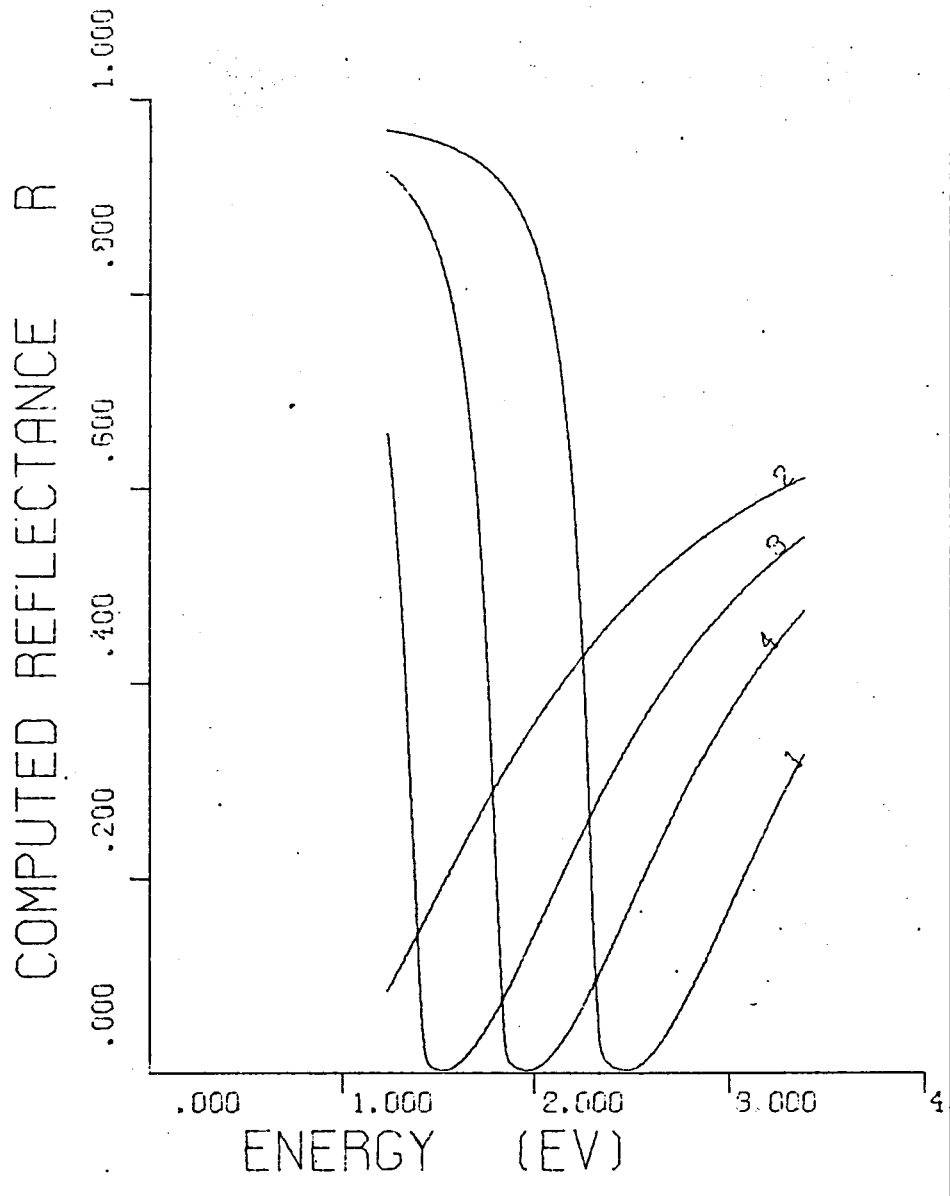

F i g. (4.9 - J)

Reflectance resulting from the computed values of the refractive index and extinction coefficient , given in Fig. (4.9-A) for film thickness of d = 150 Å .

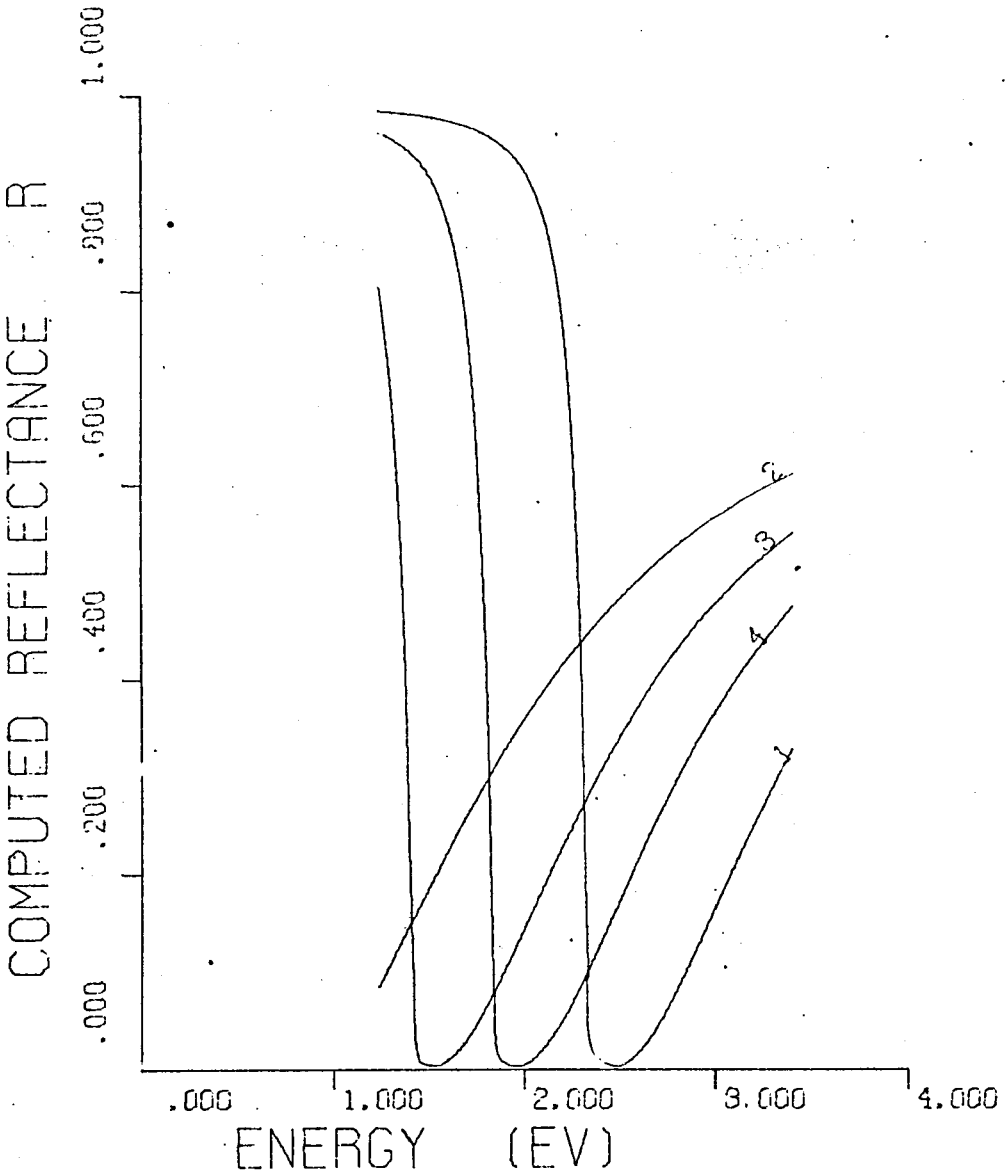

F i g. (4.9 - K)

Reflectance resulting from the computed values of the refractive index and extinction coefficient , given in Fig.(4.9 - B) for film thickness of d= 150 Å .

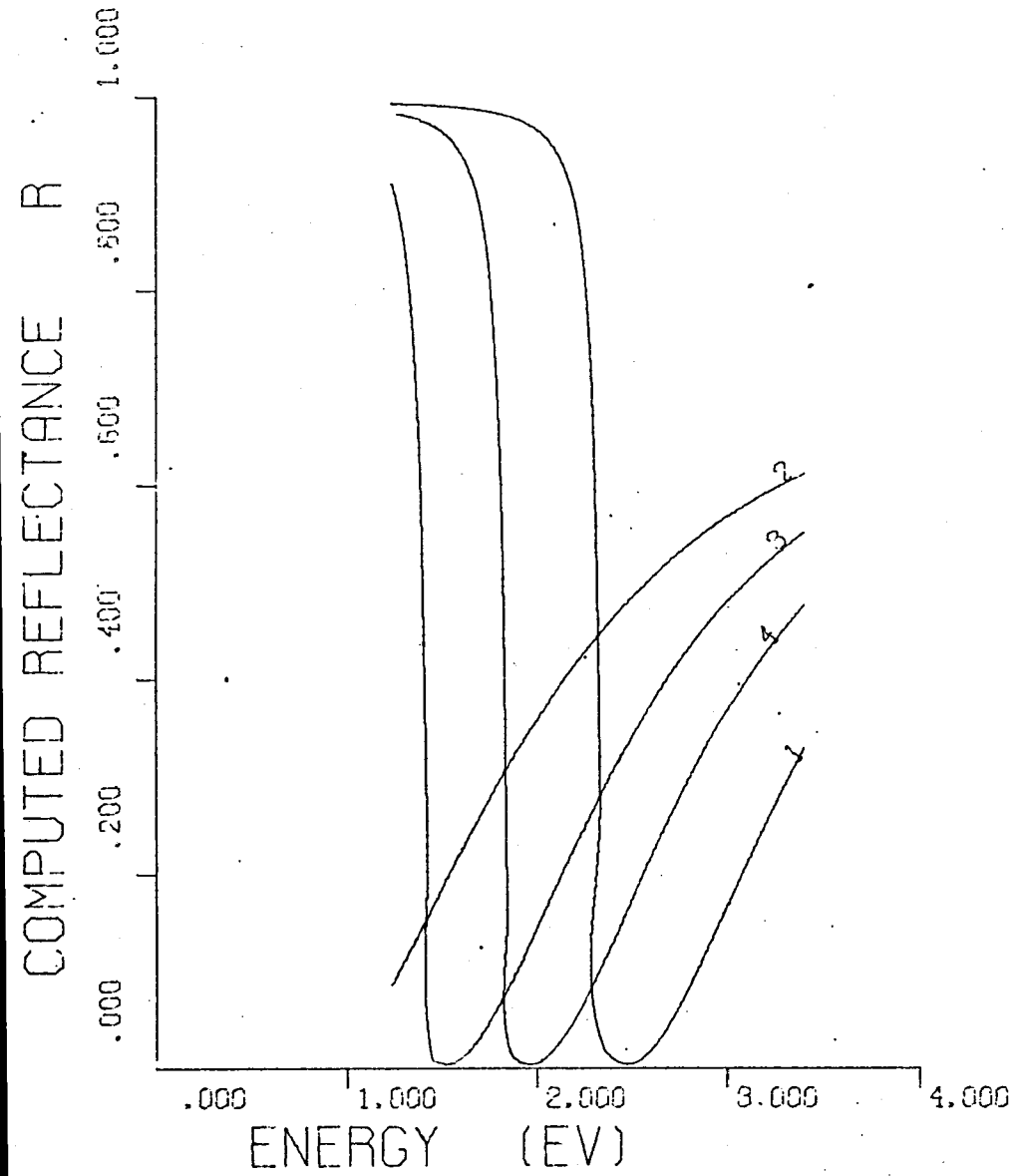

F i g. (4.9 - L)

Reflectance resulting from the computed values of the refractive index and extinction coefficient , given in Fig. (4.9 -C) for film thickness of d = 150 Å .

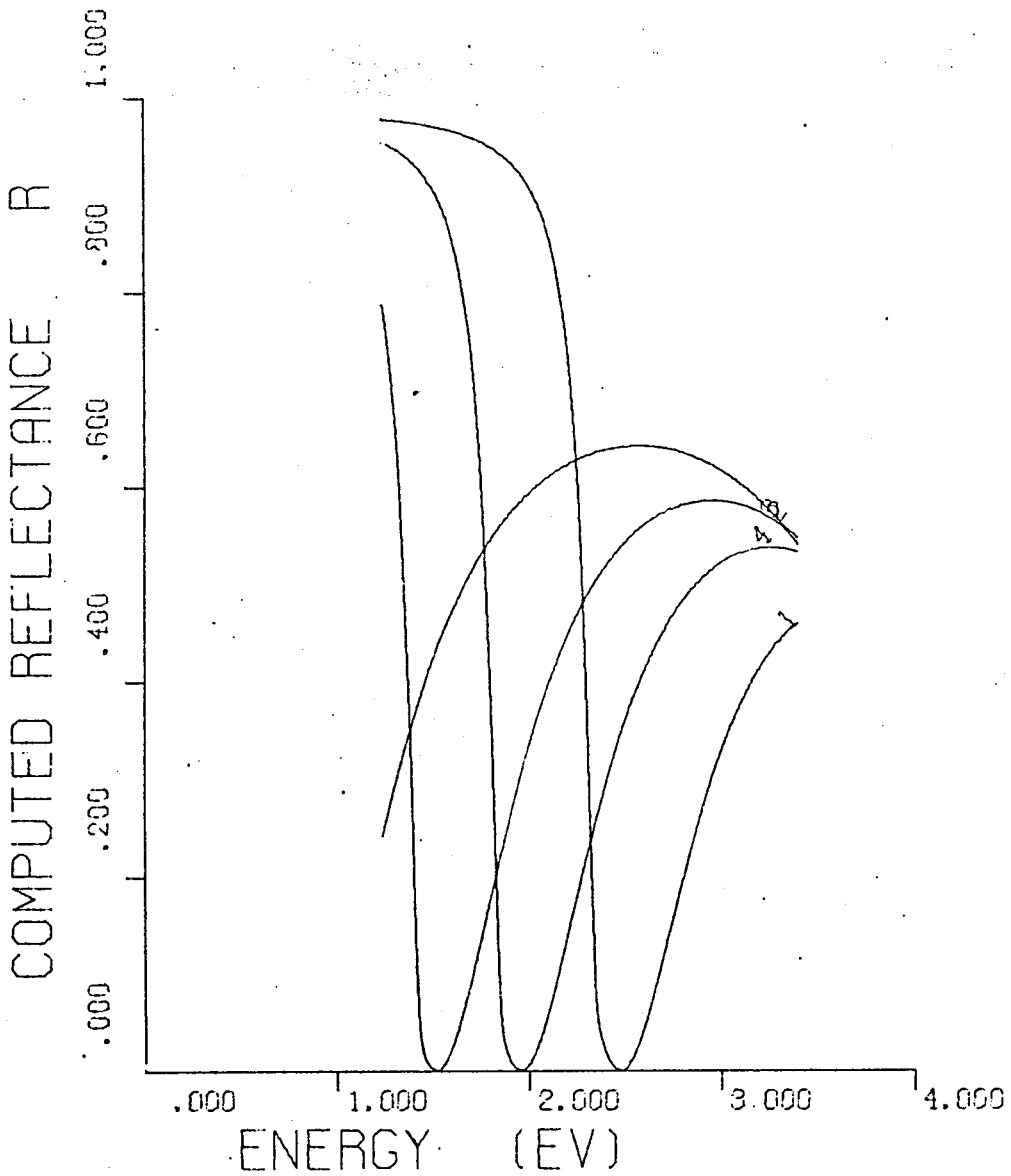

F i g. (4.9 - M)

Reflectance resulting from the computed values of the refractive index and extinction coefficient , given in Fig. (4.9-A) for film thickness of d = 300 Å .

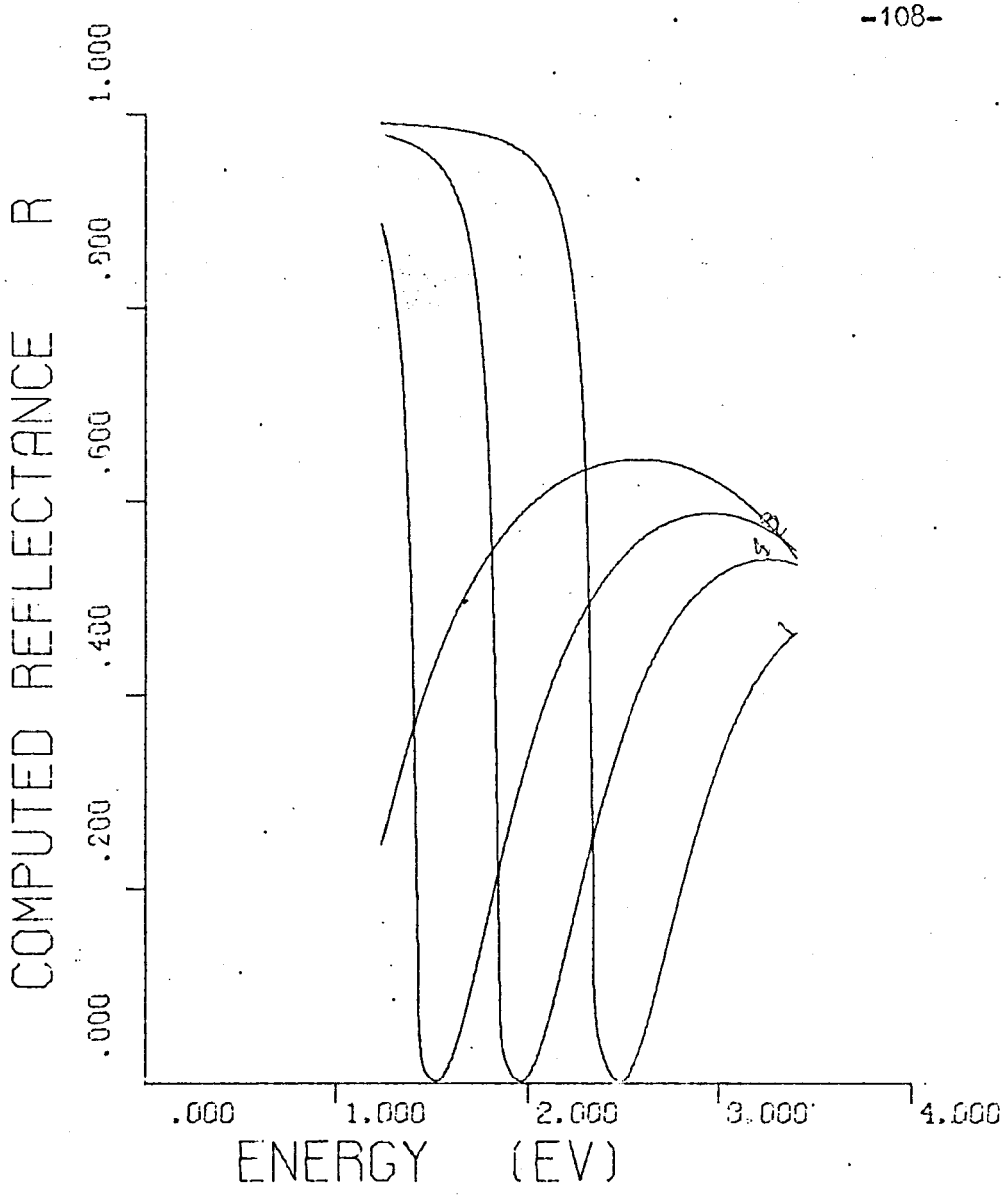

F i g. (4.9 - N)

Reflectance resulting from the computed values of the refractive index and extinction coefficient , given in Fig. (4.9-B) for film thickness of d = 300 Å .

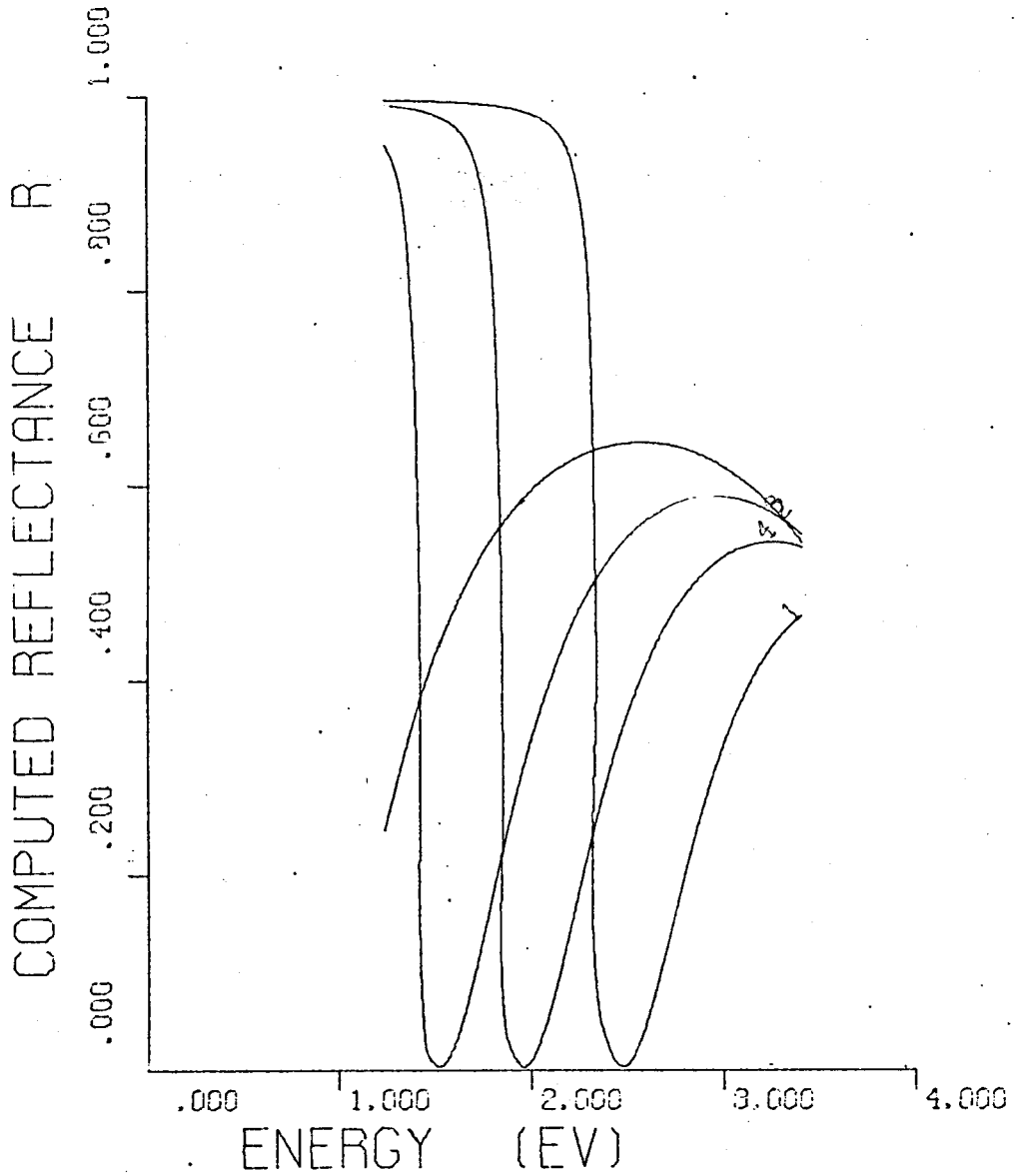

F i g. (4.9 - 0)

Reflectance resulting from the computed values of the refractive index and extinction coefficient , given in Fig. (4.9-C) for film thickness of d = 300 Å .

of reducing the absolute slope of the plasma edge and increasing the value of the minimum reflectance.

A shift of the plasma edge in frequency with temperature may be observed. This may be primarily due to a change in the electron effective mass with temperature , /31/. The mean free collision time increases on cooling and it may become very large in high purity metals at low temperatures.

All the discrepancies observed in Figs. (4.9) are mainly due to the fitting subroutine used by the plotter.

4.4 Electroreflectance in Metals

The electroreflectance (ER) of a metal has already been defined as $\Delta R/R$. Where R is the reflectance and ΔR is the change of the reflectance , due to the application of a strong electric field on the surface of a metal.

It is well established experimentally , that the main peaks of the electroreflectance spectrum for metals occur always in the region of the plasma edge. This means that the electroreflectance effect in this frequency region is associated with the free - electron plasma oscillations. This is indeed the case. The plasma frequency, which determines the location of the plasma edge in the spectrum , is a function of the carriers density (N) as it can be seen from Eq. (1.3). It has been verified experimentally /4/,/12/ that the application of a strong electric field on the surface of a metal changes the optical constants and consequently the reflectivity of the surface region. However , the applied electric field affects the

free electron concentration in the surface region. From Drude's model it becomes clear that a charge in N can be expressed macroscopically as a change of the optical constants of the surface region. And conversely a change in the optical properties denotes a change in N.

It can be proved that a suitable change of the optical constants of the surface region creates a frequency shift of the plasma edge. This already has been shown for gold /4/.

Also the maximum change in the optical constants occurs at that region of the spectrum , at which their rate of change with wavelength is high. This happens in the region where the plasma edge is located. So , we must expect the maximum change in ΔR in the spectral region of the plasma edge. Consequently the maximum of the normalized change of ΔR (i.e. the ER peak) will correspond to the plasma edge frequency - region.

The derivative -like shape of the ER spectrum gave Hansen and Prostak /11/ the wrong impression that the electroreflectance spectrum is simply a normalized first - derivative of the reflectivity with respect to energy. This model is ofcourse inapplicable. For a metal such as Ag, which exhibits a pronounced reflectivity minimum at about 3.9 eV , peaks of both signs should occur in the ER spectrum. But this does not happen /1/ , /20/ , /21/. Only one peak has been observed , corresponding to the frequency region of the plasma edge. Which means that the ER effect is related to intraband transitions , and the contribution of the interband transitions should considered as negligible. Therefore , the low frequency electric field which produces the changes in the optical constants of the surface region and consequently the changes in R , modulates only the intraband transitions

and leaves the interband transitions unaffected.

This is against McIntyre - Aspnes /13/ model which takes into account the contribution from the interband transitions.

We must expect then a peak in the ER spectrum each time the optical constants change rapidly with wavelength and this change is due mainly to intraband transitions. This approach explains qualitatively the shape of the whole experimental ER spectrum in free - electron metals , such as Au , Ag , Zn etc.

It can be concluded that the ER effect in metals is associated with the intraband transitions and it is due to the modulation of the free electron consentration on the surface region.

It is difficult to find out how the free - electron density profile , at the surface , changes with the modulating electric field , or its actual shape for a steady state. What we can estimate is , the penetration depth of the low - frequency electric field. The Thomas - Fermi screening length for a metal is approximately 0.5 Angstroms /20/ . Assuming an exponential - like free - electron density profile in this ultra - thin surface region , we can postulate that the applied electric field on the metal - surface changes only the optical constants of the interface. Which means that the local changes , in R can be expressed in terms of Δn and Δk . Where Δn and Δk are respectively the local changes in refractive index and extinction coefficient of the bulk metal , because of the application of the low frequency modulating electric field on its surface.

Based on these simple statements a new model will be proposed to explain the ER effect in metals.

4.5 Reflectance of the Enhanced Layer

It is assumed now that the application of a strong electric field on the surface of the electrode perturbes the optical constants of a ultra thin layer (ENHANCED LAYER). If $\bar{n}$ is the complex index of refraction of the bulk metal $\bar{n} + \Delta\bar{n}$ is the complex index of refraction of the enhanced layer, Fig.(4.10).

The complex Fresnel coefficients for interface 1 and 2 are given respectively by

$$\bar{r}_1 = \frac{-\bar{n} - \Delta\bar{n} + n_L}{\bar{n} + \Delta\bar{n} + n_L} = \frac{-n + n_L - \Delta n + j\,(k + \Delta k)}{n + n_L + \Delta n - j\,(k + \Delta k)} \qquad (4.34)$$

and

$$\bar{r}_2 = \frac{-\bar{n} + (\bar{n} + \Delta\bar{n})}{\bar{n} + (\bar{n} + \Delta\bar{n})} = \frac{\Delta n - j\,\Delta k}{n + n_L + \Delta n - j\,(k + \Delta k)} \qquad (4.35)$$

where n_L is the real refractive index of the electrolyte solution.

The energy reflectances are given respectively by

$$R_1 = \bar{r}_1\,\bar{r}_1^* > 0 \qquad (4.36)$$

$$R_2 = \bar{r}_2\,\bar{r}_2^* \simeq 0 \qquad (4.37)$$

The change of the refractive index is graduated into the gold film. Consequently the system can be treated as one interface i.e. the total reflectance , R , of the system is yield by

$$R = R_1 = \bar{r}_1\,\bar{r}_1^* \qquad (4.38)$$

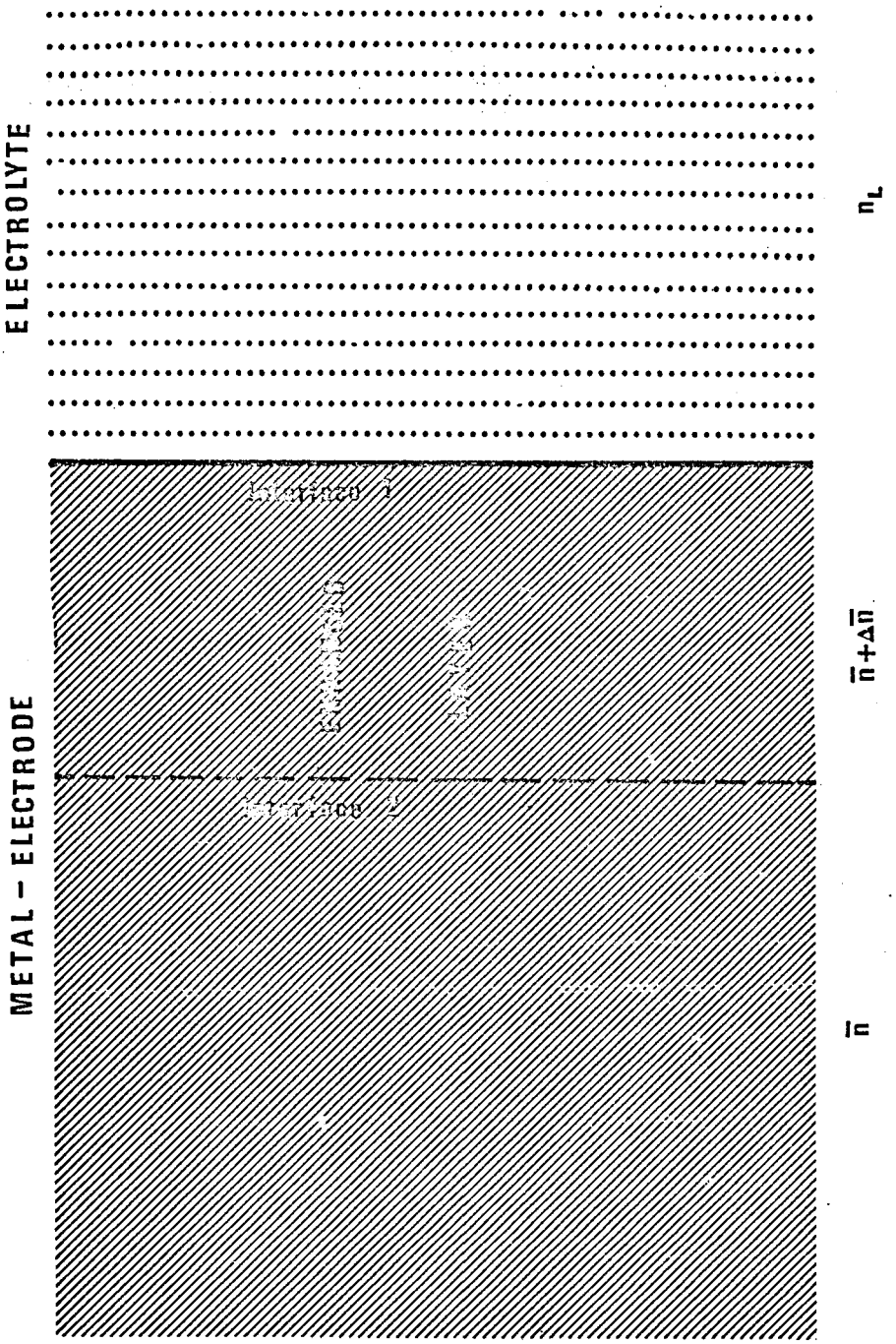

F i g. (4.10)

The enhanced layer .

4.6 Electroreflectance of a Gold - Mirror Electrode

Consider a gold - mirror electrode with a modulating electric field applied on its surface .

The complex Fresnel coefficient of reflection for the gold - electrolyte interface is

$$\bar{r} = \frac{n_L - (n - jk)}{n_L + (n - jk)} = \frac{n_L^2 - n^2 - k^2 + 2jkn_L}{(n_L + n)^2 + k^2} \qquad (4.39)$$

Consequently the energy reflectance of the same interface is given by

$$R = \bar{r}\,\bar{r}^* = \frac{(n^2 - n_L^2 + k^2)^2 + 4k^2 n_L^2}{\left[(n_L + n)^2 + k^2\right]^2} \qquad (4.40)$$

where n and k are respectively the refractive index and the extinction coefficient of gold . n_L is the refractive index of the electrolyte. The change ΔR of the energy reflectance can be expressed in terms of the changes of the optical constants of the surface of the gold mirror , by differentiating Eq. 4.40 with respect to N. Where ΔN is the change of the free electron concentration on the surface . Taking the normalized change of the reflectance , in other words the magnitude of the ER effect we have

$$\frac{\Delta R}{R\Delta N} = \frac{4(n^2 - n_L^2 + k^2)\left(n\frac{\Delta n}{\Delta N} + \frac{k\Delta k}{\Delta N}\right) + 8kn_L^2\frac{\Delta k}{\Delta N}}{\left[(n^2 - n_L^2 + k^2)^2 + 4k^2 n_L^2\right]} -$$

$$- \frac{2\left[(n + n_L)\frac{\Delta n}{\Delta N} + \frac{k\Delta k}{\Delta N}\right]}{\left[(n + n_L)^2 + k^2\right]} \qquad (4.41)$$

Making use of Drude's equations (Eqs.(4.27) , (4.28)) $\Delta n/\Delta N$ and $\Delta k / \Delta N$ can be expressed as

$$\frac{\Delta n}{\Delta N} \equiv - \frac{n}{2\cdot(n^2 + k^2)} \cdot \frac{\omega_p^2}{\omega^2 N} \qquad (4.42)$$

and

$$\frac{\Delta k}{\Delta N} = \frac{k}{2(n^2 + k^2)} \cdot \frac{\omega_p^2}{\omega^2 N} \qquad (4.43)$$

assuming

$$k \ll \tau \omega \qquad (4.44)$$

This assumption can be verified using as τ and ω the values from the section 4.3 and as k , the highest value of k which is approximatelly 4 .

Computer calculations of the quantity $\frac{1}{R} \frac{\Delta R}{\Delta N}$ as a function of energy give a spectral distribution for the magnitude of the ER effect , part of which is presented in Fig . (4.11) . Compairing our theoritical results with the experimental results of other researchers/21/ in the case of external reflection spectroscopy , we find that it fits satisfactory with the experimental ER spectrum of gold.

According to eqs. (4.41), (4.42) and (4.43) a general expression of our model can be given by .

$$\frac{\Delta R}{R} = f(n, k)\, \omega_p^2 \cdot \frac{\Delta N}{N} \cdot \omega^{-2} \qquad (4.45)$$

The above formula includes the term $f(n, k)$, which is a function of the optical constants of the bulk gold. Consequently the ER spectrum is determined by the optical constants , the plasma frequency

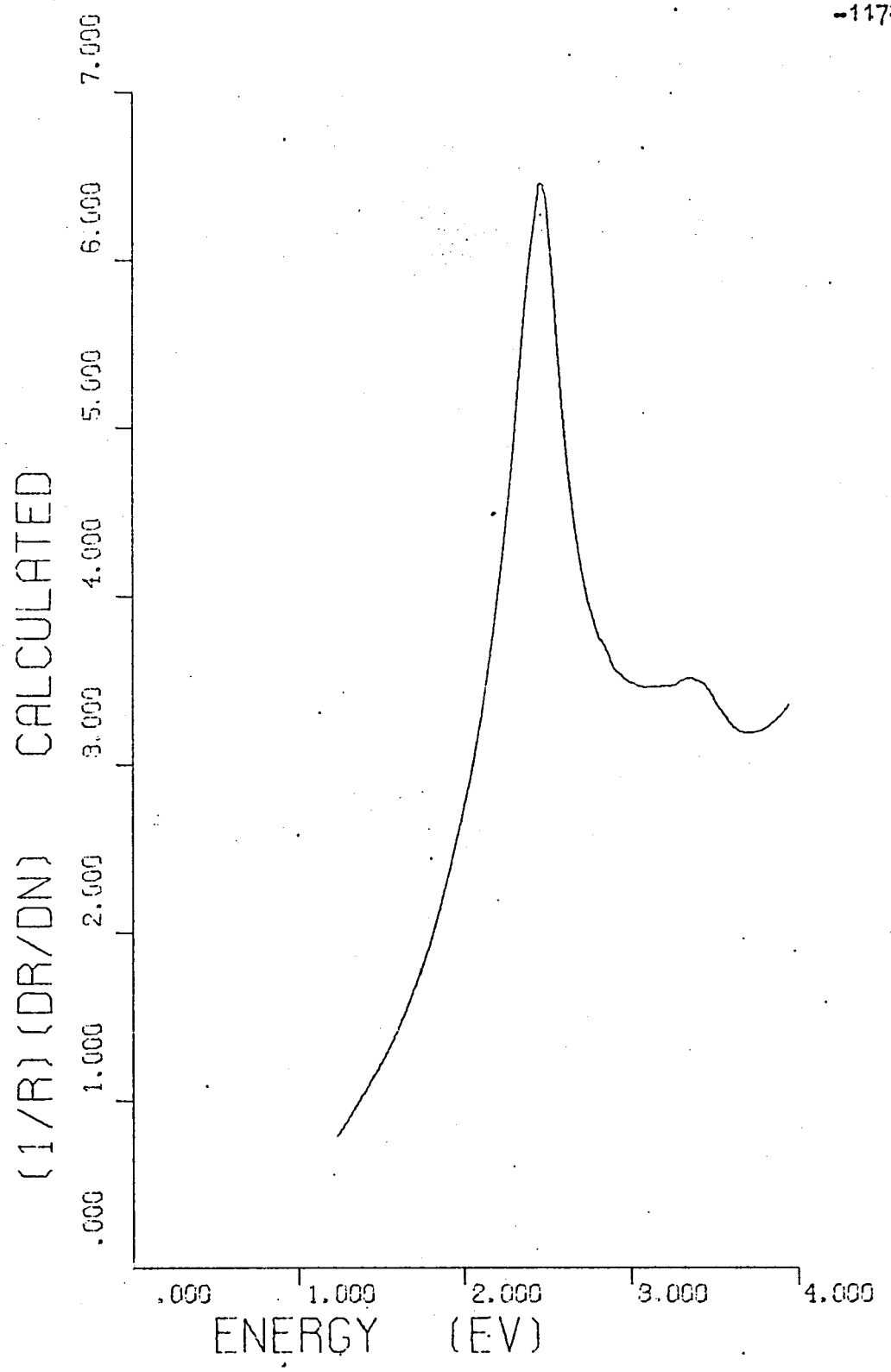

F i g. (4.11)

ER spectrum of bulk gold according to the proposed model.

and the normalized change of the free - electron concentration at the surface of the gold because of the modulating electric field.

On the other hand the ER spectrum is independent of the depth of the induced perturbation in the optical properties of the metal (i.e. the screening length). Hence the ER effect depends upon the continuous change of the free - electron surface - concentration which the incident light "sees" .

4.6.1 Application of the Proposed Model in the Case of Silver

As it has already been stated , silver exhibits a plasma edge at about 3.9 eV , and a sharp increase of the reflectance just above the plasma frequency , characteristic of interband transitions.

This characteristic feature of the reflectance spectrum of silver will help the verification of the proposed model.

The prediction of our model , i.e. Eq. (4.45), was used for the evaluation of the ER spectrum of a silver - mirror electrode. The optical constants of silver used were taken from /19a/ and /19b/. See Fig. (4.13a).

Figs. (4.12) and (4.13) show the results for the reflectance and ER spectrum of silver respectively.

The sharp ER peak is located at the photon - energy region of the plasma edge. This is in fairly good agreement with the experimental results of other researchers /1/ , /20/ and /21/ .

The existed discrepancies may due to the values of the optical constants used and to the fact that the values of the optical constants of

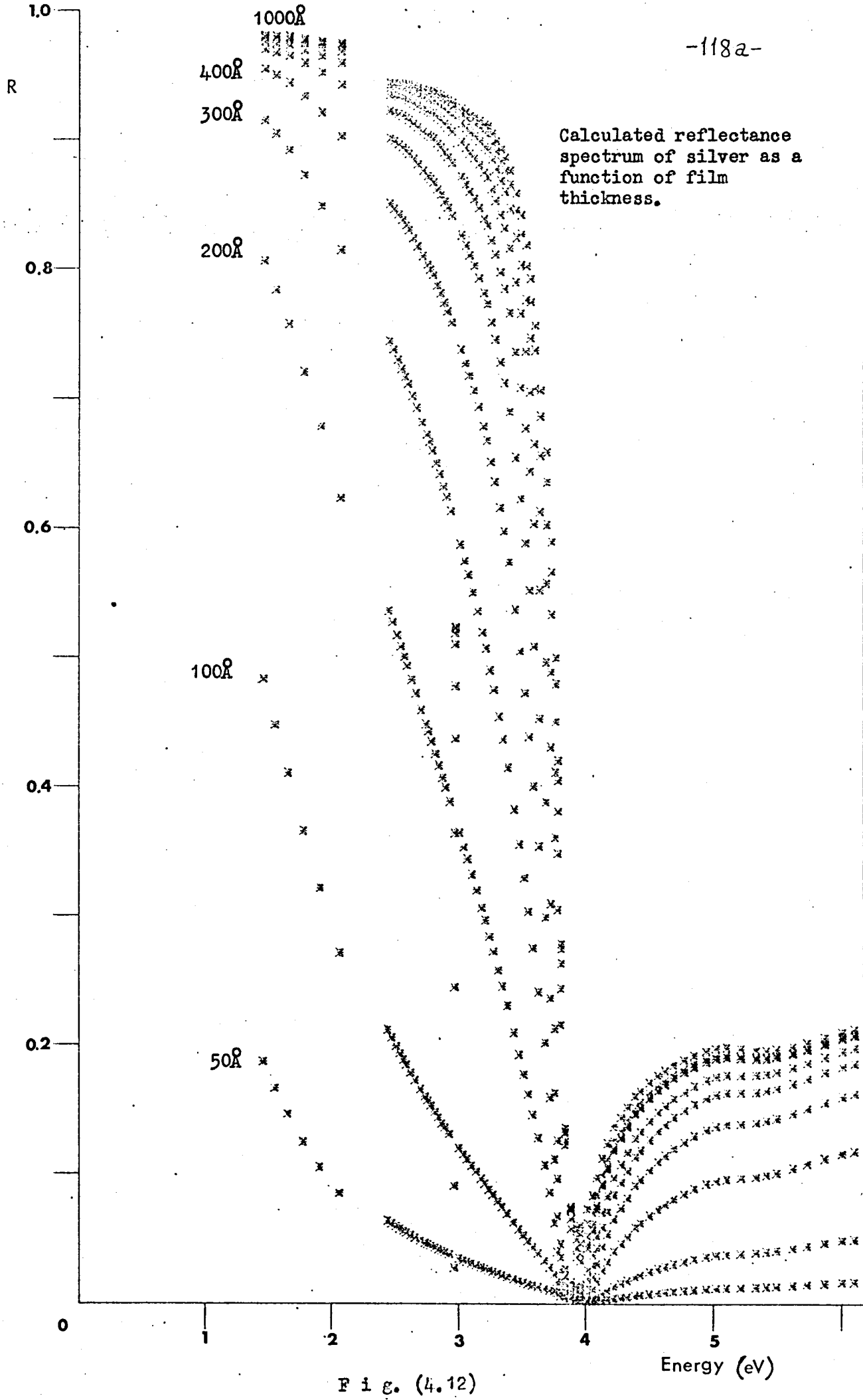

Calculated reflectance spectrum of silver as a function of film thickness.

F i g. (4.12)

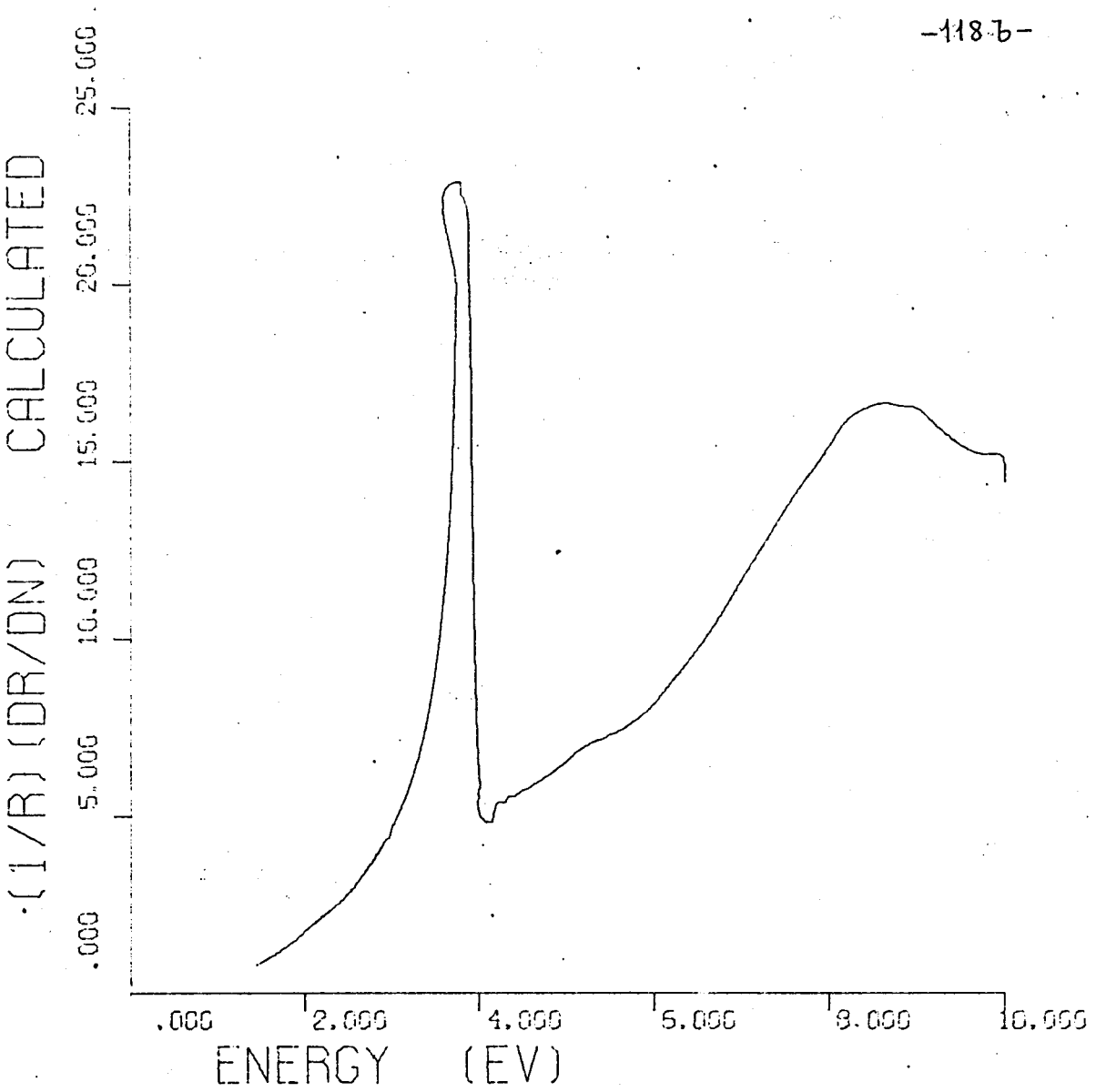

F i g. (4.13)

ER spectrum of bulk silver according to the proposed model.

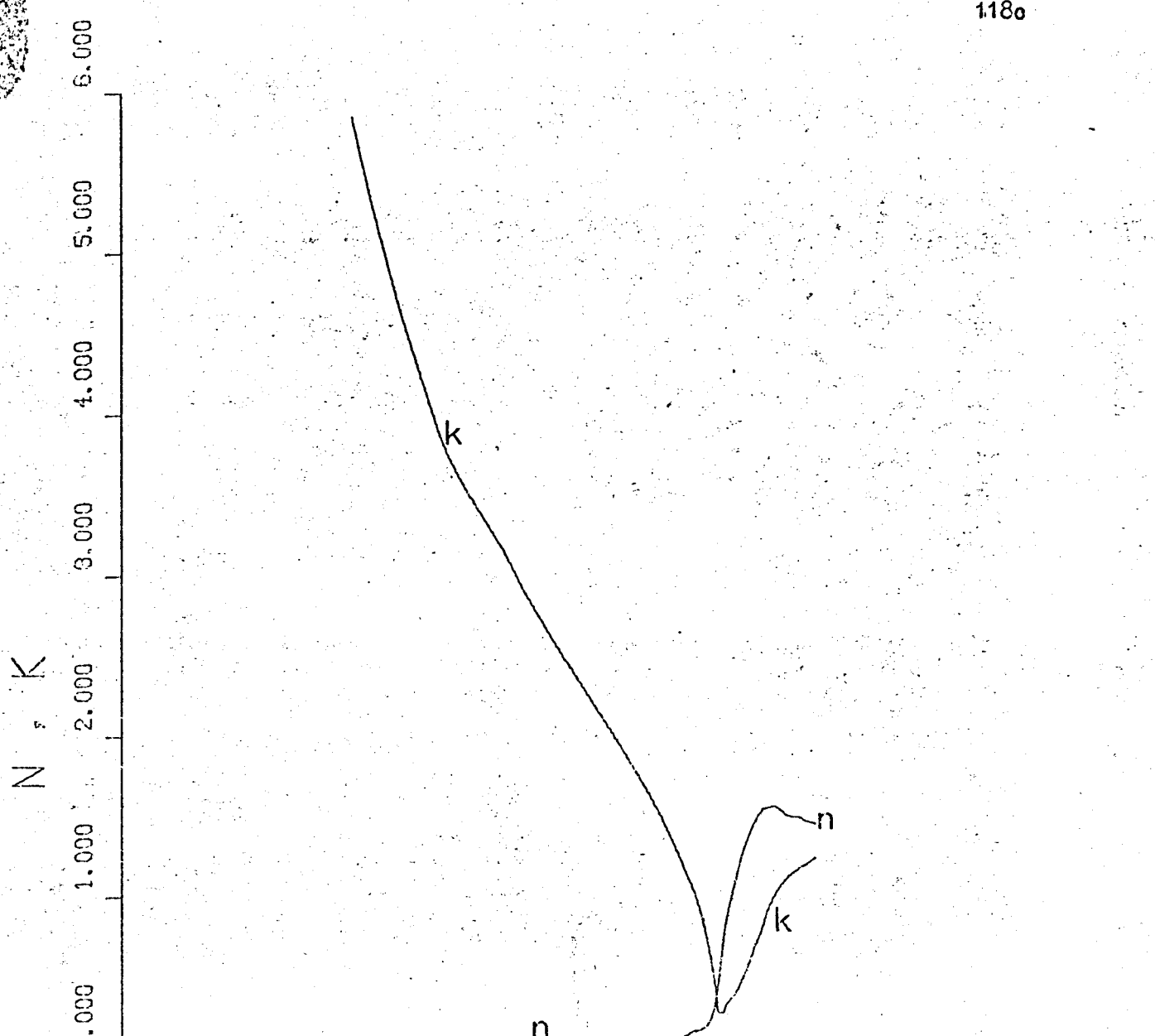

F i g . (4.13a)

Optical constants of bulk silver as a function of photon - energy.

reference /19a/ are lower than these of reference /19b/.

The reflectance curves correspond to different film thicknesses and have been drawn point by point to demostrate gaps and discontinuities in the values of the optical constants used for silver.

Computer calculations of the electron free collision time and lattice dielectric constant of silver , as in the case of gold , have shown that the approximations of our model are valid for silver in the used spectral region.

4.7 ER and ET Effect in Thin Films of Gold

The ER effect in thin films of gold can be explained in the same way as in the case of a gold - mirror electrode , i.e. considering that the optical constants of the gold - electrolyte interface only change with the applied electric field. The gold - substrate interface remains unaffected. This assumption is based on the fact that the screening length in metals is of the order of 0.1 Å . Hence, if the thickness of the film is more than 70 Å , the gold - substrate interface remains unaffected from any perturbation which occurs at the gold - electrolyte interface ,since the depth of the perturbation is only 0.1 Å .

The normalized change of the energy reflectance for a thin film can be expressed in terms of the normalized change of the Fresnel coefficient for the gold - electrolyte interface , with the aid of Eq.(4.10) , as

$$\frac{\Delta R}{R \Delta N} = \frac{\cos\phi \exp(-\beta) + \exp(-2\beta)}{r_1^2 + 2r_1 r_2 \exp(-2\beta)} \cdot R \cdot \frac{\Delta R_2}{R_2 \Delta N} \qquad (4.46)$$

Evaluation of the ER spectrum using the optical constants of bulk gold

give the curve shown in Fig. (4.14) . The ER spectrum of this figure has been calculated for a gold film of thickness 400 Å. The shape of the spectrum and the position of the peak are in very good agreement with the experimental results of gold films of the same thickness.

Following the same procedure the normalized change of energy transmittance can be expressed as

$$\frac{\Delta T}{T\,\Delta N} = \frac{r_1 r_2 \cos\Phi' + r_1^2 r_2^2}{1 + 2r_1 r_2 \cos\Phi' + r_1^2 r_2^2} \cdot \frac{\Delta R_2}{R_2 \Delta N}$$

$$- \frac{r_1 r_2 \cos\theta \exp(-\beta) + r_1^2 r_2^2 \exp(-2\beta)}{1 + 2r_1 r_2 \cos\theta \exp(-\beta) + r_1^2 r_2^2 \exp(-2\beta)} \cdot \frac{\Delta R_2}{R_2 \Delta N} \qquad (4.47)$$

Evaluation of the ET spectrum using the optical constants of bulk gold gave the curve shown in Fig. (4.15). The ET spectrum of this figure has been calculated for a gold film of thickness 300 Å. The shape of the spectrum and the position of the peak are in very good agreement with the experimental results of gold films of the same thickness.

However , when the thickness of the films is of the order of magnitude of a characteristic path length of the electrons in metals (i.e. 100 Å approximately) ,the films exhibit some particular optical properties /22/.

Hence, a different approach will be proposed for the evaluation of the ER and ET spectra of very thin films of gold , in the spectral region of the plasma edge.

As has already been shown, in the spectral region of the plasma edge of an ideal metal, the reflectance is equal to 1 for $\omega = \omega_p$ and

falls to zero as ω tends to ω_o . ω_o is given by Eq.(4.31) and $\omega_o - \omega_p$ is given by Eq.(4.32). The relative change in wavelength for which the reflectance falls from one to zero is always small in the case of gold . In other words the gold films have well defined plasma edge . Consequently the position of the plasma edge can be determined from the plasma frequency. So, in the spectral region of the plasma edge

$$\frac{\Delta R}{R\,\Delta N} = \frac{\Delta R}{R\Delta\omega}\frac{\Delta\omega}{\Delta N} = \frac{\Delta R}{R\Delta\omega}\frac{\Delta\omega_p}{\Delta N}$$

or

$$\frac{\Delta R}{R\Delta N} = M\frac{\Delta R}{R\Delta\omega} \qquad (4.48)$$

Similarly for the ET

$$\frac{\Delta T}{T\Delta N} = M\frac{\Delta T}{T\Delta\omega} \qquad (4.49)$$

where

$$M^2 = \frac{e^2}{N\varepsilon_L\varepsilon_o m\, m^*} \qquad (4.50)$$

Thus, in the spectral region of the plasma edge, the ER and ET spectra can be evaluated from the absolute slope of the reflectance and transmittance spectra respectively.

The results of this approach are in good agreement with the experimental

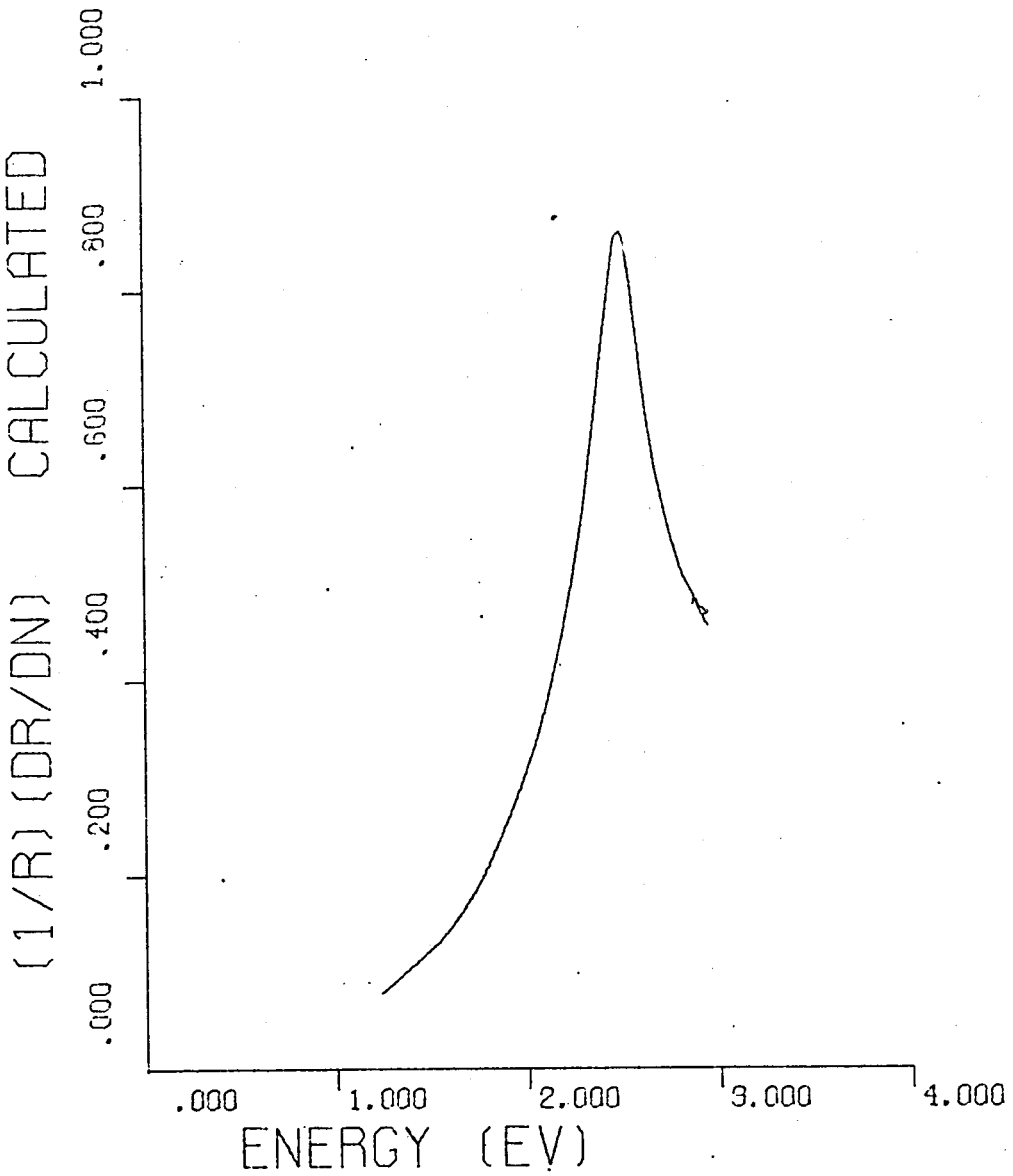

F i g. (4.14)

Application of the proposed model in the case of a gold film of thickness 400 Å.

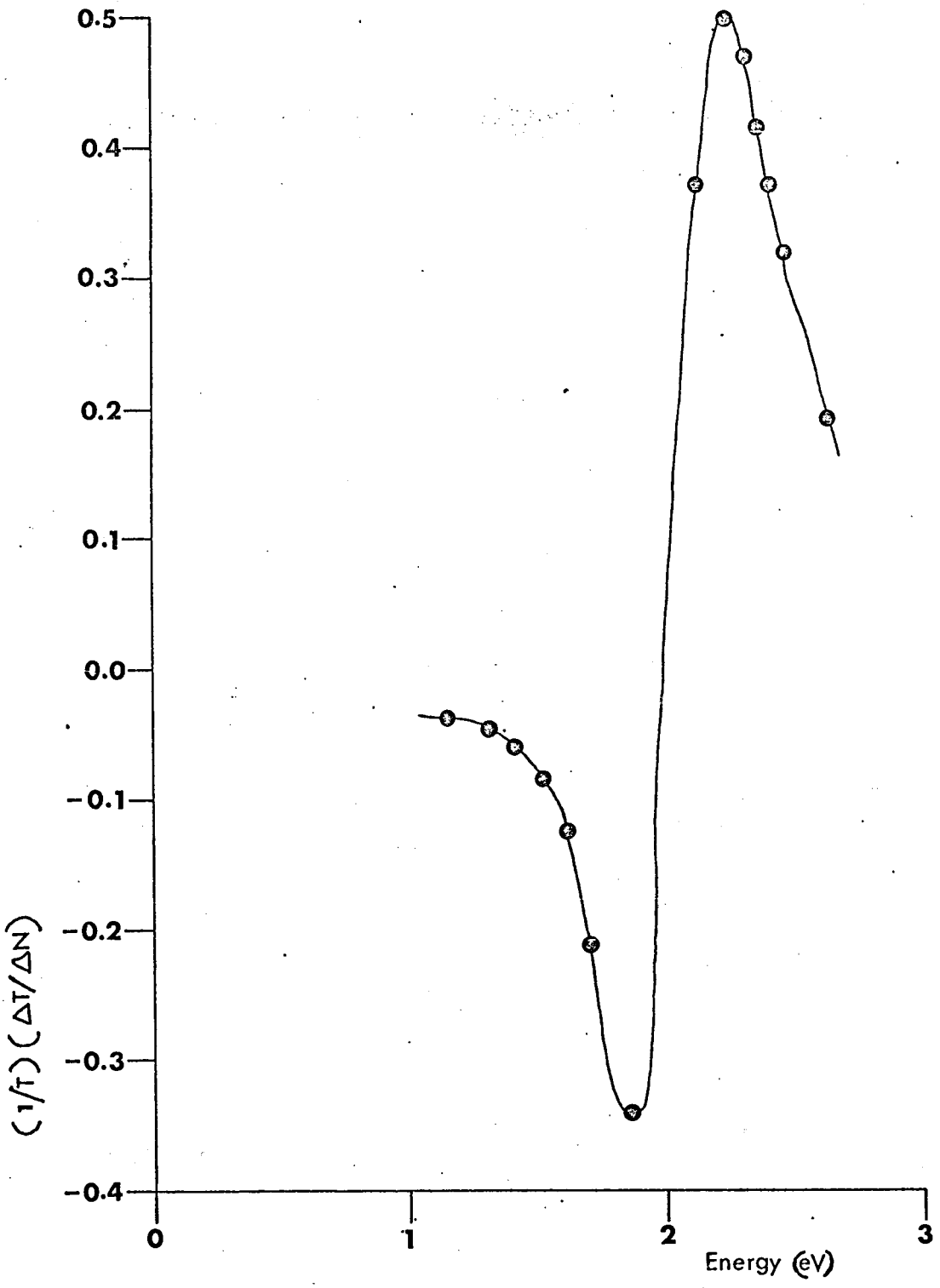

F i g . (4.15)

Calculated ET spectrum of a gold film of thickness 300 Å according to the proposed model.

results. Fig. (4.16) shows the calculated ER spectra of three films of gold . A curve-fitting subroutine was used to find the mathematical expression for the experimental curve R=f(E) . Fig. (4.17) shows the calculated ET spectrum of a thin gold film of thickness 100 Å , according to the same approach.

The calculated ER and ET spectra of very thin films of gold are in good agreement with the experimental ER and ET spectra.

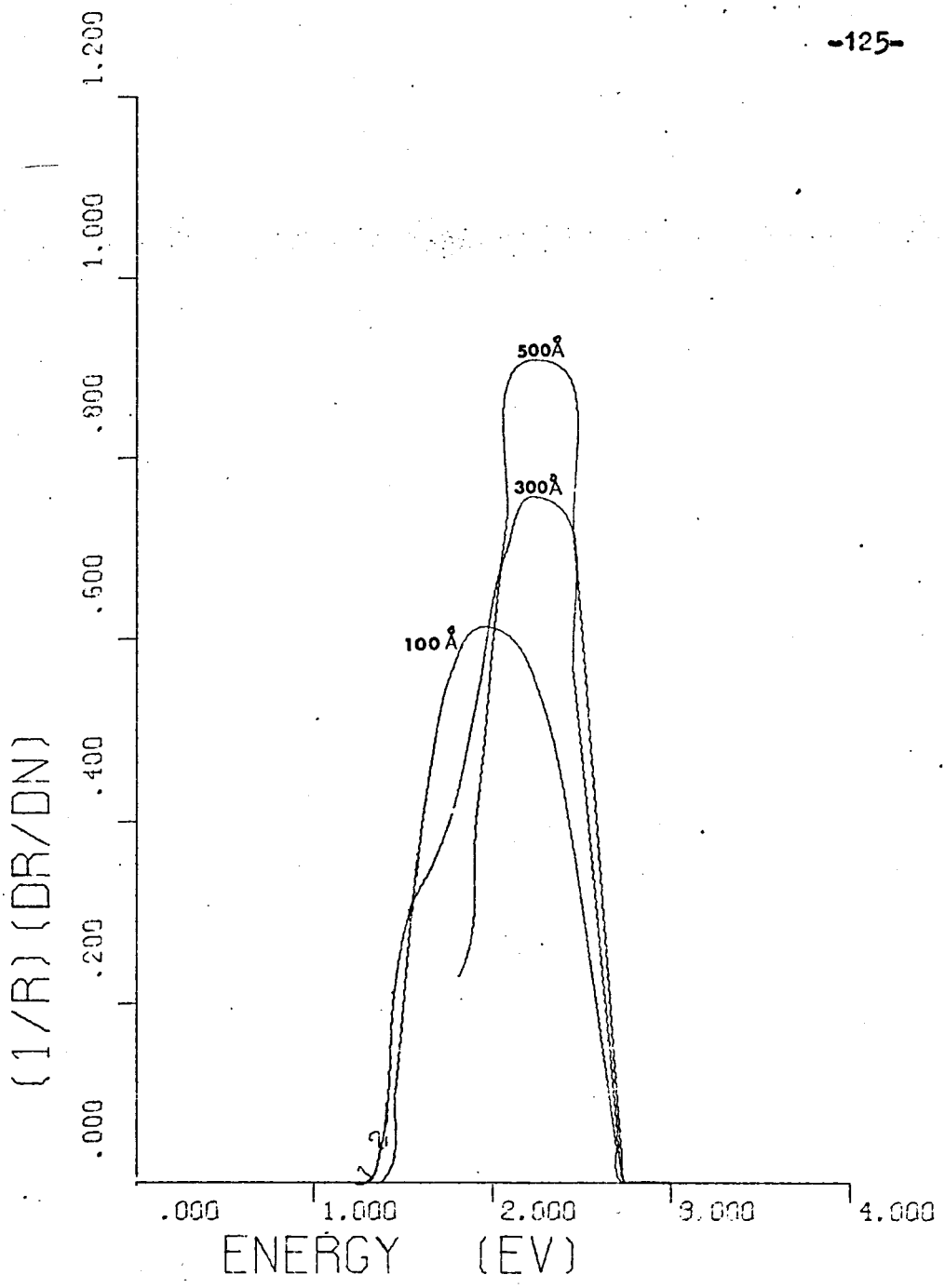

F i g. (4.16)

Calculated ER spectra of three thin films of gold. The three curves represent the normalized derivatives of the calculated reflectance spectra of the films.

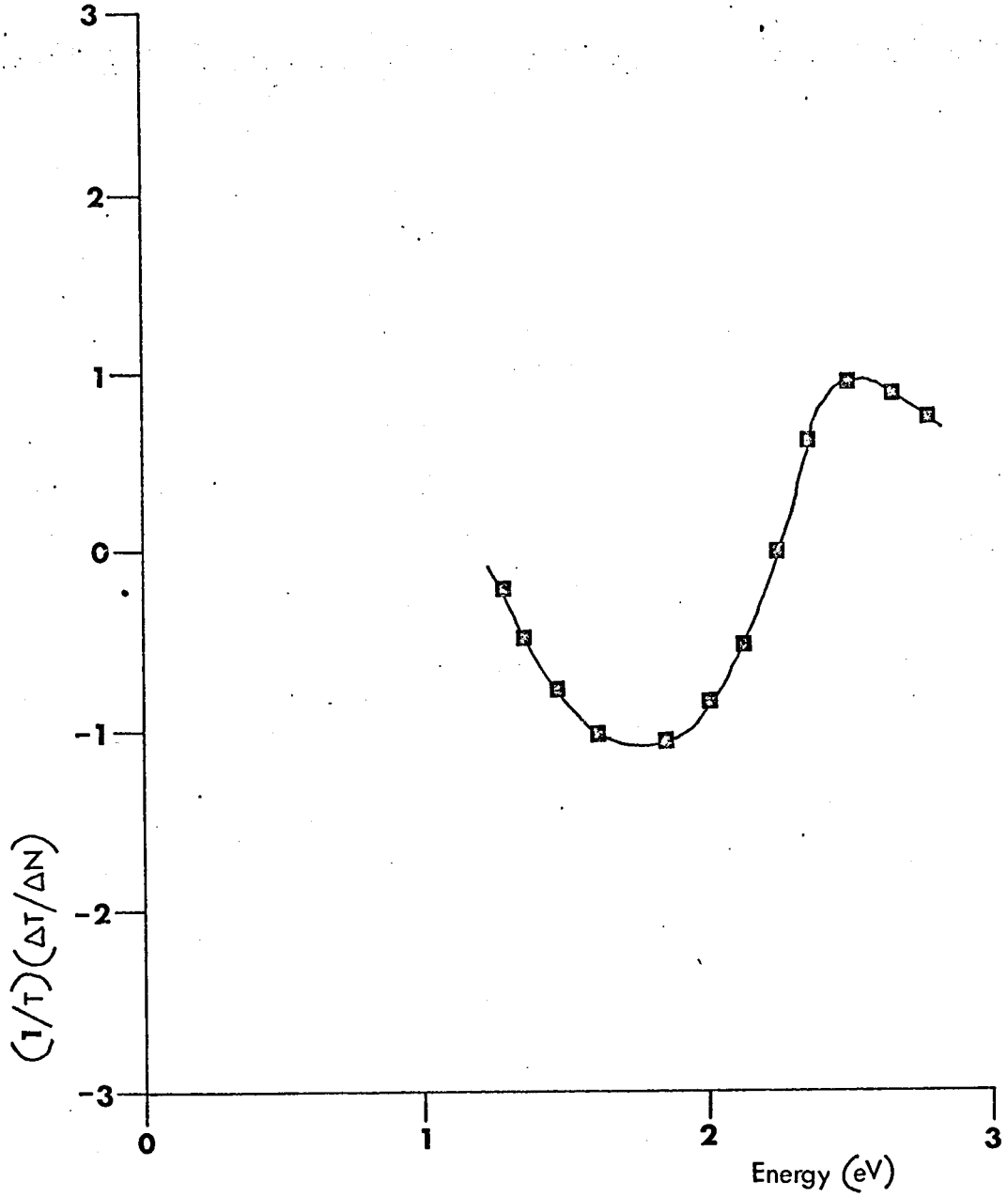

F i g . (4.17)

Calculated ET spectrum of a thin gold film of thickness 100 Å. The curve represents the normalized derivative of the calculated transmittance spectrum of the film..

4.8 Structure of the Gold Films

The structure of some gold films of different thicknesses was examined with the aid of a scanning electron microscope. The examination proved that the films were continuous and they had smooth surfaces.

A very thin film of gold about 30 Å thick was prepared under the conditions which have already been described. Examination of this film with a transmission scanning microscope gave the pictures of Figs. (4.18) and (4.19) .

Fig. (4.18) shows the typical structure of a gold film of thickness 30 Å . Although the thickness is only 30 Å the "islands" of gold on the glass substrate have been connected and the film is not discontinuous . Hence, it can be concluded that a film of gold of thickness 100 Å , prepared under the same conditions, is a continuous film. Unfortunately it was impossible to use the same technique to examine gold films thicker than 50 - 60 Å ,because they were very thick for the transmission microscope used.

Fig. (4.19) shows a ball of gold on the surface of the film. Detailed examination of three more samples proved that there was not any other similar effect on the surfaces of the examined samples.

4.9 ER as a Function of the Modulating Voltage and the Anodic Bias

It was stated in the introduction that the double layer capacity is responsible for the high electricfield applied on the surface of the gold electrode . If C is the double layer capacitance and ΔN the total excess concentration of free electrons per unit volume required to shield the applied electric field on the surface of the electrode

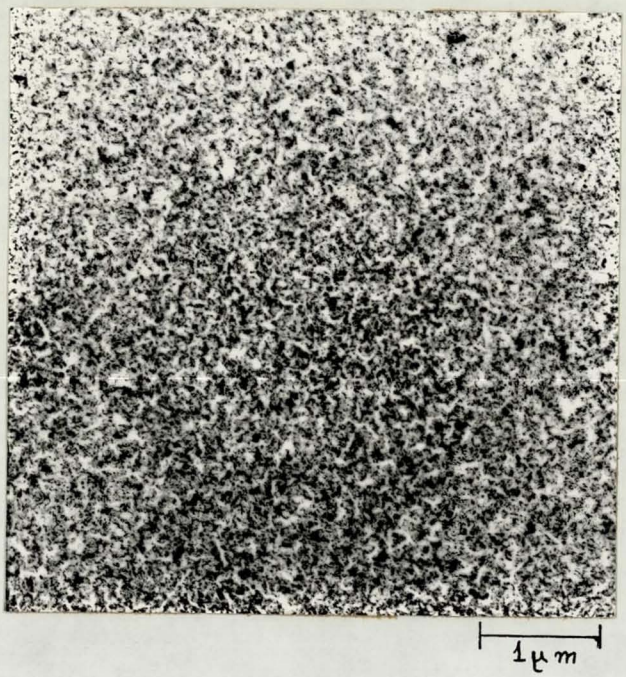

F i g. (4.18)

Typical structure of a gold film of thickness 30 Å deposited at substrate temperature 25° C.

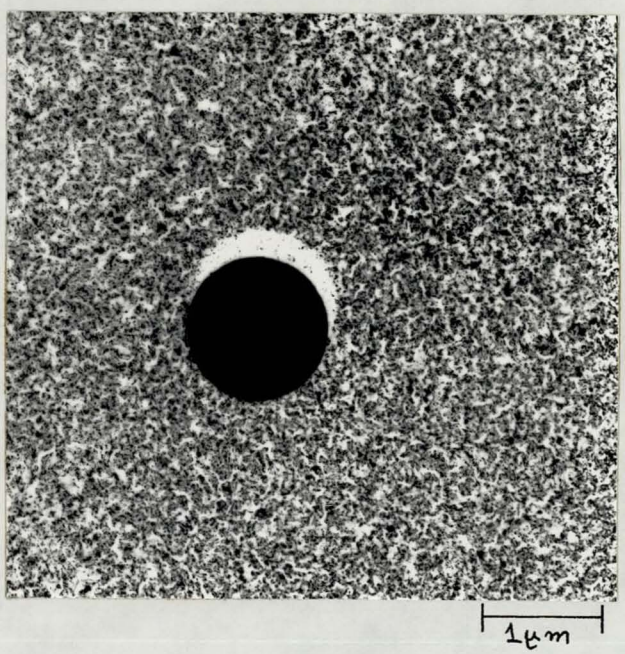

F i g. (4.19)

Droplet of gold on the surface of one of the speciments. It was the only one observed .

we can write

$$\frac{\Delta N}{N} = \frac{CE}{eNd} \cdot A^{-1} \qquad (4.51)$$

where E is the potential of the electrode , A is the effective area of the electrode and d the screening length. Substitution of the above relation in Eq. (4.45) yields

$$\frac{\Delta R}{R} = f(n,k)\omega_p^2 \cdot \frac{CEA^{-1}}{eNd} \cdot \omega^{-2} \qquad (4.52)$$

The magnitude of the ER effect is thus linearly dependent on both the applied voltage and the double layer capacity . For $C=4\times10^{-5}$F, E=0.8V, $N=8\times10^{28}m^{-3}$ and $A=1.2\times10^{-3}m^2$: d=3Å which is not far from the given value of d for metals.

The linear dependence of the value of the ER effect on the applied modulating voltage (V_m) has been verified experimentally; Fig. (3.7). $\Delta R/R$ increases linearly with the applied voltage until the voltage reaches the value of 0.9V peak . After this value the magnitude of the ER decreases continuously beacause evolution of oxygen and hydrogen takes place.

Cahan et al /23/ have observed that the spectral ER peaks shift to lower energies with increasing anodic bias. The predictions of our model (i.e. Eq. (4.52)) explain this feature of the ER effect in metals. The applied biasing voltages on the surface of the electrode change locally the free - electron concentration . So,the plasma frequency of the free - electron gas at the interface is shifted to lower energies. We have assumed that the applied field does not modulate the Fermi level and that the bound electrons are unaffected. Also, it has

been assumed that the perturbation of the optical properties of the interface only is responsible for the ER effect in metals.

The second feature which Caham et al have observed , i.e. the broadening of the ER peaks when the potential of the electrode is approximately greater than 1.0 V SCE , does not concern us as they had exceeded the linear region of the ER effect and other phenomena took place. For example chemiadsorption of species on the surface of the electrode can account for that.

Also,it can be seen from Eq. (4.52) that the ER effect is sensitive to changes in the double layer capacitance, resulting from changes in the double layer stucture with potential,specific adsorption of ions, impurity adsorption and surface - film formation .

In the region where the ER depends linearly upon the applied modulating voltage the double layer capacitance should remain approximately constant. The only effect which takes place is a local perturbation of the optical constants of the surface of the electrode. In other words the term ELECTROREFLECTANCE describes a pure field - induced modulation effect. Unfortunately this term is used some times to define optical effects of chemical origin , e.g. chemiadsorption .

All the effects which have been described and discussed are field induced modulation effects.

Fig. (3.8) shows the variation of the magnitude of the ER effect at 2.3eV as a function of the modulation frequency at 0.8v peak -to-peak. The three curves 1 ,2 and 3 correspond to three different gold films of thickness 350 Å , 200 Å and 160 Å respectively. The magnitude of the ER effect remains approximately constant over a wide frequency

region i.e. from 0 - 1 KHz. After that point the ER starts decreasing. This is in accordance to other researchers /8/, who have observed that the ER is independent from the frequency only up to a maximum frequency of 1.2KHz .

The independence of $\Delta R/R$ from frequency, in the frequency region 0 -1KHz may be explained in terms of the double layer capacitance, which should remain constant in the same frequency region.

4.10 The Magnitude of the ER

The magnitude of the ER effect depends upon the thickness of the film in the case of the Internal Reflection Spectroscopy (IRS). This is obvious from the calculated and the experimental results.

The magnitude of the ER is $2X10^{-4}$ at 2.4eV for a single reflection and a gold film 100 Å thick. Hansen and Pollak /8/ report a value $100X10^{-4}$ using a 50 Å gold film at the same energy of light. However they used multiple reflections (5 in all) to increase the magnitude of the effect. When reduced to one reflection this figure becomes $3X10^{-4}$ which is similar to that reported here.

Fig. (1.6) shows experimental data found in the literature. Differences exist in the magnitude and the sign of the experimental results of various researchers.

4.11 Reflectance Modulation Using a Schottky Barrier

Schottky diodes have been used recently /24/ , /25/ for the study of the ER effect in semiconductors. The Schottky diode is based upon the

Schottky barrier, which is a physical barrier at a metal-semiconductor interface /27/ . To explain the nature of the physical barrier consider an ideal contact between a metal of work function ϕ and an n-type semiconductor. Before equilibrium has been established the energy band scheme may be represented by Fig. (4.10).

It is known that the effective work function of semiconductor is given by the energy difference between its Fermi level and the vacuum level; let this difference be ϕ_0 . Thus if $\phi_0 < \phi$, electrons will flow from the semiconductor into the metal. Consequently the metal acquires a negative surface charge and the semiconductor charges up positively. Now because the density of donors is reletively small, the donors will become ionized over a region which extents into the semiconductor, i.e. a space charge is created. The thickness of the barrier layer thus formed can be estimated using the Poisson differntial equation for the potential energy of an electron in this region.

To a first approximation the equivalent circuit of the contact may be represented by a voltage - dependent capacitor in parallel with a non-linear resistor, the combination being in series with the bulk resistance of the semiconductor.

The Schottky barrier must be distinuished from chemical barrier layers which may be present between the metal and semiconductor as a result of chemical preparation.

Reflectance modulation using a Schottky diode depends on the formation of a Schottky barrier when a thin semitransparent metal film is deposited on the reflecting place of a semiconductor. Light reflected from the interface may then be modulated in intensity in the same manner as occurs with the electrolytic interface. Schottky diodes are

comaratively easy to fabricate and could be applied to a wide range of materials and wavelengths. Despite the intensive investigation of metal-semiconductor junctions as rectifying contacts and optical detectors the Schottky barrier has only recently been used for ER measurements in semiconductors. It was shown that for a gold on GaAs schottky diode, the magnitude of ER was similar to that obtainable with an electrolytic cell, but the energy resolution was an order of magnitude greater. In this case the modulation spectrum due to the semiconductor was investigated , but the possibility arises of observing reflectance modulation due to the metal itself corresponding to the plasma edge. Based on this fact we investigated the ER spectrum of gold using a gold - silicon Schottky diode.

Reflectance modulation was observed similar to that with the electrolytic cell. Fig. (3.17) and Fig. (3.16) show the magnitude of the observed effectas a function of the value of the modulating voltage and the frequency of the modulating signal.

The spectrum obtained is similar to that expected for a very thin film of gold,near its plasma edge. The only disadvantage was the very noisy ER signal.

It seems that the ER of silicon in the optical region of the plasma edge of the gold film does not exhibit any substantial structure /26/. Otherwise it could be impossible to distinguish the ER spectrum of the gold film from the one of the silicon .

The application of a negative D.C. bias on the Schottky diode reduces the capacitance of the Schottky barrier as it is shown in Fig.(2.16). Consequently the magnitude of the ER effect must be decreased. This

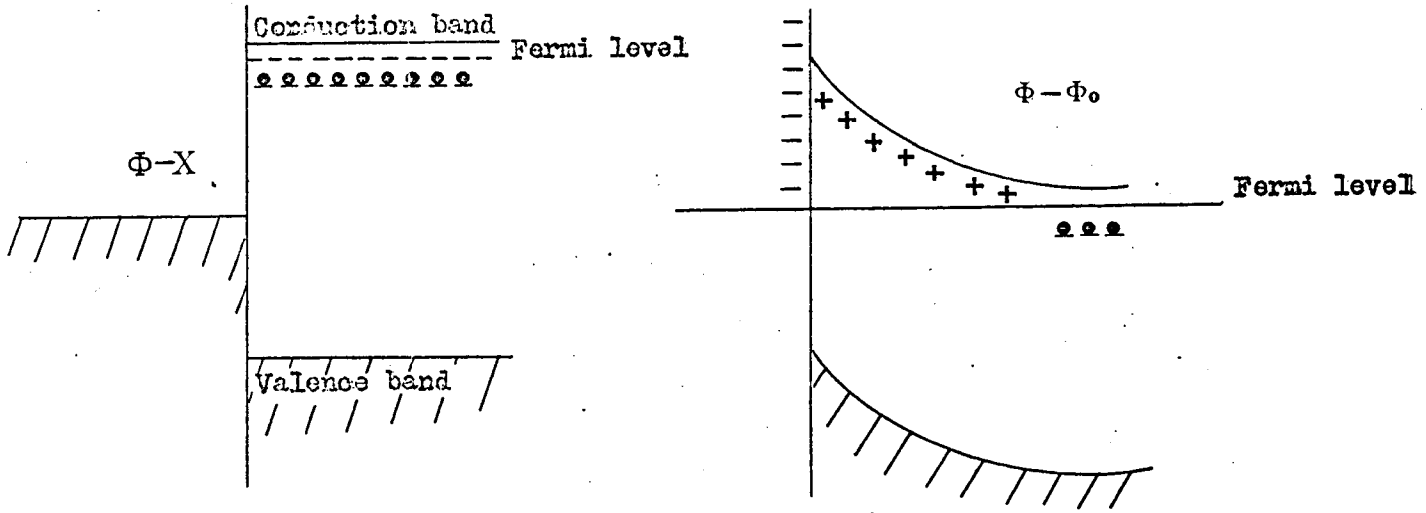

F i g . (4.20)

(a) refers to a metal-semiconductor junction not yet in equilibrium.

(b) Equilibrium has become established by the for mation of a Schottky layer.

has indeed been observed in the experimental ER spectra of the Schottky diode ; Fig. (3.14) and Fig. (3.15) .

CHAPTER 5 - CONCLUSIONS

It has been shown that the optical properties of evaporated films of gold in the visible part of the spectrum may be predicted as a function of their thickness and changes of free electron concentration. The optical constants of gold were used in a computer program for thin film behaviour.

Also, it has been shown experimentally and theoretically that the peak of the ER spectrum in thin films of gold occurs in the spectral region of the plasma edge.

Finally the ET spectrum of thin films of gold exhibits two peaks of opposite sign corresponding to the two edges of the energy - transmittance spectrum of the thin films of gold.

REFERENCES

1. Feinleib, J., Phys. Rev. Lett. , 16 , 1200 (1966) .
2. a) Gouy,G. , J. Physique , 9 , 457 (1910).
   b) Chapman,P.L., Phil. Mag. , (6) 25 , 475 (1913).
3. Grahame,D.C., Chem. Rev., 41 , 441 , (1947).
4. Takamura , T. , et al , J. Electrochem. Soc. 117 , 626 (1970) .
5. Graham,D.C. , Ann.Rev.Phys. Chem. 6 , 337 (1955).
6. a) Hansen,W.N. , Osteryoung,R.A. , and Kuwana,T., J. Amer.Chem. Soc. , 88 , 1062 (1966).
   b) Hansen,W.N. , Osteryoung,R.A. , and Kuwana,T., Anal. Chem. , 38 , 1810 (1966).
   c) Mark,H.B. , and Randall,E.N. , Symp.Faraday Soc. 4 , 157 (1970).
   d) Prostak,A. , Mark H.B. , and Hansen,W.N. , J.Phys.Chem. 72 , 2576 (1968).
7. Stadler,H.L., and Ishibashi,Y. , J.Phys.Chem.Solids 30 , 2113 (1969) .
8. Prostak,A. , and Hansen,W. , Phys. Rev. 160 , 600 (1967).
9. Hansen,W. , J.Opt.Soc.Am. 58 , 380 (1968).
10. Kittel,C. , Introduction to Solid State Physics , 3rd ed., Wiley New York,1968 , Chapter 8 , p.225.
11. Hansen,W., and Prostak,A. , Phys. Rev. 174 , 500 (1968).
12. Hansen,W., Surf.Sci., 16 , 205 (1969).
13. a) McIntyre, J.D.E.,and Aspnes,D.E., Surf.Sci. ,24,417 (1971).
   b) Advances in Electrochemistry and Electrochemical Engineering Vol. 9 , pp. 61-166.
14. McIntyre , J.D.E.,Symp.Faraday Society 4 , 50,55,61 (1970).
15. McIntyre , J.D.E.,and Aspnes,D.E., Bull Am.Phys.Soc.15 ,366 (1970).

16. Ckeyssac , P. , Garrigos , R., and Al., Surf.Sci. 37 , 683 (1973).

17. Lorrain , P., and Corson , D., "Electromagnetic Fields and Waves" (second edition) Freeman (chapter 12).

18. Howson , R.P., J.Phys.D:Appl.Phys.,3, 863 (1970).

19. a)Irari,G.B., and Al , J.Opt. Soc. Am. 61 , 128 (1971).
b)American Institute of Physics Handbook , 3rd ed.

20. McIntyre , J.D.E., paper presented at the 135th National Meeting of the Electrochemical Society , New York , May 1969 (Abstract No 231).

21. Cheyssac , P., Garrigos, R., and Al , Thin Solid Films 13 , 275 (1972).

22. Abelès , F., Physics of Thin Films p.188 , Vol.6, 1971, Acad.Press.

23. Cahan ,D., Horkans,J., and Yeager , E., Symp.Faraday Soc.4,36(1970).

24. Aspnes , D.E., and Studna , A.A. , Phys.Rev.B 7 , 4605,(1973).

25. Babyler , B.A.,et al.,Sov.Phys.-Semic.6 ,1511,(1973).

26. Babyler , B.A.,et al.,Phys.Rev. 140, A 1716 (1965).

27. Schottky,W., Z.PhysiK, 113 , 367 ,(1939).

28. Howson , P.R.,and Malina , V.,J.Phys. D. 3 , 854, (1970).

29. Moss , T., Semiconductor Optoelectronics pp. 43 and 36.

30. Moss , T.S.,et al, J.Phys. C, 1 , 1435 , (1968).

31. Elliot, R . and Gibson , A., An introduction to solid state Physics p.269.

32. Tables of Physical and Chemical Constants, G.W.C. Kaye et al.

33. Brookdeal Electronics Ltd. Application Report No 5.

34. Heavens , O.S., "Optical Properties of Thin Solid Films", Dover (1965) p.186.

35. Sennett , R.S., and Scott,G.,J.Opt.Soc.Amer.,40,203,(1950).

36. Ennos , A.,Brit.J.Appl.Phys.,9,359,(1958).

37. Delahay, P., New Instrumental Methods in Electrochemistry , Interscience Publishers (1954) , p.30.

38. Yeager , Salkind "techniques of electrochemistry" Vol.1 Wiley - Interscience , 1972, pp. 53,55,63,64.